Abscisic acid ameliorates glucose tolerance and obesity-induced inflammation

Amir Joseph Guri

Dissertation submitted to the faculty of the Virginia Polytechnic Institute and State University in partial fulfillment of the requirements for the degree of

Doctor of Philosophy
In
Human Nutrition, Foods, and Exercise

Josep Bassaganya-Riera
William Barbeau
William Huckle
David Kingston
Dongmin Liu
Forrest Thye

October 19, 2007
Blacksburg, VA

Keywords: abscisic acid, obesity, macrophage, inflammation, white adipose tissue

Abscisic acid ameliorates glucose tolerance and obesity-induced inflammation

Amir Joseph Guri

ABSTRACT

Obesity is a disease characterized by chronic inflammation and the progressive loss in systemic insulin sensitivity. One of the more effective medications in the treatment of insulin resistance have been the thiazolidinediones (TZDs), which act through the nuclear receptor peroxisome proliferator-activated receptor γ (PPAR γ). Due to the many side-effects of TZDs, our laboratory sought out a natural phytochemical, abscisic acid (ABA), with chemical similarities to TZDs. Our first study demonstrated that ABA activates PPAR γ *in vitro* and significantly ameliorates white adipose tissue (WAT) inflammation and glucose tolerance in db/db mice. We next further examined the effect of ABA on the phenotype of adipose tissue macrophages (ATMs). In doing so, we discovered two separate ATM populations which differed in their expression of the macrophage surface glycoprotein and maturation marker F4/80 ($F4/80^{hi}$ vs $F4/80^{lo}$). Dietary ABA-supplementation significantly reduced $F4/80^{hi}CCR2^{+}$ ATMs and had no effect on the $F4/80^{lo}$ population. Utilizing a tissue-specific knockout generated through Cre-lox recombination, we were able to determine that this effect was dependent on PPAR γ in immune cells. To further characterize the differences between the ATM subsets that were affected by ABA, we performed a multi-organ assessment (i.e., WAT, skeletal muscle and liver) of the effect of diet-induced obesity on the phenotype of infiltrating macrophages and T cells into metabolic organs. Based on our new data, we formulated a model by which $F4/80^{hi}CCR2^{hi}$ ATMs infiltrate WAT and ultimately induce a $CD11c^{+}$ pro-inflammatory phenotype in the resident $F4/80^{lo}CCR2^{lo}$ subset. Ultimately, our

findings provide evidence that ABA has potential as an alternative preventive

intervention, expound the role of PPAR γ in immune cells and, in general, expand our

knowledge concerning the immunopathogenesis of obesity-induced insulin resistance.

LIST OF ATTRIBUTION

Attribution

     Several colleagues and coworkers aided in the writing and research behind several of the chapters of this dissertation. A brief description of their background and their contributions are included here.

Josep-Bassaganya Riera- DVM, Ph.D. (Department of Human Nutrition, Foods, and Exercise, Virginia Tech) is the primary Advisor and Committee Chair. Dr. Bassaganya provided guidance with the experimental designs and reviewed each article before submission.

Raquel-Hontecillas- Ph.D. (Department of Human Nutrition, Foods, and Exercise, Virginia Tech) was a post-doc in the Nutritional Immunology and Molecular Nutrition Laboratory throughout the majority of my Ph.D program. Raquel provided invaluable mentorship, reviewed the manuscripts before submission, and provided guidance with data analyses.

Chapter 3: Dietary abscisic acid ameliorates glucose tolerance and obesity-related inflammation in db/db mice fed high-fat diets.

Dongmin Liu- Ph.D. (Department of Human Nutrition, Foods, and Exercise, Virginia Tech) is a committee member who provided guidance, particularly with *in vitro* cell culture protocols, and assisted in writing the methods section pertaining to cell transfection in both this chapter and the following.

Hongwei Si- (Department of Human Nutrition, Foods, and Exercise, Virginia Tech) is an HNFE graduate student and member of Dr. Liu's laboratory. Hongwei was instrumental in helping to establish the *in vitro* portion of the project and assisted in both this chapter and the following one.

Chapter 4- Loss of PPARgamma in immune cells impairs the ability of abscisic acid to improve insulin sensitivity by suppressing monocyte chemoattractant protein-1 expression and macrophage infiltration into white adipose tissue.

Gerardo Ferrer and Oriol Casagran (Department of Human Nutrition, Foods, and Exercise, Virginia Tech), both currently studying at the University of Barcelona, were members of the laboratory for approximately 3 months. During their stay, they

conducted the first project in our laboratory where we first observed the two separate macrophage populations.

Umesh Wankhade- DVM (Department of Human Nutrition, Foods, and Exercise, Virginia Tech) is a former grad student in the laboratory who assisted with the experimental protocols.

Alexis Noble- B.S. (Department of Biology, Virginia Tech) was a laboratory technician in the laboratory who assisted in the experimental protocols and animal care.

Decio Eizirik, Fernanda Ortiz, Miriam Cnop (Laboratory of Experimental Medicine, Université Libre de Bruxelles) provided the MCP-1 plasmid.

TABLE OF CONTENTS

LIST OF FIGURES

Chapter 1: Introduction

Chapter 2: Dietary abscisic acid ameliorates glucose tolerance and obesity-related inflammation in db/db mice fed high-fat diets.

Chapter 3: Dietary abscisic acid ameliorates glucose tolerance and obesity-related inflammation in db/db mice fed high-fat diets.

Chapter 4: Loss of PPARgamma in immune cells impairs the ability of abscisic acid to improve insulin sensitivity by suppressing monocyte chemoattractant protein-1 expression and macrophage infiltration into white adipose tissue.

Chapter 5: Obesity promotes macrophage infiltration into both adipose tissue and skeletal muscle and impairs the regulatory CD4+ T cell compartment.

LIST OF TABLES

LIST OF ABBREVIATIONS

ABA, abscisic acid; ADRP, adipose differentiation related protein; ANOVA, analysis of variance; AP-1, activator protein-1; ATM, adipose tissue macrophage; ATP, Adult Treatment Panel; BAT, brown adipose tissue; BP, blood pressure; β3AR, β3-andregneric receptor; CCR, chemokine receptor; C/EBP α, CCAT/enhancer binding protein α; CPT-1, carnitine palmitoyle transferase-1; CVD, coronary vascular disease; CLA, conjugated linoleic acid; COX-2, cyclooxygenase-2; DAG, diacylglyeride; DHA, decosahexaenoic acid; DIO, diet-induced obesity; DPP, diabetes prevention program; DR, direct repeat; DSS, dextran sodium sulfate; ER, endoplasmic reticulum; EPA, eicosapentaenoic acid; FFAs, free fatty acids; GTT, glucose tolerance test; HDL, high density lipoprotein; HETE, hydroxyeicosatetraenoic acid; HFD, high-fat diet; HODE, hydroxyoctadecadienoic acid; ICAM, intracellular adhesion molecule; IFG, impaired fasting glucose; IFN-γ, interferon γ; IGT, impaired glucose tolerance; IKK, inhibitor of nuclear factor κB kinase; ILS, intensive lifestyle management; IL, interleukin; IPGTT, intraperitoneal glucose tolerance test; IRS, insulin receptor substrate; IMTGs, intramuscular triglycerides; IMAT, intermuscular adipose tissue; JNK, c-Jun N-terminal kinase; LBD, ligand binding domain; LDL, low density lipoprotein; LPS, lipopolysaccharide; LXR, liver X receptor; MCP-1, monocyte chemoattractant protein 1, MIP-1α, macrophage inflammatory protein-1α, NAFLD, non-alcoholic fatty liver disease; NCor, nuclear corepressor; NF-κB, nuclear factor κB; PPAR, peroxisome proliferator-activated receptor; PAI-1, plasminogen activator inhibitor-1; PDK, pyruvate dehydrogenase kinase; PEPCK, phosphoenolpyruvate carboxykinase; PPRE, PPAR response element; ROS, reactive oxygen species; RXR, retinoid X receptor; SM, skeletal

muscle; SMP, skeletal muscle macrophage; SVCs, stromal vascular cells; SVF, stromal vascular fraction; T2D, type 2 diabetes; TGF β, transforming growth factor β; TLR, toll-like receptor; TGs, triglycerides; TNF, tumor necrosis factor, T-regs, regulatory T-cells; TZDs, thiazolidinediones; UPR, unfolded protein response; UCP, uncoupling protein; VCAM, vascular adhesion molecule; VDR, vitamin D receptor; VLDL, very low density lipoprotein; WAT, white adipose tissue; WHO, World Health Organization

CHAPTER 1: INTRODUCTION

Over the past 30 years, as obesity rates have surged towards epidemic

proportions, health practitioners have reported an attendant rise in the number of patients

diagnosed with insulin resistance (1), a condition characterized by the diminished ability

of muscle or other peripheral tissues to uptake glucose from the bloodstream. According

to the most recent World Health Organization estimates, 1.6 billion adults are overweight

and 300 million are obese. One of the consequences of insulin resistance is chronic

hyperglycemia, which induces the micro and macrovascular disorders associated with

Type 2 Diabetes (T2D) (2). In addition to T2D, however, researchers are finding that the

costs of insulin resistance extend to many chronic diseases, including coronary vascular

disease (CVD), atherosclerosis, hypertension, and obstructive sleep apnea (3).

The main tool used by clinicians to assess a patient's degree of insulin resistance

is to measure blood glucose levels after an overnight fast and 2 hours following an oral

glucose challenge. Those patients that have glucose levels greater than 125 mg/dL or 199

mg/dL following the overnight fast or glucose challenge, respectively, are diagnosed with

T2D (3). A separate classification, known as prediabetes, has been developed to describe

those patients with impaired fasting glucose (IFG, 100-125 mg/dL), impaired glucose

tolerance (IGT, 140-199 mg/dL), or both (3). While those individuals with prediabetes

do not appear to be at an immediate risk for developing the micro and macrovascular

damage associated with T2D, their probability of being diagnosed with CVD and other

insulin resistance-related co-morbidities is significantly elevated (4). Of patients

diagnosed with prediabetes in the year 2003, 94.9% had dyslipidemia, 56.5% had

hypertension, and 13.9% had microalbuminurea (5). According to the latest estimates,

20.8 million Americans have T2D and greater than 40.1 million individuals have prediabetes (3).

Because even moderate insulin resistance puts one at an elevated risk for developing CVD and other insulin resistance-related chronic diseases, a number of questions have arisen concerning when patients should begin taking an antidiabetic medication and also what type of medication they should be prescribed. The more traditional antidiabetic treatments include the sulfonylureas and α-glucosidase inhibitors, which reduce the consequences of chronic hyperglycemia by increasing pancreatic insulin secretion and inhibiting intestinal glucose absorption, respectively (3). These drugs, however, are designed to manage hyperglycemia rather than treat it, and they do not have any significant effect on the progression of insulin resistance. Because of this, they are often used in conjunction with the newer class of antidiabetic treatments known as the "insulin sensitizers."

As their name implies, "insulin sensitizers" increase the sensitivity of peripheral tissues to the actions of endogenous insulin, thereby directly counteracting the effect of obesity. The two main classes of insulin-sensitizing drugs include the biguanides (i.e. metformin) and thiazolidinediones (TZDs, i.e. rosiglitazone and pioglitazone). While both are classified as "insulin sensitizers," biguanides and TZDs act through distinct molecular mechanisms. Biguanides lower hepatic glucose production and increase intramyocellular fatty acid oxidation by increasing the activity of the signal transduction protein AMP kinase (AMPK) (6). Conversely, TZDs serve as synthetic ligands for a key metabolic regulator and transcription factor known as peroxisome proliferator-activated receptor γ (PPAR γ) (7). PPAR γ is a member of the nuclear

receptor superfamily, which consists of 48 ligand-induced transcription factors that respond to nutrients, xenobiotics, and various hormones and endogenously produced compounds, and is found in high concentrations in white adipose tissue (WAT), immune cells, and the colonic epithelium (8, 9). PPARs, which in addition to PPAR γ also include PPARs α and δ, are endogenously activated by fatty acids and products of lipid metabolism (9).

One notable difference between the biguanides and TZDs is that the latter, perhaps due to activating a central metabolic regulator, have the added benefits of being anti-hypertensive and anti-atherogenic (10, 11). In the recent PROactive (PROspective pioglitAzone Clinical Trial In macroVascular Events) clinical trial, in which T2D patients with known macrovascular disease were treated with 15 mg to 45 mg of pioglitazone or placebo, pioglitazone decreased the composite of all-cause mortality, non-fatal myocardial infarction, and stroke (12, 13). Moreover, results from the Diabetes Prevention Program (DPP), in which high-risk subjects were randomly assigned to troglitazone, placebo, metformin, or intensive lifestyle management (ILS), showed that the incidence of diabetes in those treated with the TZD was lower than those treated with placebo, metformin, or ILS (14). Comparisons between biguanides and TZDs have also indicated that TZDs are more effective in improving glycemic control and in enhancing whole body insulin sensitivity (15). Therefore, with regard to the insulin sensitizing medications, PPAR γ agonists in particular appear to represent a more promising avenue for future drug design and disease treatment/prevention.

While TZDs have shown effectiveness in improving insulin sensitivity in patients with both T2D and prediabetes (16), these compounds, as are the case with many

pharmaceutical agents, are associated with a number of unwanted side effects which limit

their desirability and availability to millions of potential users (17). For instance, in the

PROactive study, pioglitazone increased the incidences of both edema and congestive

heart failure (12, 13). TZDs are also associated with weight gain and, in the past,

hepatotoxicity (17). Recently, a study in the New England Journal of Medicine showed

that use of rosiglitazone (Avandia™) was associated with a 43% increase in myocardial

infarction and 64% increase in risk of cardiovascular mortality (18).

With regard to TZDs, there are still many questions concerning how PPAR γ

ligands improve systemic insulin sensitivity. Obesity is a condition characterized by

chronic, low-grade inflammation. During its onset, adipocytes grow in size to

accommodate the excess energy, becoming increasingly hypertrophic and dysfunctional.

This scenario has two major consequences. In white adipose tissue (WAT), the stressed,

hypertrophic adipocytes secrete pro-inflammatory cytokines and chemokines, including

tumor necrosis factor α (TNF- α) (19), IL-6 (20), monocyte chemoattractant protein-1

(MCP-1) (21), and macrophage inflammatory protein-1 α (22), which, in addition to

directly inhibiting the insulin signaling pathway through serine phosphorylation of the

insulin receptor substrates 1 and 2 (IRS1, IRS2), can also inhibit the adipocyte

differentiation (23). These cytokines, in particular MCP-1, also recruit bone marrow-

derived monocytes into the tissue (24). These monocytes differentiate into adipose tissue

macrophages (ATMs), a change that involves an increase in both size and phagocytic

ability, and primarily localize around dead adipocytes in what are referred to as "crown-

like structures" (25).

Transgenic models in which the pro-inflammatory pathways or migratory ability of myeloid cells have been compromised point to the ATM as an influential participant in progression of insulin resistance (24, 26-30). Recently, Lumeng and colleagues differentiated two distinct types of ATMs (31, 32). The first was a resident ATM population of alternative polarization (i.e., M2 macrophages) which secreted high amounts of the anti-inflammatory cytokine IL-10 and arginase (31, 32). Macrophages of this type have been shown to be adept in engulfing debris and scavenging lipid (31). During the onset of obesity, however, this population steadily gave way to an infiltrating, classically activated, M1-polarized population, which secreted more TNF- α and IL-6 and expressed higher levels of chemokine receptor 2 (CCR2) and CD11c than the resident population (31). M1 macrophages are generally involved in the development of immune responses against pathogens. The infiltration of this population was inhibited by the deletion of the MCP-1 receptor CCR2 (31). While these findings further detail the role of ATMs in the progression of insulin resistance, the involvement of other immune cells, such as regulatory T-cells (Treg), in the M1-shift of ATMs has yet to be fully elucidated.

In addition to WAT inflammation and macrophage infiltration, lipid infiltration of non-adipose tissues, including liver, skeletal muscle (SM), heart, and blood vessels is a principle consequence of obesity. Lipids and lipid intermediates, such as diacylglyceride (DAG) and ceramides, have both been shown to insulin signaling in SM (33, 34), a tissue responsible for 80% of systemic insulin-stimulated glucose uptake, and lead to the progression of non-alcoholic fatty liver disease (NAFLD), another hallmark of obesity (35).

The main way in which PPAR γ agonists are believed to function involves their direct role in alleviating adipocyte hypertrophy. Following ligand binding, PPAR γ heterodimerizes with retinoid X receptor (RXR), another member of the nuclear receptor superfamily, which induces the detachment of corepressors, the recruitment of coactivators, some of which with acetylation activity, and the subsequent binding to a PPAR response element (PPRE) on DNA that initiates the transcription of responsive genes (36). Many of the genes induced by PPAR γ, such as aP2, CD36, are important in fatty acid transport, adipogenesis, and lipid uptake, and studies have shown that PPAR γ is an essential participant in the differentiation of pre-adipocytes into adipocytes, particularly in the subcutaneous adipose tissue depots (37). The addition of newly-formed adipocytes prevents the hypertrophy of existing adipocytes, thereby indirectly preventing WAT inflammation and lipid infiltration into the peripheral tissues. While this function alone could explain the efficacy of PPAR γ ligands, numerous studies have shown that PPAR γ activation directly inhibits inflammation through multiple mechanisms, one of which involving the exportation of the nuclear factor κB (NF-κB) active subunit p65 (RelA) (38) from the nucleus and the other involving post-translational modification, whereby following activation the ligand binding domain (LBD) of PPAR γ becomes sumoylated, causing it to migrate to and inhibit the removal of the nuclear corepressor (NCor) complex of NF-κB (39). PPAR γ activation has been shown to directly inhibit MCP-1-induced migration of monocytes *in vitro* and *in vivo* (40, 41), making it very probable that the anti-inflammatory actions of PPAR γ in cells other than adipocytes are involved in the insulin-sensitizing effects of TZDs and other endogenous PPAR γ ligands.

Thus, in the context that the synthetic PPAR γ agonists have been shown to be very effective in improving systemic insulin sensitivity but yet hold strong safety concerns, our goal was to explore whether a novel, naturally occurring compound, abscisic acid (ABA), can be used to ameliorate glucose tolerance in obese, diabetic mice without the side-effects associated with the potent, synthetic compounds.

We next assessed the effect of ABA on the phenotype of ATMs and whether immune cell PPAR γ participates in its insulin sensitizing effects. From this study, we found an ATM population whose infiltration was specifically inhibited by ABA-supplementation. We then
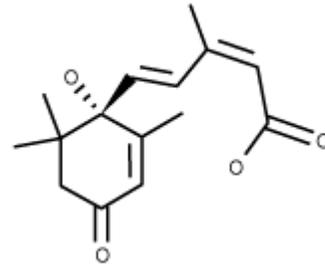
Figure 1. Chemical structure of abscisic acid

expanded the characteristics of this single ATM population and also examined the effect of obesity on immune cell infiltration into the three major metabolic tissues, WAT, liver, and skeletal muscle (SM), with the diet-induced obesity (DIO) model, formulating a new model by which ABA and other insulin sensitizing agents may inhibit inflammation. In all of the following manuscripts, the first author wrote and contributed significantly to the experimental design, data analyses, and data interpretation.

References

1.   Finkelstein EA, Fiebelkorn IC, Wang G. National medical spending attributable to overweight and obesity: how much, and who's paying? Health Aff (Millwood) 2003; Suppl Web Exclusives: W3-219-226.
2.   Vasudevan AR, Burns A, Fonseca VA. The effectiveness of intensive glycemic control for the prevention of vascular complications in diabetes mellitus. Treatments in endocrinology 2006; 5: 273-286.

3. CDC. National Diabetes Fact Sheet: general information and national estimates on diabetes in the United States, 2005. U S Department of Health and Human Services, Center for Disease Control and Prevention, 2005: Atlanta, Georgia, 2005, pp 1-10.

4. Schnell O, Standl E. Impaired glucose tolerance, diabetes, and cardiovascular disease. Endocr Pract 2006; 12 Suppl 1: 16-19.

5. Benjamin SM, Valdez R, Geiss LS, Rolka DB, Narayan KM. Estimated number of adults with prediabetes in the US in 2000: opportunities for prevention. Diabetes care 2003; 26: 645-649.

6. Zhou G, Myers R, Li Y, Chen Y, Shen X, Fenyk-Melody J, et al. Role of AMP-activated protein kinase in mechanism of metformin action. The Journal of clinical investigation 2001; 108: 1167-1174.

7. Lehmann JM, Moore LB, Smith-Oliver TA, Wilkison WO, Willson TM, Kliewer SA. An antidiabetic thiazolidinedione is a high affinity ligand for peroxisome proliferator-activated receptor gamma (PPAR gamma). The Journal of biological chemistry 1995; 270: 12953-12956.

8. Braissant O, Foufelle F, Scotto C, Dauca M, Wahli W. Differential expression of peroxisome proliferator-activated receptors (PPARs): tissue distribution of PPAR-alpha, -beta, and -gamma in the adult rat. Endocrinology 1996; 137: 354-366.

9. Desvergne B, Wahli W. Peroxisome proliferator-activated receptors: nuclear control of metabolism. Endocr Rev 1999; 20: 649-688.

10. Wang G, Wei J, Guan Y, Jin N, Mao J, Wang X. Peroxisome proliferator-activated receptor-gamma agonist rosiglitazone reduces clinical inflammatory responses in type 2 diabetes with coronary artery disease after coronary angioplasty. Metabolism: clinical and experimental 2005; 54: 590-597.

11. Dobrian AD, Schriver SD, Khraibi AA, Prewitt RL. Pioglitazone prevents hypertension and reduces oxidative stress in diet-induced obesity. Hypertension 2004; 43: 48-56.

12. Dormandy JA, Charbonnel B, Eckland DJ, Erdmann E, Massi-Benedetti M, Moules IK, et al. Secondary prevention of macrovascular events in patients with type 2 diabetes in the PROactive Study (PROspective pioglitAzone Clinical Trial In macroVascular Events): a randomised controlled trial. Lancet 2005; 366: 1279-1289.

13. Scheen AJ, Lefebvre PJ. [Proactive study: secondary cardiovascular prevention with pioglitazione in type 2 diabetic patients]. Revue medicale de Liege 2005; 60: 896-901.

14. Knowler WC, Hamman RF, Edelstein SL, Barrett-Connor E, Ehrmann DA, Walker EA, et al. Prevention of type 2 diabetes with troglitazone in the Diabetes Prevention Program. Diabetes 2005; 54: 1150-1156.

15. Seufert J, Lubben G, Dietrich K, Bates PC. A comparison of the effects of thiazolidinediones and metformin on metabolic control in patients with type 2 diabetes mellitus. Clinical therapeutics 2004; 26: 805-818.

16. Dumasia R, Eagle KA, Kline-Rogers E, May N, Cho L, Mukherjee D. Role of PPAR- gamma agonist thiazolidinediones in treatment of pre-diabetic and diabetic individuals: a cardiovascular perspective. Current drug targets 2005; 5: 377-386.

17. Nesto RW, Bell D, Bonow RO, Fonseca V, Grundy SM, Horton ES, et al. Thiazolidinedione use, fluid retention, and congestive heart failure: a consensus statement from the American Heart Association and American Diabetes Association. October 7, 2003. Circulation 2003; 108: 2941-2948.

18. Nissen SE, Wolski K. Effect of rosiglitazone on the risk of myocardial infarction and death from cardiovascular causes. The New England journal of medicine 2007; 356: 2457-2471.

19. Hotamisligil GS, Shargill NS, Spiegelman BM. Adipose expression of tumor necrosis factor-alpha: direct role in obesity-linked insulin resistance. Science 1993; 259: 87-91.

20. Bruun JM, Lihn AS, Madan AK, Pedersen SB, Schiott KM, Fain JN, et al. Higher production of IL-8 in visceral vs. subcutaneous adipose tissue. Implication of nonadipose cells in adipose tissue. American journal of physiology 2004; 286: E8-13.

21. Bruun JM, Lihn AS, Pedersen SB, Richelsen B. Monocyte chemoattractant protein-1 release is higher in visceral than subcutaneous human adipose tissue (AT): implication of macrophages resident in the AT. J Clin Endocrinol Metab 2005; 90: 2282-2289.

22. Gerhardt CC, Romero IA, Cancello R, Camoin L, Strosberg AD. Chemokines control fat accumulation and leptin secretion by cultured human adipocytes. Mol Cell Endocrinol 2001; 175: 81-92.

23. Cawthorn WP, Heyd F, Hegyi K, Sethi JK. Tumour necrosis factor-alpha inhibits adipogenesis via a beta-catenin/TCF4(TCF7L2)-dependent pathway. Cell death and differentiation 2007; 14: 1361-1373.

24. Weisberg SP, McCann D, Desai M, Rosenbaum M, Leibel RL, Ferrante AW, Jr. Obesity is associated with macrophage accumulation in adipose tissue. The Journal of clinical investigation 2003; 112: 1796-1808.

25. Cinti S, Mitchell G, Barbatelli G, Murano I, Ceresi E, Faloia E, et al. Adipocyte death defines macrophage localization and function in adipose tissue of obese mice and humans. J Lipid Res 2005; 46: 2347-2355.

26. Xu H, Barnes GT, Yang Q, Tan G, Yang D, Chou CJ, et al. Chronic inflammation in fat plays a crucial role in the development of obesity-related insulin resistance. The Journal of clinical investigation 2003; 112: 1821-1830.

27. Weisberg SP, Hunter D, Huber R, Lemieux J, Slaymaker S, Vaddi K, et al. CCR2 modulates inflammatory and metabolic effects of high-fat feeding. The Journal of clinical investigation 2006; 116: 115-124.

28. Kanda H, Tateya S, Tamori Y, Kotani K, Hiasa K, Kitazawa R, et al. MCP-1 contributes to macrophage infiltration into adipose tissue, insulin resistance, and hepatic steatosis in obesity. The Journal of clinical investigation 2006; 116: 1494-1505.

29. Kamei N, Tobe K, Suzuki R, Ohsugi M, Watanabe T, Kubota N, et al. Overexpression of monocyte chemoattractant protein-1 in adipose tissues causes macrophage recruitment and insulin resistance. The Journal of biological chemistry 2006; 281: 26602-26614.

30.   Arkan MC, Hevener AL, Greten FR, Maeda S, Li ZW, Long JM, et al. IKK-beta links inflammation to obesity-induced insulin resistance. Nature medicine 2005; 11: 191-198.

31.   Lumeng CN, Bodzin JL, Saltiel AR. Obesity induces a phenotypic switch in adipose tissue macrophage polarization. The Journal of clinical investigation 2007; 117: 175-184.

32.   Lumeng CN, Deyoung SM, Bodzin JL, Saltiel AR. Increased inflammatory properties of adipose tissue macrophages recruited during diet-induced obesity. Diabetes 2007; 56: 16-23.

33.   Holland WL, Brozinick JT, Wang LP, Hawkins ED, Sargent KM, Liu Y, et al. Inhibition of ceramide synthesis ameliorates glucocorticoid-, saturated-fat-, and obesity-induced insulin resistance. Cell metabolism 2007; 5: 167-179.

34.   Chavez JA, Summers SA. Characterizing the effects of saturated fatty acids on insulin signaling and ceramide and diacylglycerol accumulation in 3T3-L1 adipocytes and C2C12 myotubes. Archives of biochemistry and biophysics 2003; 419: 101-109.

35.   Kotronen A, Yki-Jarvinen H. Fatty Liver. A Novel Component of the Metabolic Syndrome. Arterioscler Thromb Vasc Biol 2007.

36.   Lehrke M, Lazar MA. The many faces of PPARgamma. Cell 2005; 123: 993-999.

37.   Guri A, Hontecillas R, Bassaganya-Riera J. Peroxisome Proliferator-Activated Receptors: Bridging Metabolic Syndrome with Molecular Nutrition. Clinical Nutrition 2006.

38.   Kelly D, Campbell JI, King TP, Grant G, Jansson EA, Coutts AG, et al. Commensal anaerobic gut bacteria attenuate inflammation by regulating nuclear-cytoplasmic shuttling of PPAR-gamma and RelA. Nat Immunol 2004; 5: 104-112.

39.   Pascual G, Fong AL, Ogawa S, Gamliel A, Li AC, Perissi V, et al. A SUMOylation-dependent pathway mediates transrepression of inflammatory response genes by PPAR-gamma. Nature 2005; 437: 759-763.

40.   Tanaka T, Fukunaga Y, Itoh H, Doi K, Yamashita J, Chun TH, et al. Therapeutic potential of thiazolidinediones in activation of peroxisome proliferator-activated receptor gamma for monocyte recruitment and endothelial regeneration. Eur J Pharmacol 2005; 508: 255-265.

41.   Babaev VR, Yancey PG, Ryzhov SV, Kon V, Breyer MD, Magnuson MA, et al. Conditional knockout of macrophage PPARgamma increases atherosclerosis in C57BL/6 and low-density lipoprotein receptor-deficient mice. Arterioscler Thromb Vasc Biol 2005; 25: 1647-1653.

CHAPTER 2: PEROXISOME PROLIFERATOR-ACTIVATED RECEPTORS: BRIDGING METABOLIC SYNDROME WITH MOLECULAR NUTRITION

INTRODUCTION

The publisher for this copyrighted material is Elsevier. By clicking "accept" in connection with completing this licensing transaction, you agree that the following terms and conditions apply to this transaction (along with the Billing and Payment terms and conditions established by Copyright Clearance Center, Inc. ("CCC"), at the time that you opened your Rightslink account and that are available at any time at http://myaccount.copyright.com).

GENERAL TERMS

Elsevier hereby grants you permission to reproduce the aforementioned material subject to the terms and conditions indicated.

Acknowledgement: If any part of the material to be used (for example, figures) has appeared in our publication with credit or acknowledgement to another source, permission must also be sought from that source. If such permission is not obtained then that material may not be included in your publication/copies. Suitable acknowledgement to the source must be made, either as a footnote or in a reference list at the end of your publication, as follows:

"Reprinted from Publication title, Vol number, Author(s), Title of article, Pages No., Copyright (Year), with permission from Elsevier [OR APPLICABLE SOCIETY COPYRIGHT OWNER]." Also Lancet special credit - "Reprinted from The Lancet, Vol. number, Author(s), Title of article, Pages No., Copyright (Year), with permission from Elsevier."

Reproduction of this material is confined to the purpose and/or media for which permission is hereby given.

Altering/Modifying Material: Not Permitted. However figures and illustrations may be altered/adapted minimally to serve your work. Any other abbreviations, additions, deletions and/or any other alterations shall be made only with prior written authorization of Elsevier Ltd. (Please contact Elsevier at permissions@elsevier.com)

If the permission fee for the requested use of our material is waived in this instance, please be advised that your future requests for Elsevier materials may attract a fee.

Reservation of Rights: Publisher reserves all rights not specifically granted in the combination of (i) the license details provided by you and accepted in the course of this licensing transaction, (ii) these terms and conditions and (iii) CCC's Billing and Payment terms and conditions.

License Contingent Upon Payment: While you may exercise the rights licensed immediately upon issuance of the license at the end of the licensing process for the transaction, provided that you have disclosed complete and accurate details of your

proposed use, no license is finally effective unless and until full payment is received from you (either by publisher or by CCC) as provided in CCC's Billing and Payment terms and conditions. If full payment is not received on a timely basis, then any license preliminarily granted shall be deemed automatically revoked and shall be void as if never granted. Further, in the event that you breach any of these terms and conditions or any of CCC's Billing and Payment terms and conditions, the license is automatically revoked and shall be void as if never granted. Use of materials as described in a revoked license, as well as any use of the materials beyond the scope of an unrevoked license, may constitute copyright infringement and publisher reserves the right to take any and all action to protect its copyright in the materials.

Warranties: Publisher makes no representations or warranties with respect to the licensed material.

Indemnity: You hereby indemnify and agree to hold harmless publisher and CCC, and their respective officers, directors, employees and agents, from and against any and all claims arising out of your use of the licensed material other than as specifically authorized pursuant to this license.

No Transfer of License: This license is personal to you and may not be sublicensed, assigned, or transferred by you to any other person without publisher's written permission.

No Amendment Except in Writing: This license may not be amended except in a writing signed by both parties (or, in the case of publisher, by CCC on publisher's behalf).

Objection to Contrary Terms: Publisher hereby objects to any terms contained in any purchase order, acknowledgment, check endorsement or other writing prepared by you, which terms are inconsistent with these terms and conditions or CCC's Billing and Payment terms and conditions. These terms and conditions, together with CCC's Billing and Payment terms and conditions (which are incorporated herein), comprise the entire agreement between you and publisher (and CCC) concerning this licensing transaction. In the event of any conflict between your obligations established by these terms and conditions and those established by CCC's Billing and Payment terms and conditions, these terms and conditions shall control.

Revocation: Elsevier or Copyright Clearance Center may deny the permissions described in this License at their sole discretion, for any reason or no reason, with a full refund payable to you. Notice of such denial will be made using the contact information provided by you. Failure to receive such notice will not alter or invalidate the denial. In no event will Elsevier or Copyright Clearance Center be responsible or liable for any costs, expenses or damage incurred by you as a result of a denial of your permission request, other than a refund of the amount(s) paid by you to Elsevier and/or Copyright Clearance Center for denied permissions.

<div align="center">LIMITED LICENSE</div>

The following terms and conditions apply to specific license types:

Translation: This permission is granted for non-exclusive world **English** rights only unless your license was granted for translation rights. If you licensed translation rights you may only translate this content into the languages you requested. A professional translator must perform all translations and reproduce the content word for word preserving the integrity of the article. If this license is to re-use 1 or 2 figures then permission is granted for non-exclusive world rights in all languages.

Website: The following terms and conditions apply to electronic reserve and author websites:
Electronic reserve: If licensed material is to be posted to website, the web site is to be password-protected and made available only to bona fide students registered on a relevant course if:
This license was made in connection with a course,
This permission is granted for 1 year only. You may obtain a license for future website posting,
All content posted to the web site must maintain the copyright information line on the bottom of each image,
A hyper-text must be included to the Homepage of the journal from which you are licensing at http://www.sciencedirect.com/science/journal/xxxxx , and
Central Storage: This license does not include permission for a scanned version of the material to be stored in a central repository such as that provided by Heron/XanEdu.

Author website with the following additional clauses: This permission is granted for 1 year only. You may obtain a license for future website posting,
All content posted to the web site must maintain the copyright information line on the bottom of each image, and
The permission granted is limited to the personal version of your paper. You are not allowed to download and post the published electronic version of your article (whether PDF or HTML, proof or final version), nor may you scan the printed edition to create an electronic version,
A hyper-text must be included to the Homepage of the journal from which you are licensing at http://www.sciencedirect.com/science/journal/xxxxx , and
Central Storage: This license does not include permission for a scanned version of the material to be stored in a central repository such as that provided by Heron/XanEdu.

Website (regular and for author): "A hyper-text must be included to the Homepage of the journal from which you are licensing at http://www.sciencedirect.com/science/journal/xxxxx."

Thesis/Dissertation: If your license is for use in a thesis/dissertation your thesis may be submitted to your institution in either print or electronic form. Should your thesis be published commercially, please reapply for permission. These requirements include permission for the Library and Archives of Canada to supply single copies, on demand, of the complete thesis and include permission for UMI to supply single copies, on demand, of

the complete thesis. Should your thesis be published commercially, please reapply for permission.

Other conditions: None

ELSEVIER

REVIEW

Peroxisome proliferator-activated receptors: Bridging metabolic syndrome with molecular nutrition

Amir J. Guri, Raquel Hontecillas, Josep Bassaganya-Riera*

Laboratory of Nutritional Immunology and Molecular Nutrition; Department of Human Nutrition, Foods and Exercise; Virginia Polytechnic Institute and State University, Blacksburg, VA 24061, USA

Summary Over recent years, obesity rates and the onset of obesity-induced chronic diseases have risen dramatically. The more we learn about the physiological and morphological changes that occur during obesity, the more it is becoming clear that obesity-related disorders can be traced back to adipocyte hypertrophy and inflammation at white adipose tissue (WAT). To combat this problem, the body has developed a regulatory system specifically designed at mediating the systemic response to obesity, utilizing free fatty acids (FFAs) and their metabolites as nutrient messengers to signal adaptations from peripheral tissues. These messages are predominantly interceded through the peroxisome proliferator-activated receptors (PPARs), a family of ligand-induced transcription factors that serve as a net of lipid sensors throughout the body. Understanding how and why nutrients, nutrient derivatives and metabolites exert their physiological effects are the key goals in the study of molecular nutrition. By learning about the mechanisms and tissue-specific effects of endogenous PPAR ligands and expanding our knowledge of the body's integrated homeostatic system, we will significantly increase our odds of designing safe and effective preventive and therapeutic interventions that keep us one step ahead of obesity-related diseases.
© 2006 Elsevier Ltd and European Society for Clinical Nutrition and Metabolism. All rights reserved.

*Corresponding author. Tel.: +1 540 231 7421; fax: +1 540 231 3916.
E-mail address: jbassaga@vt.edu (J. Bassaganya-Riera).

Contents

Introduction

At its core, obesity is an endocrine disease whose manifestations and complications result from the body's inability to handle excess energy intake. During the last few decades, as obesity rates have surged towards epidemic proportions, the incidences of all obesity-induced complications, including type 2 diabetes mellitus (T2D), coronary heart disease, hypertension, dyslipidemia, stroke, gallbladder disease, osteoarthritis and sleep apnea, have risen dramatically, attributing to 9.1% of total health care costs in the United States.[1] Metabolic syndrome has been defined by the Third Report of the National Cholesterol Education Program's Adult Treatment panel (ATP III) as patients being diagnosed with three of five conditions: abdominal obesity, elevated triglycerides, low HDL cholesterol, blood pressure (BP) equal to or greater than 130/85 mmHg, and fasting glucose equal to or greater than 110 mg/dl.[2] However, the term "metabolic syndrome" has been imprecisely defined, as separate institutions, including the World Health Organization (WHO) and American Association of Clinical Endocrinologists, have each listed separate definitions on what constitutes metabolic syndrome.[3–5] Moreover, there still exists a lack of certainty regarding the pathogenesis of metabolic syndrome, making its treatment as a "syndrome" extremely difficult and somewhat controversial.[3] Thus far, the strategy for combating metabolic syndrome has been to treat the complications as they manifest individually. For instance, obese patients who become diabetic are commonly prescribed sulfonylureas to increase insulin secretion from the pancreas, α-glucosidase inhibitors to reduce the absorption of glucose at the intestinal level, or thiazolidinediones (TZDs) to enhance systemic insulin sensitivity.[6] For hypertriglyceridemia and hypercholesterolemia, fenofibrates and statins, respectively, are often utilized.

Obesity complications arise when adipose tissue is over-capacitated, resulting in the deposition of lipids in liver, pancreas, heart, skeletal muscle, and blood vessels. To cope with this situation, the body must expand its lipid-storing capacity while also attempting to prevent hyperglycemia, the underlying cause of many obesity complications. Understanding and harnessing the built-in regulatory mechanisms the body uses to offset obesity is the key to generating novel, safer, and more effective treatments. An emerging field that may help us achieve this goal is molecular nutrition—the study of the molecular mechanisms by which nutrients maintain homeostasis and prevent chronic diseases.[7] While much of this science has been devoted to exploring how vitamins, minerals, and their combination affect biological processes, macronutrients, which include carbohydrates, proteins, and lipids, can also act through distinct molecular mechanisms. For instance, a number of studies have directly correlated the increase in

plasma free fatty acids (FFAs) and their deposition into peripheral organs with the onset of metabolic syndrome.[8] However, in addition to serving as an oxidative fuel, FFAs and their metabolites bind nutrient receptors, activating a homeostatic mechanism that allows tissues to adapt to the sudden increase in the concentrations of lipids.[9]

The peroxisome proliferator-activated receptors (PPARs), which include PPAR α, PPAR δ, and PPAR γ, are the main receptors acted upon by lipids.[9,10] PPARs are members of the nuclear receptor superfamily, which consist of 48 ligand-induced transcription factors, including the retinoid X receptor (RXR) and vitamin D receptor (VDR), that regulate many of the biochemical and physiological effects elicited by nutrients, nutraceuticals and phytochemicals.[11] Following ligand binding, PPARs heterodimerize with RXR, inducing the detachment of corepressors, recruitment of coactivators, some of which with acetylation activity, and subsequent binding to a PPAR response element (PPRE) on DNA that initiates the transcription of responsive genes (Fig. 1).[11] While present in many different organs, PPARs are heavily concentrated in key metabolic areas, including adipose tissue, skeletal muscle, liver, and pancreas and in immune cells.[9] In this review, we will discuss how metabolic syndrome develops and explore the role of endogenous PPAR ligands in shaping the systemic response to obesity.

Obesity, adipocyte hypertrophy, and the inflammatory cascade

Fifteen years ago, the only known function for white adipose tissue (WAT) was the storage of excess energy.[12] Current evidence now indicates that WAT holds much more complexity, which is exemplified by the many different types of cells this tissue encompasses and its varied biological functions beyond energy mobilization and storage. The parenchimal cells in WAT are the adipocytes. While energy storage is still recognized as a main function of adipocytes, these cells also serve as key regulators of local inflammation.[13] Adipocytes secrete a number of bioactive polypeptides, including leptin, adiponectin, and cytokines
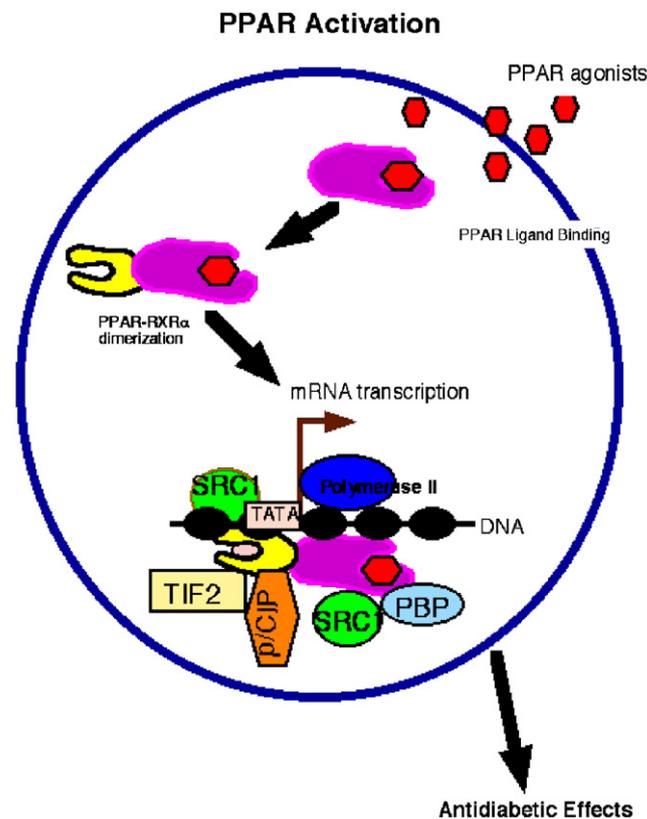
Figure 1 Activation of peroxisome proliferator-activated receptors (PPARs). After binding with an endogenous ligand, PPARs form a heterodimer with retinoid X receptor α (RXRα), initiating the detachment of corepressors and addition of coactivators. Coactivators promote histone acetylation, which aids in the unwinding DNA to grant the PPAR–RXRα heterodimer easier access to the PPAR response element, thereby inducing the transcription of genes which regulate metabolic processes.

(i.e. TNF-α, IL-6), that affect metabolic and inflammatory processes both locally and systemically.[14] Of these compounds, adiponectin is particularly interesting since it is the principal anti-inflammatory protein released by adipocytes.[15] Adiponectin acts through an AMP-activated kinase (AMPK) pathway to increase glucose disposal in muscle, inhibit hepatic glucose production, and promote the oxidation of intramuscular triglycerides (IMTG).[16–18] Adipocytes also produce chemokines, including monocyte chemoattractant protein 1 (MCP-1), macrophage inflammatory protein 1 α (MIP-1α) and interleukin 8 (IL-8), which foster leukocyte extravasation into the stromal-vascular fraction (SVF) of WAT.[19–21] The non-parenchimal cells in this region, referred to as stromal-vascular cells (SVCs), consist of endothelial cells, macrophages, pre-adipocytes, and lymphocytes.[21,22] The presence of lymphocytes in WAT was initially reported by Robker and colleagues and was also verified in our laboratory.[22] In comparison to the adipocyte fraction, SVCs secrete larger amounts of pro-inflammatory mediators, including TNF-α, IL-6, and IL1β.[19]

During the onset of obesity, adipocytes are ostensibly the primary cells affected in WAT. As more space is needed to accommodate excess energy intake, adipocytes steadily become larger. The continuous increase in adipocyte size and dysfunction are believed to be the initiating factors in the development of WAT inflammation.[23] Adipocyte hypertrophy puts a significant amount of strain on the cell, resulting in endoplasmic reticulum (ER) stress.[24] ER stress results from glucose or nutrient deprivation, increased synthesis of secretory proteins, or the presence of unfolded or misfolded proteins in the ER lumen, though its origin as it pertains to adipocyte hypertrophy is still unclear.[24] The ER stress causes the activation of a signal transduction system known as the unfolded protein response (UPR) that is designed to maintain ER homeostasis through UPR effectors and modulators connected to important signaling pathways.[24] In adipocytes, this response induces the serine/threonine kinases c-Jun N-terminal kinase (JNK) and inhibitor of nuclear factor-κB (NF-κB) kinase (IKK), thus beginning an inflammatory cascade.[13]

JNK proteins and IKK, respectively, activate activator protein 1 (AP-1) and NF-κB, transcription factors that increase the expression of TNF-α and IL-6 from adipocytes, the genes of which contain AP-1 and NF-κB binding sites in their promoter regions.[13] TNF-α stimulates serine phosphorylation of insulin receptor substrate 1 (IRS-1), which inhibits the ability of IRS-1 to act as a substrate for

the insulin receptor.[25] Subsequently, it was demonstrated that both JNK and IKK can also directly phosphorylate IRS-1.[13] The disruption of the IRS-1 signaling pathway by pro-inflammatory stimuli is at the core of insulin resistance, and dampening the inflammatory response has been shown to ameliorate insulin resistance.[26] In 1993, Hotamisligil et al.[12] were among the first to demonstrate that neutralizing the TNF-α receptor in obese mice significantly increases peripheral glucose uptake. More recent studies have also determined that disrupting JNK1 or IKK confers protection from obesity-induced insulin resistance.[27,28]

Role of WAT stromal cells in inflammation

While the effects of adipocyte-derived cytokines may play a role in the development of obesity-induced inflammation, the production of these compounds is nominal when compared to that of the SVCs.[19] As adipocytes continue to become hypertrophic during the onset of obesity, the rate of cell death is significantly increased.[23] Concomitantly, chemokine secretion from WAT becomes upregulated, fostering the extravasation of leukocytes into the SVF.[29] A considerable portion of the infiltrating cells is comprised of bone-marrow derived macrophages.[19] Though the role of macrophages in WAT has not been fully characterized, over 90% of them localize around dead adipocytes, alluding that their main function is the clearance of dead adipocytes and debris from the region.[23]

Despite this potentially reparative and beneficial function, several lines of evidence directly implicate macrophages in the pathogenesis of T2D and cardiovascular disease. First, isolation of macrophages by selecting for the surface marker F4/80 has illustrated that the vast majority of pro-inflammatory cytokine and chemokine gene expression in WAT stems directly from macrophages.[19,30] Second, the development of insulin resistance in C57BL6/J mice fed high-fat diets is immediately preceded by a surge in WAT pro-inflammatory cytokine and chemokine production.[31] Finally, inhibiting the migratory response of macrophages by knocking out the MCP-1 receptor, chemokine receptor 2 (CCR2), had profound beneficial effects on obesity-induced insulin resistance.[32] Obese CCR2 knockout mice, despite showing no differences in average adipocyte area when compared to wild type mice, exhibited less WAT macrophage infiltration, lower pro-inflammatory gene expression, and higher insulin sensitivity.[32] Treatment with a pharmacological CCR2 antagonist for 14

days also yielded insulin-sensitizing effects.[32] Interestingly, there were no differences in WAT pro-inflammatory gene expression between mice treated and untreated with the CCR2 antagonist, perhaps indicating that macrophage extravasation into other tissues may also play an important role in the development of insulin resistance.

The PPARs

Often times the question is asked as to why adipocytes increase inflammation and heighten the risk of chronic diseases. In other words, what is the biological significance of a non-productive inflammatory response in WAT? A possible explanation is that over the last few decades, we have been asking adipocytes to store more energy than ever before. Eventually, hypertrophic adipocytes will not be able to expand any larger, and they will ultimately undergo apoptosis. However, prior to cell death, the adipocyte becomes dysfunctional and irresponsive to circulating FFAs and activates pro-inflammatory pathways to lower the infusion of nutrients through the IRS-1 signaling pathway.[26] There is also a decrease in the production of adiponectin[33], possibly since adiponectin would increase glucose uptake through an alternative AMPK mechanism. Finally, the adipocyte secretes chemokines that will attract leukocytes to clean up the cell debris associated with cell death through phagocytosis.[21]

The progressive termination of nutrient absorption by hypertrophic adipocytes dramatically increases the concentrations of FFA and lipid metabolites in plasma, a rise that occurs prior to the development of insulin resistance.[8] Acting as endogenous PPAR ligands, these nutrients signal PPAR-expressing organs, including the liver, WAT, heart, pancreas, and skeletal muscle, that their oxidative, metabolic and lipid-storing capabilities are needed. Accordingly, studies have shown that adipose, liver, and skeletal muscle levels of PPAR γ expression is significantly higher in obese mice and humans than in their lean counterparts, results most likely stemming from the greater availability of endogenous ligands.[34] The presence of direct repeat (DR) 1, 2, and 4 sequences specific for PPAR γ in the PPAR γ promoter region [35] suggests that PPAR γ activation, in addition of up-regulating the expression of PPAR γ-responsive genes, induces PPAR γ expression. Essentially, PPARs may have been created by nature to regulate the systemic metabolic and inflammatory responses to obesity, and each one of these receptors is required for this task to be accomplished properly.

Endogenous and dietary PPAR ligands

One of the main effects of adipocyte hypertrophy in WAT is the increased circulation of fatty acids and their metabolites. While fatty acids have been shown to be endogenous ligands for all three PPARs, the differences in the compositions of their respective ligand binding domains PPAR make them more amenable to certain types of fatty acids than others.[9] In addition, co-crystal structure analyses on PPAR γ and its ligands suggest that the shape complementarity may be particularly important for subtype selectivity.[36] For instance, polyunsaturated fatty acids, including linoleic acid, linolenic acid, and the fish oils docosahexaenoic acid (DHA) and eicosapentaenoic acid (EPA), have all been shown to bind and activate PPAR γ and δ, though their affinity is higher for PPAR α.[9,37] Saturated and monounsaturated fatty acids, including palmitic, oleic, and arachidonic acids, also bind for PPAR α with greater affinity than either PPAR γ or δ[9,38].

Enzymatic modification, either through acylation or conversion into eicosanoids, is a key manner in which PPAR ligands are formed.[9,39] Eicosanoids, which are produced mainly from arachidonic acid via the lipoxygenase or cyclooxygenase pathways, tend to be more specific for the type of PPAR in which they bind than fatty acids. For example, the eicosanoid 8-S-hydroxyeicosatetraenoic acid (8S-HETE), among the higher affinity endogenous PPAR α ligands[40], only moderately binds PPAR γ or δ[9]. However, 9-hydroxy-octadecadienoic acid (9–HODE) and 13-HODE, which are produced from linoleic acid via the 15-lipoxygenase pathway, and 15-delta-prostaglandin J2 (15dPGJ2) tend to be more specific for PPAR γ[41,42] For PPAR δ, which contains the largest binding pocket, there are indications that VLDL-delivered fatty acids may serve as endogenous ligands.[43]

In addition to the endogenously produced ligands, there are numerous natural compounds which can significantly add to the pool of endogenous PPAR ligands. For instance, our laboratory has recently discovered that abscisic acid, a phytochemical and vitamin A derivative found in all photosynthetic organisms, significantly improves glucose tolerance and increases WAT PPAR γ expression in db/db mice fed high-fat diets without the weight-gain commonly associated with TZDs.[44] We have also previously demonstrated that dietary supplementation of conjugated linoleic acid (CLA), a fatty acid found in high amounts in beef and dairy products, provides protection from dextran sodium sulfate (DSS)-induced colitis through a PPAR γ-dependent mechanism. Because of the control endogenous PPAR ligands exert on both metabolic

20

and inflammatory processes, identifying the conditions these ligands are produced and how we can naturally increase the pool of endogenous ligands will continue to be a high priority.

White adipose tissue

Adipocyte hypertrophy

In 1995, Lehmann et al.[45] discovered that TZDs are specific ligands of PPAR γ, a finding that has led to much about what we currently know about this receptor. The initiation of all obesity-induced complications centers on the generation of hypertrophic adipocytes in WAT and the limited uptake of FFAs and triglycerides. Because of their high expression of PPAR γ, adipocytes are the first cells that can respond to subtle changes in the concentration of these circulating nutrients.

There are two prevailing theories commonly cited to explain the antidiabetic effects of PPAR γ ligands in adipocytes. In the first, insulin sensitization is due to increasing adipogenesis and the differentiation of new adipocytes. PPAR γ is recognized as a central regulator of adipogenesis.[46] Upon activation, PPAR γ upregulates the transcription of genes involved in FFA uptake and storage, including aP2, CD36, lipoprotein lipase, acyl coenzyme A synthase, and LDL R1 receptor.[11,47] PPAR γ activation also positively regulates CCAAT/enhancer binding protein α (C/EBPα), a pleiotropic transcriptional activator that is required for pre-adipocyte differentiation.[47] The smaller adipocytes that result from increased differentiation are more insulin sensitive than larger cells and, most importantly, represent a new pool that can enhance the absorption of circulating FFAs and triglycerides, thereby limiting their deposition into peripheral tissues.[48] In addition to increasing differentiation, activation PPAR γ has also been shown to increase oxygen consumption and palmitate oxidation WAT, indicating that increased lipid utilization could also contribute to a reduction in adipocyte hypertrophy.[49]

To examine the effects of PPAR γ in adipocytes, Jones et al.[50] used the Cre-lox recombination system to create conditional knockout mice which specifically lacked PPAR γ in adipocytes. These mice were generated by crossing PPAR γ-floxed mice with aP2-Cre mice, which constitutively express the Cre recombinase under control of the aP2 promoter. As the authors pointed out, since aP2 does not become fully expressed until adipocyte differentiation has already occurred, the resulting mice lack PPAR γ

only in mature adipocytes. After an 18–week period of diet-induced obesity, the investigators found that disruption of PPAR γ in adipocytes actually improves the metabolic profile and enhances systemic insulin sensitivity.[50] One conclusion we can make from these findings is that transcriptional regulation in fully differentiated adipocytes by PPAR γ ligands does not contribute significantly to their antidiabetic effects. Rather, disrupting PPAR γ with aP2-Cre most likely impaired adipocyte uptake of FFAs, making them less likely to become hypertrophic, and increased the availability of endogenous ligands to promote pre-adipocyte differentiation. Differentiating pre-adipocytes are remarkably insulin sensitive and absorb significant levels of FFAs and triglycerides in comparison to mature adipocytes.[51] Though the authors did not determine whether WAT from the tissue-specific PPAR γ null mice showed increased expression of genes involved in adipocyte differentiation, they did find that hepatic PPAR γ and CD36 were upregulated, suggesting that the increased availability of endogenous PPAR γ ligands to act upon peripheral metabolic tissues may have also contributed to the improved metabolic profile (Table 1).[50]

Recently, Tsuchida et al.[52] demonstrated that a PPAR α agonist significantly improves insulin sensitivity and glucose tolerance in obese mice. In similar regard to PPAR γ activation, PPAR α activation also attenuated adipocyte hypertrophy[52], though the mechanisms behind these analogous effects differed significantly. As opposed to increasing the differentiation of new adipocytes, PPAR α activation reduced adipocyte hypertrophy by increasing triglyceride uptake and oxidation. In line with this reasoning, expression of β3-andrenergic receptor (β3AR), a protein expressed in WAT and brown adipose tissue (BAT) that plays an important role in lipolysis and thermogenesis, was significantly elevated following PPAR α activation.[52] Increased fatty acid oxidation in other tissues, such as the liver and skeletal muscle, could also have contributed to this effect.[52]

Similar to PPAR γ and PPAR α, there is reason to believe that endogenous PPAR δ ligands also attenuate adipocyte hypertrophy, as transgenic mice with virally-induced, constitutively active PPAR δ in adipocytes are protected from its development.[53] The constant activation of PPAR δ in adipocytes significantly increased the expression of genes involved in fatty acid oxidation (i.e. acyl-CoA oxidase, long-chain acyl-CoA synthase) in brown adipocytes while white adipocytes showed increased expression of uncoupling protein 1 (UCP-1).[53] Considering the different mechanisms by

Table 1 Tissue-specific effects of PPAR activation.

	PPAR α	PPAR γ	PPAR δ	Reference
White adipose tissue				
Adipocyte hypertrophy	−	−	−	52,53
FA oxidation	+	+/−	+	49,52,53
Macrophage infiltration	−	−		31,44,52
Liver				
Hepatic glucose production	+	−	−	70,73,74
Skeletal muscle				
FA oxidation	+	−	+	83,87,88,89
Pancreas				
Lipotoxicity and glucose-stimulated insulin secretion	+/−	+/−		72,95,97,98
Blood vessels				
Reverse cholesterol transport	+	+	+/−	106,107,108,109
Vascular inflammation	−	−	−	110,111

which the PPARs act upon, the findings that each of them improves systemic insulin sensitivity and attenuates adipocyte hypertrophy are among the few phenotypical characteristics that these receptors have in common.

Adipokines

The second theory concerning the antidiabetic effects of PPAR γ activation in adipocytes involves differentially modulating the production of adiponectin and inflammatory mediators. PPAR γ activation increases the production of the anti-inflammatory adiponectin and decreases the production of IL-6, TNF-α, plasminogen activator inhibitor 1 (PAI-1), and other pro-inflammatory molecules released from adipocytes.[54] Interestingly, the upregulation of pro-inflammatory adipokine expression occurs when adipocytes become hypertrophic, raising the question as to whether the anti-inflammatory effects of PPAR γ activation in adipocytes are an indirect result of increasing adipocyte differentiation and attenuating adipocyte hypertrophy as opposed to direct transcriptional regulation. As we have seen, PPAR α activation also prevents adipocytes from becoming hypertrophic; however, Tsuchida et al.[52] observed no effect on serum adiponectin levels following treatment with a PPAR α agonist.[52] Instead, PPAR α activation significantly upregulated WAT expression of the adiponectin receptors, AdipoR1 and AdipoR2. In addition, the presence of a PPAR γ DR1 sequence in the PPAR α promoter region[35] represent two findings that exemplify that PPAR γ and PPAR α act in concert to regulate metabolic processes.[52]

WAT inflammation and macrophage activation

Other possible contributors to the antidiabetic effects of endogenous PPAR ligands in WAT are the SVCs. Recent studies have demonstrated that ligands for PPAR γ and PPAR α inhibit macrophage infiltration and chemokine production in WAT of obese mice.[19,29,52] While a some of these effects may be secondary to a reduction of adipocyte hypertrophy, the key role that macrophages play in the progression of WAT inflammation along with their high expression of PPARs makes them prime targets for endogenous PPAR ligands.

Following their extravasation into WAT, bone marrow-derived monocytes differentiate into macrophages, a process that greatly increases their size, phagocytic ability, and proteolytic enzyme activity.[55] They can then take on one of two distinct phenotypes. In the first phenotype (M1), macrophages secrete significant amounts of pro-inflammatory cytokines (i.e. TNF-α and IL-6), chemokines (i.e. MCP-1, IL-8), and reactive oxygen species (ROS).[21] In contrast, if macrophages are alternatively activated (M2)[21], they will develop into a reparative phenotype characterized by the secretion of high amounts of the anti-inflammatory cytokines IL-10 and transforming growth factor β (TGF-β).[21] Because of the significant functional differences between these two phenotypes, the ratio of alternatively activated to classically activated macrophages may have a significant impact on development of inflammation in WAT. In obese patients, the majority of macrophages isolated from WAT are classically activated[21], though Cancello et al.[56] recently demonstrated that weight loss induced by gastric bypass surgery

significantly increases the percentage of IL-10–expressing macrophages after 3 months. While the reason behind the induction of classically activated macrophages in WAT from obese individuals has not been fully elucidated, hypoxia occurring as a result of adipocyte hypertrophy may be involved. Studies have shown that human monocytes exposed to hypoxic conditions (3% oxygen) secrete significantly more TNF-α than under normoxic conditions.[57] Whatever the cause may be, it appears likely that increased WAT inflammation is a negative byproduct associated with the macrophage infiltration and adipocyte hypertrophy rather than an essential contributor to WAT homeostasis. Accordingly, the body has developed countermeasures to downregulate macrophage activation and obesity-related inflammation, with PPARs acting as principal effectors.

Both PPAR γ and PPAR δ are induced early during differentiation of human macrophages.[58] Ligand activation of PPAR γ and PPAR δ induces the expressions of the CD36 and adipose differentiation-related protein (ADRP), respectively[58], enhancing the lipid-loading capabilities of macrophages. To address the effects of PPAR γ activation on macrophage inflammatory gene expression, Chawla et al.[59] treated wild type and PPAR γ-deficient macrophages with TZDs and the endogenous PPAR γ ligands 15d-PGJ2 following stimulation with lipopolysaccharide (LPS). Though pro-inflammatory cytokines secretion was inhibited, the mechanism was independent of PPAR γ. These findings in macrophages differ from those obtained in other cell types, including a recent study which demonstrated that in the colonic mucosa, PPAR γ binds the active p65 (RelA) subunit of NF-κB and exports it from the nucleus after ligand binding, thus decreasing P65-induced inflammation.[60]

In 2003, Welch et al.[61] determined that a significant portion of the PPAR γ-independent effects in macrophages can in fact be attributed to PPAR δ. Another possible explanation is that TZDs and endogenous PPAR γ ligands can also act upon toll-like receptors (TLRs) in WAT macrophages. Studies have shown that saturated and polyunsaturated fatty acids exert differential effects on TLR activation.[62] As opposed to the pro-inflammatory effects of saturated fatty acids, polyunsaturated and oxidized fatty acids, which are the more common PPAR ligands, antagonize LPS-induced TLR4 activation and NF-κB activation.[62] In particular docosahexanoic acid (DHA), an n-3 polyunsaturated fatty acid, inhibited NF-κB activation and cyclooxygenase 2 (COX-2) expression induced by different TLR ligands, including lipopetides (TLR2), double-stranded RNA (TLR3), LPS (TLR4), and CpG (TLR9), and was even able to block pro-inflammatory gene expression in macrophages that constitutively expressed TLR4.[63] In support of the argument that some endogenous PPAR ligands inhibit TLR4, Eun and colleagues found that treatment with 15d-PGJ2 significantly reduces LPS-induced stimulation of TLR4 and decreases TLR4 mRNA and protein expression in the colonic epithelium.[64] More research, however, will be needed to confirm whether endogenous PPAR ligands act to antagonize macrophage TLR activity in vivo during the development of obesity-induced inflammation.

Liver

Oxidation and hepatic glucose production

While inflammation in WAT represents one of the key initiating factors in the development of obesity-induced insulin resistance, the contribution made by the liver in regulating systemic glucose homeostasis during the onset of obesity far exceeds that of WAT. The liver upregulates or downregulates the metabolism and storage of glucose and fatty acids based on messages provided by circulating hormones (i.e. insulin, glucagon, glucocorticoids) and nutrients (i.e. fatty acids, cholesterol, vitamins, lipid metabolites). With obesity, the greater availability of fatty acids as a metabolic substrate provides the gluconeogenesis pathway with glycerol, reducing equivalents, and ATP that all act to increase hepatic glucose production.[65] PPARs, and PPAR α in particular, serve as important lipid sensors in hepatocytes.[65] As adipose stores become overcapacitated and the availability of endogenous PPAR ligands progressively rises with obesity, the ultimate objective of the liver is to increase fatty acid oxidation without enhancing hepatic glucose production.

In hepatocytes, PPAR α activation upregulates the expression of carnitine palmitoyl transferase 1 (CPT-1)[66], a protein involved in the transport of fatty acids into the mitochondria, and other enzymes involved in β-oxidation, including acyl-CoA synthetase, very-long- and medium-chain acyl-CoA dehydrogenases, and 3-ketoacyl-CoA thiolase.[67] The benefits of PPAR α activation in increasing fatty acid oxidation and triglyceride catabolism reduces the production of very low-density lipoproteins (VLDLs), indirectly reducing small dense LDL numbers and enhancing HDL formation.[68,69] However, PPAR α also increases hepatic glucose production by inducing gluconeogenic enzymes, including glycerol-3-phosphate dehydrogenase

(GPDH), glycerol-3-kinase, and the hepatic glycerol transporters aquaporin 3 and aquaporin 9.[70] The importance of PPAR α in promoting hepatic glucose production is illustrated in PPAR α deficient mice, which become severely hypoglycemic after only 24 h of fasting.[71] Despite promoting hepatic glucose production, treatment with PPAR α activation has been shown to lower fasting glucose blood glucose levels and insulin levels.[52] One explanation for these antidiabetic effects is increased energy expenditure, as PPAR α activation increases hepatic uncoupling protein 2 (UCP2) expression and BAT UCP1 expression.[52] Also, a recent study has demonstrated that PPAR α activation potentiates glucose-induced insulin secretion in the pancreatic β-cells[72], thus improving cellular uptake of the glucose produced in hepatocytes.

During the onset of obesity, the increase in hepatic glucose production by PPAR α activation can be simultaneously mitigated by PPAR γ activation, which directly reduces the transcription of phosphoenolpyruvate carboxykinase (PEPCK).[73,74] The inhibition in hepatic glucose production is potentiated by increased oxidation in skeletal muscle by inhibition of pyruvate dehydrogenase kinase 4 (PDK4) and PDK2.[75] While the exact role PPAR γ plays in hepatocytes is not completely understood, a number of studies have confirmed that liver activation of PPAR γ improves hepatic insulin sensitivity despite increasing liver triglyceride accumulation in leptin deficient ob/ob mice.[76,77] Interestingly, in wild type mice fed high fat diets the effects are reversed, and PPAR γ activation reduces triglyceride content.[77] These findings imply that adipocyte-derived leptin may also play a role in regulating the liver triglyceride content.

Skeletal muscle

Glucose and fatty acid oxidation

Skeletal muscle makes up 38.4% total body mass in males and 30.6% in females[78], and accounts for 80% of insulin-stimulated glucose disposal in the body.[79] Despite this fact the contribution of this tissue to the antidiabetic effects of PPAR γ activation does not appear to be significant.[80] The concentration of PPAR γ mRNA in skeletal muscle is only 5% the amount in WAT[81], making this tissue far less sensitive than WAT to the increase in circulating and/or local endogenous PPAR γ ligands that occur with obesity. In skeletal muscle PPAR α and PPAR δ increase the oxidation of fatty acids.[79,82] However,

Norris et al.[80] found that mice deficient in muscle PPAR γ have increased adiposity and are more insulin resistant that controls despite lowered food intake, suggesting that it too may share in this role.[80] Insulin-stimulated glucose disposal in skeletal muscle is not significantly affected by the loss of PPAR γ. Rather, the systemic insulin resistance observed in muscle-specific PPAR γ null mice developed as a result of impaired hepatic insulin action, and treatment of muscle-specific PPAR γ knockouts and control mice with rosiglitazone was equally effective in improving systemic insulin sensitivity.[80] We suspect that the hepatic insulin resistance in the muscle-specific PPAR γ knockout mice stems from the importance of PPAR γ in enhancing glucose oxidation.[83] In contrast to PPAR α and PPAR δ, PPAR γ activation increases PDK2 and PDK4 expression in muscle, promoting the use of glucose as an energy source as opposed to fatty acids.[83] In the liver, PPAR γ acts to inhibit the increase in hepatic glucose production that results from the increased oxidation of fatty acids.[83] Without PPAR γ in the muscle to simultaneously increase glucose oxidation, the liver may have found itself overworked, resulting in its insulin resistance. Treatment with the synthetic ligands, however, seemed to be all that was necessary to better enable to liver to cope with this problem. The importance of PPAR γ in promoting glucose oxidation in muscle is further supported by the increased adiposities of the muscle-specific knockouts, as glucose that does not become oxidized readily undergoes de novo lipogenesis in rodents.[84,85]

While the contribution of myocyte PPAR γ to the antidiabetic effects of endogenous PPAR ligands is still uncertain, PPAR δ and PPAR α are expressed at levels 50 and 10 times greater than PPAR γ in myocytes[79], and therefore, most likely hold more physiological relevance to the effects of common endogenous ligands than PPAR γ. One commonly cited effect of PPAR δ activation in skeletal muscle is a shifting of muscle fibers from glycolytic fast-twitch muscles (type II) to oxidative slow-twitch muscles (type I), which preferentially express enzymes that oxidize fatty acids as opposed to glucose.[79,86] By increasing lipid oxidation and fatty acid disposal into myocytes[87,88], the metabolic reshuffling of skeletal muscle fibers by PPAR δ ligands indirectly prevent adipocyte hypertrophy in WAT.

Similar to PPAR δ, PPAR α activation also appears to promote fatty acid utilization in skeletal muscle though the contribution of this tissue to the antidiabetic effects of PPAR α ligands have been called into question. Finck et al.[89] recently

demonstrated that transgenic mice overexpressing PPAR α in skeletal muscle are glucose intolerant despite their protection from high-fat diet-induced obesity. While one cannot conclude that PPAR α is pro-diabetic based on this transgenic study, this finding does raise concerns about synthetic PPAR α agonists, which can produce very high levels of activation.

Intermuscular adipocyte morphology

Though the majority of cells in skeletal muscle are myocytes, endogenous PPAR ligands may still be acting on other cells residing in and around skeletal muscle. The deposition of FFAs and triglycerides in skeletal muscle and the subsequent formation of intramuscular triglycerides IMTGs is a hallmark of obesity-induced insulin resistance.[90] However, since IMTG accumulation occurs in insulin sensitive endurance athletes at levels comparable to that of T2D patients[90], the increase IMTGs in both groups is most likely a result of increased circulation of FFAs during obesity and endurance exercise. Instead of examining the intramuscular lipid droplets, we may instead want to shift our attention nearby to the adipose tissue dispersed between muscle fibers, referred to as intermuscular adipose tissue (IMAT) or infiltrating adipose tissue. IMAT accumulation is significantly associated with insulin resistance.[91] A recent study also revealed that African-Americans, a group highly susceptible to insulin resistance, have a greater amount of IMAT than either Caucasians or Asians.[92] Currently, very little is known about this adipose depot, but given what we know about the effects of adipose hypertrophy on macrophage infiltration and local inflammation and the importance of muscle for insulin-stimulated glucose disposal, we suspect that hypertrophic adipocytes in IMAT may be one of the more significant events leading to skeletal muscle inflammation and insulin resistance. In support of this assertion, comparative analysis of skeletal muscle from lean and obese mice revealed that macrophages do infiltrate IMAT and to a much greater degree in the obese mice[19], a finding that substantiates earlier works showing that TNF-α expression is significantly elevated in skeletal muscle of obese mice and humans.[93] Thus, while the anti-diabetic effects of endogenous PPAR γ ligands may not be dependent on skeletal muscle PPAR γ, the effects of these compounds on the progression of IMAT hypertrophy and the infiltration skeletal muscle macrophages warrant significantly more attention.

Pancreas

Lipotoxicity

It is well established that acute FFA exposure potentiates glucose-stimulated insulin secretion in pancreatic β-cells[72,94], an effect that is almost certainly mediated by the PPARs. However, such is the case in every other tissue, long-term exposure to fatty acids negatively affects tissue function and induces lipotoxicity, a condition characterized by increased basal insulin secretion and reduced glucose-stimulated insulin secretion.[72] Pancreatic β-cells express all three members of the PPAR family and, similar to other metabolic sites, most of our knowledge concerns the roles of PPAR γ and PPAR α· However, findings concerning the functions of these receptors have been inconsistent at best.

A number of recent studies have challenged the beneficial role PPAR α exerts on the pancreas in part due to its promotion of UCP2.[95] Lipotoxicity and β-cell glucose insensitivity are associated with UCP2 induction, the formation of ROS, and reduced hyperpolarization of the mitochondial membrane.[72,96] Ectopic expression PPAR α and treatment with a PPAR α agonist in insulinoma cells significantly reduced glucose-stimulated insulin secretion and led to β-cell dysfunction.[95] However, when PPAR α was overexpressed with RXR α, fatty acid oxidation and glucose-stimulated insulin secretion were significantly enhanced, suggesting that endogenous RXR α levels were insufficient in the previous experiment.[72] While UCP2 levels were elevated in response to PPAR α overexpression, the levels were too low to dissipate the mitochondrial proton gradient.

Similar to PPAR α, information regarding the role of pancreatic PPAR γ is ambiguous. While some studies have shown that ectopic PPAR γ increases fatty acid disposal and prevents lipotoxicity in β-cells[97], other studies suggest that PPAR γ enhances lipogenesis and represses glucose-stimulated insulin secretion.[72] As opposed to the negative effects found in β-cell lines, Yajima et al.[98] found that PPAR γ activation preserves GLUT2 expression and significantly ameliorates glucose-stimulated insulin disposal and insulin content in the pancreas of db/db mice. Dual treatment PPAR γ and PPAR α activation was even more effective.[98] Despite all of the inconsistent in vitro findings concerning the role of pancreatic PPAR α and PPAR γ, we must remember that, to date, there have been no in vivo findings suggesting that either of these receptors is anything but beneficial to pancreatic function.

Blood vessels

Lipoprotein metabolism

Artery walls in obese patients are repleted with low-density lipoproteins (LDLs), which are unable to deposit their cargo into the insulin resistant, hypertrophic adipocytes.[99] In the blood vessels, lipids in LDLs are highly susceptible to oxidation by numerous pro-oxidants, including 12/15 lipooxygenase[100] and superoxide.[101] The oxidized LDL activates endothelial cells and increases smooth muscle proliferation, leading to the development of the atherosclerotic plaque.[102] There is also a recruitment of macrophages and lymphocytes by the oxidized LDLs and endothelial cells.[102] The role of the macrophage in this environment is to uptake the lipid and cholesterol from oxidized LDLs, which is accomplished by scavenger receptors CD36, CD68, and scavenger receptor A (SR-A).[77] However, similar to what occurs in insulin resistance, these macrophages become classically activated and appear to have a proatherogenic effect, as inhibiting their transmigration using mice deficient in MCP-1 or CCR2 prevents the development of the atherosclerotic plaque.[103,104] Studies have shown that inhibiting the uptake of oxidized LDLs by macrophages and the subsequent production of foam cells by knocking out CD36 decreases the progression of atherosclerosis.[105] One of the main actions of PPAR γ activation in macrophages is the upregulation of CD36, suggesting that their ligands would exert a proatherogenic effect.[77] However, CD36 upregulation in macrophages is coupled with PPAR γ and PPAR α-induced transcriptional activation of liver X receptor α (LXR α), a nuclear receptor that increases reverse cholesterol transport through promotion of the ATP-binding cassette transporters ABCA-1 and ABCG-1 along with other genes involved in this process.[77,106,107] Thus, while PPAR α and γ act to increase the uptake of the oxidized LDLs by macrophages, they simultaneously promote cholesterol efflux onto high-density lipoproteins (HDLs) to inhibit foam cell production.[77] Findings concerning the contribution of PPAR δ in macrophage cholesterol efflux have been inconsistent thus far, and while there is some reason to believe that PPAR δ activation may play a role in increasing levels of ABCA-1[108], its involvement does not appear to be critical.[109]

Inhibition of vascular inflammation

All three PPARs also exert an anti-inflammatory effect in the atherosclerotic lesion, as several genes involved in inflammation and macrophage infiltration, including MCP-1, interferon γ (IFN-γ), TNF-α, IL-1β, vascular adhesion molecule-1 (VCAM-1), and intracellular adhesion molecule-1 (ICAM-1), are significantly downregulated after treatment with their respective synthetic ligands.[110] The decrease in pro-inflammatory cytokine expression in the atherosclerotic lesion signified that macrophage infiltration or macrophage function was altered following treatment. In the vascularature, PPAR ligands inhibit macrophage infiltration by inhibiting endothelial cell activation.[111] Endothelial cells are activated through stimulation by pro-inflammatory cytokines, oxidative stress, or high glucose levels.[102,112] Once activated, endothelial cells upregulate adhesion molecule expression and chemokine secretion, greatly contributing to leukocyte infiltration.[102] Ligands for both PPAR α and PPAR γ inhibit endothelial cell activation, a key step in the development of atherosclerotic plaque.[111,112] Studies have shown that omega-3 fatty acids inhibit NF-κB activation in endothelial cells in a PPAR α-dependent manner.[113] PPAR γ ligands, in addition to directly inhibiting TNF-α-induced endothelial cell activation[114], also increase plasma adiponectin, which inhibits NF-κB activation.[115] In addition to inhibiting endothelial cell activation, PPAR γ ligands downregulate the chemotactic response of THP-1 macrophages by repressing CCR2 expression.[116] In support of this finding, mice with macrophage-specific deletion of PPAR γ show a significantly increased presence of macrophages in atherosclerotic lesions.[117] Thus, both endogenous and dietary ligands of PPAR γ are likely to play an important role as protective/therapeutic vasoactive agents in patients with CVD.

Concluding remarks and future directions

Throughout this review, we have seen how PPARs regulate glucose homeostasis, lipid metabolism, and inflammation by responding to the flux of circulating nutrients. It is fitting that nature has selected lipids and their metabolites, whose fasting levels are dependent on the storing capacity of adipose tissue, to be the endogenous ligands and, therefore, key metabolic regulators. While obesity causes a rise in endogenous ligands, resulting in increased adipocyte differentiation and fatty acid oxidation, FFA and lipids are promptly stored in WAT under lean conditions, thereby decreasing systemic expression of PPARs. Ultimately understanding how the body utilizes all three PPARs to

regulate overall metabolic homeostasis will enable us to develop more effective therapies and preventative options to obesity, T2D, CVD and metabolic syndrome. However, the many side effects and risks associated with pharmaceutical usage require us to identify natural PPAR ligands such as ABA, which could be incorporated into our daily diets or taken as dietary supplements. In addition to discovering natural PPAR ligands, there is significant potential for combinational approaches in which dual or pan-PPAR ligands are provided in doses similar to that of physiological levels. Though the knowledge we obtain from molecular nutrition analysis and the tissue-specific functions of PPARs is unlikely to significantly impede obesity rates, it will someday allow us to keep ahead of the development of inflammation and the onset of metabolic syndrome.

References

1. Finkelstein EA, Fiebelkorn IC, Wang G. National medical spending attributable to overweight and obesity: how much, and who's paying? *Health Aff (Millwood) Suppl. Web Exclusives* 2003; W3-219–226.
2. Executive Summary of The Third Report of The National Cholesterol Education Program (NCEP) Expert Panel on Detection. Evaluation, and treatment of high blood cholesterol in adults (adult treatment panel III). *JAMA* 2001;**285**:2486–97.
3. Kahn R, Buse J, Ferrannini E, Stern M. The metabolic syndrome: time for a critical appraisal: joint statement from the american diabetes association and the european association for the study of diabetes. *Diabetes Care* 2005;**28**:2289–304.
4. Alberti KG, Zimmet PZ. Definition, diagnosis and classification of diabetes mellitus and its complications. Part 1: diagnosis and classification of diabetes mellitus provisional report of a WHO consultation. *Diabet Med* 1998;**15**:539–53.
5. Eckel RH, Grundy SM, Zimmet PZ. The metabolic syndrome. *Lancet* 2005;**365**:1415–28.
6. CDC: National diabetes fact sheet: general information and national estimates on diabetes in the United States. US Department of Health and Human Services, Center for Disease Control and Prevention, Atlanta, Georgia, 2005. p. 1–10.
7. Zempleni J. *Molecular nutrition*. Lincoln, Nebraska: CABI Publishing; 2003.
8. Kovacs P, Stumvoll M. Fatty acids and insulin resistance in muscle and liver. *Best Pract Res Clin Endocrinol Metab* 2005;**19**:625–35.
9. Desvergne B, Wahli W. Peroxisome proliferator-activated receptors: nuclear control of metabolism. *Endocr Rev* 1999;**20**:649–88.
10. Kliewer SA, Sundseth SS, Jones SA, et al. Fatty acids and eicosanoids regulate gene expression through direct interactions with peroxisome proliferator-activated receptors alpha and gamma. *Proc Natl Acad Sci USA* 1997;**94**:4318–23.
11. Lehrke M, Lazar MA. The many faces of PPARgamma. *Cell* 2005;**123**:993–9.
12. Hotamisligil GS, Shargill NS, Spiegelman BM. Adipose expression of tumor necrosis factor-alpha: direct role in obesity-linked insulin resistance. *Science* 1993;**259**:87–91.
13. Wellen KE, Hotamisligil GS. Inflammation, stress, and diabetes. *J Clin Invest* 2005;**115**:1111–9.
14. Trayhurn P, Wood IS. Adipokines: inflammation and the pleiotropic role of white adipose tissue. *Br J Nutr* 2004;**92**:347–55.
15. Ouchi N, Kihara S, Arita Y, et al. Adiponectin, an adipocyte-derived plasma protein, inhibits endothelial NF-kappaB signaling through a cAMP-dependent pathway. *Circulation* 2000;**102**:1296–301.
16. Berg AH, Combs TP, Du X, Brownlee M, Scherer PE. The adipocyte-secreted protein Acrp30 enhances hepatic insulin action. *Nat Med* 2001;**7**:947–53.
17. Fruebis J, Tsao TS, Javorschi S, et al. Proteolytic cleavage product of 30-kDa adipocyte complement-related protein increases fatty acid oxidation in muscle and causes weight loss in mice. *Proc Natl Acad Sci USA* 2001;**98**:2005–10.
18. Yamauchi T, Kamon J, Minokoshi Y, et al. Adiponectin stimulates glucose utilization and fatty-acid oxidation by activating AMP-activated protein kinase. *Nat Med* 2002;**8**:1288–95.
19. Weisberg SP, McCann D, Desai M, Rosenbaum M, Leibel RL, Ferrante Jr AW. Obesity is associated with macrophage accumulation in adipose tissue. *J Clin Invest* 2003;**112**:1796–808.
20. Bruun JM, Pedersen SB, Richelsen B. Interleukin-8 production in human adipose tissue. Inhibitory effects of anti-diabetic compounds, the thiazolidinedione ciglitazone and the biguanide metformin. *Horm Metab Res* 2000;**32**:537–41.
21. Bouloumie A, Curat CA, Sengenes C, Lolmede K, Miranville A, Busse R. Role of macrophage tissue infiltration in metabolic diseases. *Curr Opin Clin Nutr Metab Care* 2005;**8**:347–54.
22. Robker RL, Collins RG, Beaudet AL, Mersmann HJ, Smith CW. Leukocyte migration in adipose tissue of mice null for ICAM-1 and Mac-1 adhesion receptors. *Obes Res* 2004;**12**:936–40.
23. Cinti S, Mitchell G, Barbatelli G, et al. Adipocyte death defines macrophage localization and function in adipose tissue of obese mice and humans. *J Lipid Res* 2005;**46**:2347–55.
24. Ozcan U, Cao Q, Yilmaz E, et al. Endoplasmic reticulum stress links obesity, insulin action, and type 2 diabetes. *Science* 2004;**306**:457–61.
25. Gao Z, Hwang D, Bataille F, et al. Serine phosphorylation of insulin receptor substrate 1 by inhibitor kappa B kinase complex. *J Biol Chem* 2002;**277**:48115–21.
26. Hotamisligil GS. Inflammatory pathways and insulin action. *Int J Obes Relat Metab Disord* 2003;**27**(Suppl. 3):S53–5.
27. Hirosumi J, Tuncman G, Chang L, et al. A central role for JNK in obesity and insulin resistance. *Nature* 2002;**420**:333–6.
28. Yuan M, Konstantopoulos N, Lee J, et al. Reversal of obesity- and diet-induced insulin resistance with salicylates or targeted disruption of Ikkbeta. *Science* 2001;**293**:1673–7.
29. Xu A, Wang Y, Keshaw H, Xu LY, Lam KS, Cooper GJ. The fat-derived hormone adiponectin alleviates alcoholic and nonalcoholic fatty liver diseases in mice. *J Clin Invest* 2003;**112**:91–100.
30. Curat CA, Wegner V, Sengenes C, et al. Macrophages in human visceral adipose tissue: increased accumulation in

obesity and a source of resistin and visfatin. *Diabetologia* 2006;**49**:744–7.

31. Xu H, Barnes GT, Yang Q, et al. Chronic inflammation in fat plays a crucial role in the development of obesity-related insulin resistance. *J Clin Invest* 2003;**112**:1821–30.

32. Weisberg SP, Hunter D, Huber R, et al. CCR2 modulates inflammatory and metabolic effects of high-fat feeding. *J Clin Invest* 2006;**116**:115–24.

33. Kadowaki T, Hara K, Yamauchi T, Terauchi Y, Tobe K, Nagai R. Molecular mechanism of insulin resistance and obesity. *Exp Biol Med (Maywood)* 2003;**228**:1111–7.

34. Kruszynska YT, Mukherjee R, Jow L, Dana S, Paterniti JR, Olefsky JM. Skeletal muscle peroxisome proliferator-activated receptor-gamma expression in obesity and non-insulin-dependent diabetes mellitus. *J Clin Invest* 1998;**101**:543–8.

35. Selvaraj RK, Klasing KC. Lutein and eicosapentaenoic acid interact to modify iNOS mRNA levels through the PPAR-gamma/RXR pathway in chickens and HD11 cell lines. *J Nutr* 2006;**136**:1610–6.

36. Epple R, Azimioara M, Russo R, et al. 1,3,5-Trisubstituted aryls as highly selective PPARdelta agonists. *Bioorg Med Chem Lett* 2006;**16**:2969–73.

37. Willson TM, Wahli W. Peroxisome proliferator-activated receptor agonists. *Curr Opin Chem Biol* 1997;**1**:235–41.

38. Banner CD, Gottlicher M, Widmark E, Sjovall J, Rafter JJ, Gustafsson JA. A systematic analytical chemistry/cell assay approach to isolate activators of orphan nuclear receptors from biological extracts: characterization of peroxisome proliferator-activated receptor activators in plasma. *J Lipid Res* 1993;**34**:1583–91.

39. Hostetler HA, Kier AB, Schroeder F. Very-long-chain and branched-chain fatty acyl-CoAs are high affinity ligands for the peroxisome proliferator-activated receptor alpha (PPARalpha). *Biochemistry* 2006;**45**:7669–81.

40. Forman BM, Chen J, Evans RM. Hypolipidemic drugs, polyunsaturated fatty acids, and eicosanoids are ligands for peroxisome proliferator-activated receptors alpha and delta. *Proc Natl Acad Sci USA* 1997;**94**:4312–7.

41. Nagy L, Tontonoz P, Alvarez JG, Chen H, Evans RM. Oxidized LDL regulates macrophage gene expression through ligand activation of PPARgamma. *Cell* 1998;**93**:229–40.

42. Forman BM, Tontonoz P, Chen J, Brun RP, Spiegelman BM, Evans RM. 15-Deoxy-delta 12,14-prostaglandin J2 is a ligand for the adipocyte determination factor PPARgamma. *Cell* 1995;**83**:803–12.

43. Chawla A, Lee CH, Barak Y, et al. PPARdelta is a very low-density lipoprotein sensor in macrophages. *Proc Natl Acad Sci USA* 2003;**100**:1268–73.

44. Guri A, Hontecillas R, Si H, Lui D, Bassaganya-Riera J. Dietary abscisic acid ameliorates glucose tolerance and obesity-related inflammation in db/db mice fed high fat diets. *Clin Nutr* 2006; in press, doi:10.1016/j.clnu.2006.07.008.

45. Lehmann JM, Moore LB, Smith-Oliver TA, Wilkison WO, Willson TM, Kliewer SA. An antidiabetic thiazolidinedione is a high affinity ligand for peroxisome proliferator-activated receptor gamma (PPARgamma). *J Biol Chem* 1995;**270**:12953–6.

46. Ren D, Collingwood TN, Rebar EJ, Wolffe AP, Camp HS. PPARgamma knockdown by engineered transcription factors: exogenous PPARgamma2 but not PPARgamma1 reactivates adipogenesis. *Genes Dev* 2002;**16**:27–32.

47. Otto TC, Lane MD. Adipose development: from stem cell to adipocyte. *Crit Rev Biochem Mol Biol* 2005;**40**:229–42.

48. Bassaganya-Riera J, Guri A, King J, Hontecillas R. Peroxisome proliferator-activated receptors: the nutritionally controlled molecular networks that integrate inflammation, immunity and metabolism. *Curr Nutr Food Sci* 2005;**1**:179–87.

49. Wilson-Fritch L, Nicoloro S, Chouinard M, et al. Mitochondrial remodeling in adipose tissue associated with obesity and treatment with rosiglitazone. *J Clin Invest* 2004;**114**:1281–9.

50. Jones JR, Barrick C, Kim KA, et al. Deletion of PPARgamma in adipose tissues of mice protects against high fat diet-induced obesity and insulin resistance. *Proc Natl Acad Sci USA* 2005;**102**:6207–12.

51. Reed BC, Lane MD. Insulin receptor synthesis and turnover in differentiating 3T3-L1 preadipocytes. *Proc Natl Acad Sci USA* 1980;**77**:285–9.

52. Tsuchida A, Yamauchi T, Takekawa S, et al. Peroxisome proliferator-activated receptor (PPAR)alpha activation increases adiponectin receptors and reduces obesity-related inflammation in adipose tissue: comparison of activation of PPARalpha, PPARgamma, and their combination. *Diabetes* 2005;**54**:3358–70.

53. Wang YX, Lee CH, Tiep S, et al. Peroxisome-proliferator-activated receptor delta activates fat metabolism to prevent obesity. *Cell* 2003;**113**:159–70.

54. Hammarstedt A, Andersson CX, Rotter Sopasakis V, Smith U. The effect of PPARgamma ligands on the adipose tissue in insulin resistance. *Prostaglandins Leukot Essent Fatty Acids* 2005;**73**:65–75.

55. Holevinsky KO, Nelson DJ. Simultaneous detection of free radical release and membrane current during phagocytosis. *J Biol Chem* 1995;**270**:8328–36.

56. Cancello R, Henegar C, Viguerie N, et al. Reduction of macrophage infiltration and chemoattractant gene expression changes in white adipose tissue of morbidly obese subjects after surgery-induced weight loss. *Diabetes* 2005;**54**:2277–86.

57. Guida E, Stewart A. Influence of hypoxia and glucose deprivation on tumour necrosis factor-alpha and granulocyte-macrophage colony-stimulating factor expression in human cultured monocytes. *Cell Physiol Biochem* 1998;**8**:75–88.

58. Castrillo A, Tontonoz P. Nuclear receptors in macrophage biology: at the crossroads of lipid metabolism and inflammation. *Annu Rev Cell Dev Biol* 2004;**20**:455–80.

59. Chawla A, Barak Y, Nagy L, Liao D, Tontonoz P, Evans RM. PPAR-gamma dependent and independent effects on macrophage-gene expression in lipid metabolism and inflammation. *Nat Med* 2001;**7**:48–52.

60. Kelly D, Campbell JI, King TP, et al. Commensal anaerobic gut bacteria attenuate inflammation by regulating nuclear-cytoplasmic shuttling of PPAR-gamma and RelA. *Nat Immunol* 2004;**5**:104–12.

61. Welch JS, Ricote M, Akiyama TE, Gonzalez FJ, Glass CK. PPARgamma and PPARdelta negatively regulate specific subsets of lipopolysaccharide and IFN-gamma target genes in macrophages. *Proc Natl Acad Sci USA* 2003;**100**:6712–7.

62. Lee JY, Hwang DH. The modulation of inflammatory gene expression by lipids: mediation through Toll-like receptors. *Mol Cells* 2006;**21**:174–85.

63. Lee JY, Zhao L, Youn HS, et al. Saturated fatty acid activates but polyunsaturated fatty acid inhibits Toll-like receptor 2 dimerized with Toll-like receptor 6 or 1. *J Biol Chem* 2004;**279**:16971–9.

64. Eun CS, Han DS, Lee SH, et al. Attenuation of colonic inflammation by PPARgamma in intestinal epithelial cells:

effect on Toll-like receptor pathway. *Dig Dis Sci* 2006; **51**:693–7.

65. Lefebvre P, Chinetti G, Fruchart JC, Staels B. Sorting out the roles of PPAR alpha in energy metabolism and vascular homeostasis. *J Clin Invest* 2006;**116**:571–80.

66. Nagasawa T, Inada Y, Nakano S, et al. Effects of bezafibrate, PPAR pan-agonist, and GW501516, PPARdelta agonist, on development of steatohepatitis in mice fed a methionine- and choline-deficient diet. *Eur J Pharmacol* 2006;**536**:182–91.

67. Oh KS, Kim M, Lee J, et al. Liver PPARalpha and UCP2 are involved in the regulation of obesity and lipid metabolism by swim training in genetically obese db/db mice. *Biochem Biophys Res Commun* 2006;**345**:1232–9.

68. Packard CJ. Triacylglycerol-rich lipoproteins and the generation of small, dense low-density lipoprotein. *Biochem Soc Trans* 2003;**31**:1066–9.

69. Caslake MJ, Packard CJ, Gaw A, et al. Fenofibrate and LDL metabolic heterogeneity in hypercholesterolemia. *Arterioscler Thromb* 1993;**13**:702–11.

70. Patsouris D, Mandard S, Voshol PJ, et al. PPARalpha governs glycerol metabolism. *J Clin Invest* 2004;**114**:94–103.

71. Kersten S, Seydoux J, Peters JM, Gonzalez FJ, Desvergne B, Wahli W. Peroxisome proliferator-activated receptor alpha mediates the adaptive response to fasting. *J Clin Invest* 1999;**103**:1489–98.

72. Ravnskjaer K, Boergesen M, Rubi B, et al. Peroxisome proliferator-activated receptor alpha (PPARalpha) potentiates, whereas PPARgamma attenuates, glucose-stimulated insulin secretion in pancreatic beta-cells. *Endocrinology* 2005;**146**:3266–76.

73. Tontonoz P, Hu E, Devine J, Beale EG, Spiegelman BM. PPARgamma 2 regulates adipose expression of the phosphoenolpyruvate carboxykinase gene. *Mol Cell Biol* 1995; **15**:351–7.

74. Devine JH, Eubank DW, Clouthier DE, et al. Adipose expression of the phosphoenolpyruvate carboxykinase promoter requires peroxisome proliferator-activated receptor gamma and 9-cis-retinoic acid receptor binding to an adipocyte-specific enhancer in vivo. *J Biol Chem* 1999;**274**:13604–12.

75. Holness MJ, Bulmer K, Smith ND, Sugden MC. Investigation of potential mechanisms regulating protein expression of hepatic pyruvate dehydrogenase kinase isoforms 2 and 4 by fatty acids and thyroid hormone. *Biochem J* 2003;**369**: 687–95.

76. Tanaka T, Masuzaki H, Ebihara K, et al. Transgenic expression of mutant peroxisome proliferator-activated receptor gamma in liver precipitates fasting-induced steatosis but protects against high-fat diet-induced steatosis in mice. *Metabolism* 2005;**54**:1490–8.

77. Walczak R, Tontonoz P. PPARadigms and PPARadoxes: expanding roles for PPARgamma in the control of lipid metabolism. *J Lipid Res* 2002;**43**:177–86.

78. Janssen I, Heymsfield SB, Wang ZM, Ross R. Skeletal muscle mass and distribution in 468 men and women aged 18–88 yr. *J Appl Physiol* 2000;**89**:81–8.

79. Barish GD, Narkar VA, Evans RM. PPAR delta: a dagger in the heart of the metabolic syndrome. *J Clin Invest* 2006;**116**: 590–7.

80. Norris AW, Chen L, Fisher SJ, et al. Muscle-specific PPARgamma-deficient mice develop increased adiposity and insulin resistance but respond to thiazolidinediones. *J Clin Invest* 2003;**112**:608–18.

81. Vidal-Puig AJ, Considine RV, Jimenez-Linan M, et al. Peroxisome proliferator-activated receptor gene expression in human tissues. Effects of obesity, weight loss, and regulation by insulin and glucocorticoids. *J Clin Invest* 1997;**99**:2416–22.

82. De Souza AT, Cornwell PD, Dai X, Caguyong MJ, Ulrich RG. Agonists of the peroxisome proliferator activated receptor alpha (PPAR{alpha}) induce a fiber-type selective transcriptional response in rat skeletal muscle. *Toxicol Sci* 2006.

83. Abbot EL, McCormack JG, Reynet C, Hassall DG, Buchan KW, Yeaman SJ. Diverging regulation of pyruvate dehydrogenase kinase isoform gene expression in cultured human muscle cells. *FEBS J* 2005;**272**:3004–14.

84. Kersten S. Mechanisms of nutritional and hormonal regulation of lipogenesis. *EMBO Rep* 2001;**2**:282–6.

85. Wang Y, Jones Voy B, Urs S, et al. The human fatty acid synthase gene and de novo lipogenesis are coordinately regulated in human adipose tissue. *J Nutr* 2004;**134**: 1032–8.

86. He J, Watkins S, Kelley DE. Skeletal muscle lipid content and oxidative enzyme activity in relation to muscle fiber type in type 2 diabetes and obesity. *Diabetes* 2001;**50**: 817–23.

87. Dressel U, Allen TL, Pippal JB, Rohde PR, Lau P, Muscat GE. The peroxisome proliferator-activated receptor beta/delta agonist, GW501516, regulates the expression of genes involved in lipid catabolism and energy uncoupling in skeletal muscle cells. *Mol Endocrinol* 2003;**17**:2477–93.

88. Luquet S, Lopez-Soriano J, Holst D, et al. Roles of peroxisome proliferator-activated receptor delta (PPARdelta) in the control of fatty acid catabolism. A new target for the treatment of metabolic syndrome. *Biochimie* 2004; **86**:833–7.

89. Finck BN, Han X, Courtois M, et al. A critical role for PPARalpha-mediated lipotoxicity in the pathogenesis of diabetic cardiomyopathy: modulation by dietary fat content. *Proc Natl Acad Sci USA* 2003;**100**:1226–31.

90. van Loon LJ, Goodpaster BH. Increased intramuscular lipid storage in the insulin-resistant and endurance-trained state. *Pflugers Arch* 2006;**451**:606–16.

91. Goodpaster BH, Thaete FL, Kelley DE. Thigh adipose tissue distribution is associated with insulin resistance in obesity and in type 2 diabetes mellitus. *Am J Clin Nutr* 2000;**71**: 885–92.

92. Gallagher D, Kuznia P, Heshka S, et al. Adipose tissue in muscle: a novel depot similar in size to visceral adipose tissue. *Am J Clin Nutr* 2005;**81**:903–10.

93. Saghizadeh M, Ong JM, Garvey WT, Henry RR, Kern PA. The expression of TNF alpha by human muscle. Relationship to insulin resistance. *J Clin Invest* 1996;**97**:1111–6.

94. Stein DT, Stevenson BE, Chester MW, et al. The insulinotropic potency of fatty acids is influenced profoundly by their chain length and degree of saturation. *J Clin Invest* 1997;**100**:398–403.

95. Tordjman K, Standley KN, Bernal-Mizrachi C, et al. PPARalpha suppresses insulin secretion and induces UCP2 in insulinoma cells. *J Lipid Res* 2002;**43**:936–43.

96. Koshkin V, Wang X, Scherer PE, Chan CB, Wheeler MB. Mitochondrial functional state in clonal pancreatic beta-cells exposed to free fatty acids. *J Biol Chem* 2003;**278**: 19709–15.

97. Parton LE, Diraison F, Neill SE, et al. Impact of PPARgamma overexpression and activation on pancreatic islet gene expression profile analyzed with oligonucleotide microarrays. *Am J Physiol Endocrinol Metab* 2004;**287**: E390–404.

98. Yajima K, Hirose H, Fujita H, et al. Combination therapy with PPARgamma and PPARalpha agonists increases glu-

cose-stimulated insulin secretion in db/db mice. *Am J Physiol Endocrinol Metab* 2003;**284**:E966–71.

99. Imbeault P, Lemieux S, Prud'homme D, et al. Relationship of visceral adipose tissue to metabolic risk factors for coronary heart disease: is there a contribution of sub-cutaneous fat cell hypertrophy? *Metabolism* 1999;**048**: 355–62.

100. George J, Afek A, Shaish A, et al. 12/15-Lipoxygenase gene disruption attenuates atherogenesis in LDL receptor-deficient mice. *Circulation* 2001;**104**:1646–50.

101. Hiramatsu K, Rosen H, Heinecke JW, Wolfbauer G, Chait A. Superoxide initiates oxidation of low density lipoprotein by human monocytes. *Arteriosclerosis* 1987;**7**:55–60.

102. Szmitko PE, Wang CH, Weisel RD, de Almeida JR, Anderson TJ, Verma S. New markers of inflammation and endothelial cell activation: Part I. *Circulation* 2003;**108**:1917–23.

103. Guo J, Van Eck M, de Waard V, et al. The presence of leukocyte CC-chemokine receptor 2 in CCR2 knockout mice promotes atherogenesis. *Biochim Biophys Acta* 2005;**1740**: 453–9.

104. Gu L, Okada Y, Clinton SK, et al. Absence of monocyte chemoattractant protein-1 reduces atherosclerosis in low density lipoprotein receptor-deficient mice. *Mol Cell* 1998;**2**:275–81.

105. Febbraio M, Abumrad NA, Hajjar DP, et al. A null mutation in murine CD36 reveals an important role in fatty acid and lipoprotein metabolism. *J Biol Chem* 1999;**274**: 19055–62.

106. Chawla A, Boisvert WA, Lee CH, et al. A PPARgamma-LXR-ABCA1 pathway in macrophages is involved in cholesterol efflux and atherogenesis. *Mol Cell* 2001;**7**:161–71.

107. Chinetti G, Lestavel S, Bocher V, et al. PPAR-alpha and PPAR-gamma activators induce cholesterol removal from human macrophage foam cells through stimulation of the ABCA1 pathway. *Nat Med* 2001;**7**:53–8.

108. Oliver Jr WR, Shenk JL, Snaith MR, et al. A selective peroxisome proliferator-activated receptor delta agonist promotes reverse cholesterol transport. *Proc Natl Acad Sci USA* 2001;**98**:5306–11.

109. Vosper H, Patel L, Graham TL, et al. The peroxisome proliferator-activated receptor delta promotes lipid accu-mulation in human macrophages. *J Biol Chem* 2001;**276**: 44258–65.

110. Li AC, Binder CJ, Gutierrez A, et al. Differential inhibition of macrophage foam-cell formation and atherosclerosis in mice by PPARalpha, beta/delta, and gamma. *J Clin Invest* 2004;**114**:1564–76.

111. Verrier E, Wang L, Wadham C, et al. PPARgamma agonists ameliorate endothelial cell activation via inhibition of diacylglycerol-protein kinase C signaling pathway: role of diacylglycerol kinase. *Circ Res* 2004;**94**:1515–22.

112. Dragomir E, Tircol M, Manduteanu I, Voinea M, Simionescu M. Aspirin and PPAR-alpha activators inhibit monocyte chemoattractant protein-1 expression induced by high glucose concentration in human endothelial cells. *Vasc Pharmacol* 2006;**44**:440–9.

113. Mishra A, Chaudhary A, Sethi S. Oxidized omega-3 fatty acids inhibit NF-kappaB activation via a PPARalpha-depen-dent pathway. *Arterioscler Thromb Vasc Biol* 2004;**24**: 1621–7.

114. Roberts CK, Won D, Pruthi S, et al. Effect of a diet and exercise intervention on oxidative stress, inflammation, MMP-9 and monocyte chemotactic activity in men with metabolic syndrome factors. *J Appl Physiol* 2005.

115. Ajuwon KM, Spurlock ME. Adiponectin inhibits LPS-induced NF-kappaB activation and IL-6 production and increases PPARgamma2 expression in adipocytes. *Am J Physiol Regul Integr Comp Physiol* 2005;**288**:R1220–5.

116. Tanaka T, Fukunaga Y, Itoh H, et al. Therapeutic potential of thiazolidinediones in activation of peroxisome prolif-erator-activated receptor gamma for monocyte recruit-ment and endothelial regeneration. *Eur J Pharmacol* 2005; **508**:255–65.

117. Babaev VR, Yancey PG, Ryzhov SV, et al. Conditional knockout of macrophage PPARgamma increases athero-sclerosis in C57BL/6 and low-density lipoprotein receptor-deficient mice. *Arterioscler Thromb Vasc Biol* 2005;**25**: 1647–53.

30

CHAPTER 3: DIETARY ABSCISIC ACID AMELIORATES GLUCOSE TOLERANCE AND OBESITY-RELATED INFLAMMATOIN IN DB/DB MICE FED HIGH-FAT DIETS

INTRODUCTION

The publisher for this copyrighted material is Elsevier. By clicking "accept" in connection with completing this licensing transaction, you agree that the following terms and conditions apply to this transaction (along with the Billing and Payment terms and conditions established by Copyright Clearance Center, Inc. ("CCC"), at the time that you opened your Rightslink account and that are available at any time at http://myaccount.copyright.com).

GENERAL TERMS

Elsevier hereby grants you permission to reproduce the aforementioned material subject to the terms and conditions indicated.

Acknowledgement: If any part of the material to be used (for example, figures) has appeared in our publication with credit or acknowledgement to another source, permission must also be sought from that source. If such permission is not obtained then that material may not be included in your publication/copies. Suitable acknowledgement to the source must be made, either as a footnote or in a reference list at the end of your publication, as follows:

"Reprinted from Publication title, Vol number, Author(s), Title of article, Pages No., Copyright (Year), with permission from Elsevier [OR APPLICABLE SOCIETY COPYRIGHT OWNER]." Also Lancet special credit - "Reprinted from The Lancet, Vol. number, Author(s), Title of article, Pages No., Copyright (Year), with permission from Elsevier."

Reproduction of this material is confined to the purpose and/or media for which permission is hereby given.

Altering/Modifying Material: Not Permitted. However figures and illustrations may be altered/adapted minimally to serve your work. Any other abbreviations, additions, deletions and/or any other alterations shall be made only with prior written authorization of Elsevier Ltd. (Please contact Elsevier at permissions@elsevier.com)

If the permission fee for the requested use of our material is waived in this instance, please be advised that your future requests for Elsevier materials may attract a fee.

Reservation of Rights: Publisher reserves all rights not specifically granted in the combination of (i) the license details provided by you and accepted in the course of this licensing transaction, (ii) these terms and conditions and (iii) CCC's Billing and Payment

terms and conditions.

License Contingent Upon Payment: While you may exercise the rights licensed immediately upon issuance of the license at the end of the licensing process for the transaction, provided that you have disclosed complete and accurate details of your proposed use, no license is finally effective unless and until full payment is received from you (either by publisher or by CCC) as provided in CCC's Billing and Payment terms and conditions. If full payment is not received on a timely basis, then any license preliminarily granted shall be deemed automatically revoked and shall be void as if never granted. Further, in the event that you breach any of these terms and conditions or any of CCC's Billing and Payment terms and conditions, the license is automatically revoked and shall be void as if never granted. Use of materials as described in a revoked license, as well as any use of the materials beyond the scope of an unrevoked license, may constitute copyright infringement and publisher reserves the right to take any and all action to protect its copyright in the materials.

Warranties: Publisher makes no representations or warranties with respect to the licensed material.

Indemnity: You hereby indemnify and agree to hold harmless publisher and CCC, and their respective officers, directors, employees and agents, from and against any and all claims arising out of your use of the licensed material other than as specifically authorized pursuant to this license.

No Transfer of License: This license is personal to you and may not be sublicensed, assigned, or transferred by you to any other person without publisher's written permission.

No Amendment Except in Writing: This license may not be amended except in a writing signed by both parties (or, in the case of publisher, by CCC on publisher's behalf).

Objection to Contrary Terms: Publisher hereby objects to any terms contained in any purchase order, acknowledgment, check endorsement or other writing prepared by you, which terms are inconsistent with these terms and conditions or CCC's Billing and Payment terms and conditions. These terms and conditions, together with CCC's Billing and Payment terms and conditions (which are incorporated herein), comprise the entire agreement between you and publisher (and CCC) concerning this licensing transaction. In the event of any conflict between your obligations established by these terms and conditions and those established by CCC's Billing and Payment terms and conditions, these terms and conditions shall control.

Revocation: Elsevier or Copyright Clearance Center may deny the permissions described in this License at their sole discretion, for any reason or no reason, with a full refund payable to you. Notice of such denial will be made using the contact information provided by you. Failure to receive such notice will not alter or invalidate the denial. In no event will Elsevier or Copyright Clearance Center be responsible or liable for any costs, expenses or damage incurred by you as a result of a denial of your permission request, other than a refund of the

amount(s) paid by you to Elsevier and/or Copyright Clearance Center for denied permissions.

LIMITED LICENSE

The following terms and conditions apply to specific license types:

Translation: This permission is granted for non-exclusive world **English** rights only unless your license was granted for translation rights. If you licensed translation rights you may only translate this content into the languages you requested. A professional translator must perform all translations and reproduce the content word for word preserving the integrity of the article. If this license is to re-use 1 or 2 figures then permission is granted for non-exclusive world rights in all languages.

Website: The following terms and conditions apply to electronic reserve and author websites:
Electronic reserve: If licensed material is to be posted to website, the web site is to be password-protected and made available only to bona fide students registered on a relevant course if:
This license was made in connection with a course,
This permission is granted for 1 year only. You may obtain a license for future website posting,
All content posted to the web site must maintain the copyright information line on the bottom of each image,
A hyper-text must be included to the Homepage of the journal from which you are licensing at http://www.sciencedirect.com/science/journal/xxxxx , and
Central Storage: This license does not include permission for a scanned version of the material to be stored in a central repository such as that provided by Heron/XanEdu.

Author website with the following additional clauses: This permission is granted for 1 year only. You may obtain a license for future website posting,
All content posted to the web site must maintain the copyright information line on the bottom of each image, and
The permission granted is limited to the personal version of your paper. You are not allowed to download and post the published electronic version of your article (whether PDF or HTML, proof or final version), nor may you scan the printed edition to create an electronic version,
A hyper-text must be included to the Homepage of the journal from which you are licensing at http://www.sciencedirect.com/science/journal/xxxxx , and
Central Storage: This license does not include permission for a scanned version of the material to be stored in a central repository such as that provided by Heron/XanEdu.

Website (regular and for author): "A hyper-text must be included to the Homepage of the journal from which you are licensing at http://www.sciencedirect.com/science/journal/xxxxx."

Thesis/Dissertation: If your license is for use in a thesis/dissertation your thesis may be submitted to your institution in either print or electronic form. Should your thesis be published commercially, please reapply for permission. These requirements include permission for the Library and Archives of Canada to supply single copies, on demand, of the complete thesis and include permission for UMI to supply single copies, on demand, of the complete thesis. Should your thesis be published commercially, please reapply for permission.

Other conditions: None

ORIGINAL ARTICLE

Dietary abscisic acid ameliorates glucose tolerance and obesity-related inflammation in db/db mice fed high-fat diets

Amir J. Guri, Raquel Hontecillas, Hongwei Si, Dongmin Liu, Josep Bassaganya-Riera*

Laboratory of Nutritional Immunology and Molecular Nutrition, Department of Human Nutrition, Foods and Exercise, Virginia Polytechnic Institute and State University, 319 Wallace Hall, Blacksburg, VA 24061, USA

Summary
Background & Aims: Despite their efficacy in improving insulin sensitivity, thiazolidine-diones (TZDs) are associated with a number of side effects (i.e. weight gain, hepatotoxicity, congestive heart failure) that have limited their use by millions of diabetic patients. We have investigated whether abscisic acid (ABA), a naturally occurring phytochemical with structural similarities to TZDs, could be used as an alternative to TZDs to improve glucose homeostasis.
Methods: We first examined whether ABA, similar to TZDs, activates PPARγ in vitro. We next determined the lowest effective dose of dietary ABA (100 mg/kg) and assessed its effect on glucose tolerance, obesity-related inflammation, and mRNA expression of PPARγ and its responsive genes in white adipose tissue (WAT) of db/db mice fed high-fat diets.
Results: We found that ABA induced transactivation of PPARγ in 3T3-L1 pre-adipocytes in vitro. Dietary ABA-supplementation for 36 days decreased fasting blood glucose concentrations, ameliorated glucose tolerance, and increased mRNA expression of PPARγ and its responsive genes (i.e., adiponectin, aP2, and CD36) in WAT. We also found that adipocyte hypertrophy, tumor necrosis factor-α (TNF-α) expression, and macrophage infiltration in WAT were significantly attenuated in ABA-fed mice.
Conclusions: These findings suggest that ABA could be used as a nutritional intervention against type II diabetes and obesity-related inflammation.
© 2006 Elsevier Ltd and European Society for Clinical Nutrition and Metabolism. All rights reserved.

*Corresponding author. Tel.: +1 540 231 7421; fax: +1 540 231 3916.
E-mail address: jbassaga@vt.edu (J. Bassaganya-Riera).

Introduction

In spite of efforts by public health officials to encourage physical activity and reduce energy intake, the obesity rate in the US, Europe and worldwide has continued to climb and it has reached epidemic proportions. According to estimates by the Center for Disease Control and Prevention in the year 2000, 30% of Americans are obese and 65% are overweight.[1] One of the manifestations associated with this obesity epidemic is the growing number of people diagnosed with type II diabetes (T2D). T2D is a widespread and debilitating disease characterized by insulin resistance and inflammation that can lead to coronary heart disease, hypertension, blindness, neuropathy, nephropathy, and limb amputations.[2] It was recently estimated that 20.8 million Americans had T2D and 40.1% of middle-aged adults had prediabetes, a condition characterized by either impaired glucose tolerance or high fasting blood glucose concentrations.[2] Future predictions indicate that one of three children born in 2000 will one day become diabetic.[3] The impending consequence is that millions of people will soon become dependent on oral palliative antidiabetic medications to maintain their quality of life.

During the onset of obesity, adipocytes become increasingly hypertrophic. One of the outcomes of adipocyte hypertrophy is endoplasmic reticulum stress, which results in the activation of IkappaB kinase and c-Jun N-terminal Kinase and production of pro-inflammatory cytokines.[4] These inflammatory mediators inhibit insulin signaling by promoting serine phosphorylation of insulin receptor substrate 1 (IRS-1), thereby inhibiting its ability to act as a substrate for the insulin receptor. Hypertrophic adipocytes also promote the infiltration bone-marrow-derived macrophages, which aggregate in the stromal vascular fraction (SVF) and are able to fuse into multinucleate giant cells (MGCs), hallmarks of inflammation that can persist for extended periods of time.[5]

One of the most effective of the currently available medications for T2D is the thiazolidinedione (TZDs) class of insulin-sensitizing drugs. Subsequent to their use as oral antidiabetic agents, Lehmann et al.[6] demonstrated that TZDs function by binding to the nuclear receptor peroxisome proliferator-activated receptor γ (PPARγ). In WAT, PPARγ activation promotes adipogenesis and the differentiation of new adipocytes. Despite increasing total adipose tissue mass, TZDs are believed to improve systemic insulin sensitivity, in part by expanding the pool of insulin-sensitive cells and increasing the production of adiponectin, a glucose-sensitizing peptide that holds anti-inflammatory properties.[7] PPARγ ligands also markedly reduce the production of pro-inflammatory cytokine secretion in WAT, an effect that is associated with a significant reduction in macrophage infiltration.[8,9]

The major factors limiting the use of TZDs by millions of diabetic patients are the numerous side effects, including weight gain, hepatotoxicity, and congestive heart failure.[7,10] For instance, the TZD troglitazone (Rezulin®) was launched in 1997 and withdrawn from the market in March of 2000 due to reports of serious liver injury when compared to other TZDs.[11] While other Food and Drug Administration (FDA)-approved TZDs for T2D treatment, including rosiglitazone (Avandia®) and pioglitazone (Actos®), continue to

be widely prescribed, concerns regarding their safety persist. In this regard, the FDA recommended that the presence of liver enzymes in blood of diabetic patients taking Avandia® be periodically monitored. Furthermore, due to the risk factors and side effects connected with TZDs and other oral synthetic antidiabetic agents, their use as preventative medications is contraindicated for the millions of people with prediabetes. The aim of this study was to determine whether abscisic acid (ABA), a phytochemical found in all photosynthetic organisms, could improve glucose homeostasis and obesity-related inflammation and, as a result, be used an alternative to TZDs. We chose to use ABA based on structural similarities to TZDs and other known PPARγ ligands. Similar to other PPARγ ligands, ABA contains both a polar head group and a hydrophobic component, which are needed for binding to the PPARγ ligand-binding domain and for entry through the plasma and nuclear membranes, respectively.[12] The hydrophobic component also plays another key role in that its size controls the stability of the ligand/receptor interaction.[12] Chemical synthesis of ABA results in the racemic 1:1 mixture of its enantiomers, namely the natural hormone, S-(+)-ABA, and its mirror image, R-(−)-ABA, which elicit similar biological responses in plants.[13] While the role of ABA as a phytohormone has been studied extensively, this is the first study designed to investigate the effect of ABA in the prevention and treatment of T2D and obesity-related inflammation.

Research design and methods

Transfection of 3T3-L1 preadipocytes

A pCMX.PPARγ expression plasmid and a pTK.PPRE3x luciferase reporter plasmid driven by the PPRE-containing Acyl-CoA oxidase promoter (kindly provided by Dr. R.M. Evans, The Salk Institute, San Diego, CA) were purified using Qiagen's Maxi kit (Valencia, CA). 3T3-L1 cells (American Type Culture Collection, Manassas, VA) were grown in 24-well plates in DMEM high glucose medium (Invitrogen, Carlsbad, CA) containing 10% fetal bovine serum (FBS) until 60–70% confluence. Before transfection, the medium was changed to 1% FBS. The cells cultured in 24-well plates were co-transfected with 0.8 μg plasmid DNA and 1 ng of pRL reporter control plasmid per well using F-1 transfection reagents (Targeting Systems, Santee, CA) according to the manufacturer's protocol. Transfection efficiencies were determined by cotransfecting the cells with a pcDNA™ 3.1/His/lacZ control vector at 24 h. The transfected cells were then treated with either a racemic ABA mixture (3.125, 6.25, 12.5, 25, and 50 μM; Sigma) or rosiglitazone (1, 5, 10 μM; Cayman Chemicals, Ann Arbor, MI) for 24 h. Designated wells were also pretreated with the PPARγ antagonist GW9662 (10 μM; Caymen Chemicals) for 1 h prior to treatment with either ABA (12.5 μM) or rosiglitazone (1 μM). Transfected cells were harvested in reporter lysis reagent. Luciferase activity, normalized to pRL activity in the cell extracts was determined by using the dual luciferase reporter assay system (Promega, Madison, WI) in a TD-20/20 Single-Tube Luminometer (Turner Biosystems, Sunnyvale, CA). Relative luciferase activity (RLA) was calculated as a ratio of the chemiluminescence 10 s after

the Luciferase Assay Reagent II (Promega) was added over the chemiluminescence 10 s after the Stop and Glo Reagent (Promega).

Mice and dietary treatments

Male BKS.Cg-+Lepr^{db}/+Lepr^{db}/OlaHsd (db/db) mice, 4–5-week-old, were purchased from Harlan Laboratories (Indianapolis, IN) and housed at the animal facilities at Virginia Polytechnic Institute and State University in a room maintained at 75 °F, with a 12:12 h light–dark cycle starting from 6:00 AM. All experimental procedures were approved by the Institutional Animal Care and Use Committee of Virginia Polytechnic Institute and State University and met or exceeded requirements of the Public Health Service/ National Institutes of Health and the Animal Welfare Act.

Experiment 1: Mice ($n = 25$) were fed high-fat ($>40\%$ energy from fat), isocaloric, isonitrogenous diets containing 0, 100, 200, 400, and 800 mg of a racemic ($\pm$) ABA mixture/ kg diet for 36 days (Table 1). These doses were chosen based on the standard concentrations of TZDs utilized in the treatment of T2D. The mice were weighed and their food intake was recorded daily. On day 36, fasted mice (12 h) were bled through the caudal vein and fasting blood glucose concentrations were determined with an Accu-Chek® Glucometer (Roche, Indianapolis, IN). Mice were then killed by CO_2 narcosis and WAT was excised and stored in RNA Later (Ambion, Austin, TX), a commercial solution that inhibits RNases. Weights were recorded for WAT and interscapular brown adipose tissue (BAT).

Experiment 2: Mice ($n = 14$) were fed high-fat diets containing 0 or 100 mg ABA/kg for 36 days. The ABA dose utilized (100 mg ABA/kg) was based on the lowest effective dose based on the results obtained from the ABA titration study (i.e., Experiment 1). Their body weights and food intake was recorded daily, and blood was collected on day 36 of the study. To investigate the ability of ABA to normalize glucose concentrations, an intraperitoneal glucose tolerance test (IPGTT) was performed on day 36 on the fasted mice. Briefly, mice were bled at 0, 10, 25, 45, and 100 min following the administration of glucose (2 g/kg) for measurement of plasma glucose levels. Following the IPGTT, the mice were sacrificed by CO_2 narcosis and abdominal WAT was

---

Table 1 Composition of experimental diets.*

Ingredient (g)	Dietary treatments				
	Control	100 mg ABA	200 mg ABA	400 mg ABA	800 mg ABA
Casein	232	232	232	232	232
L-cystein	3	3	3	3	3
DL-methionine	3.5	3.5	3.5	3.5	3.5
Corn starch	137	137	137	137	137
Maltodextrin	150	150	150	150	150
Sucrose	162.595	162.595	162.595	162.595	162.595
Cellulose	50	50	50	50	50
Cholesterol	1.9	1.9	1.9	1.9	1.9
Mineral mix (AIN-93)†	40.60	40.60	40.60	40.60	40.60
Calcium phosphate dibasic	4.64	4.64	4.64	4.64	4.64
Vitamin mix (AIN-93)‡	16.24	16.24	16.24	16.24	16.24
Choline bitartrate§	5	5	5	5	5
Tert-butylhydroquinone¶	0.02	0.02	0.02	0.02	0.02
Vitamin K1	0.005	0.005	0.005	0.005	0.005
Soybean oil	30	30	30	30	30
Lard	163.5	163.5	163.5	163.5	163.5
Abscisic acid (ABA)**	—	0.100	0.200	0.400	0.800

*Supplied per kg diet. Provides approximately 19.6% fat, 0.2% total cholesterol and 4.4 kcal/g it obtains 40% kcal from fat. kcal density is approximately 16% higher than typical AIN-93G-based diets.

†Supplied per kg of mineral mix: 357 g calcium carbonate, 196 potassium phosphate monobasic, 70.78 potassium citrate, 74 g sodium chloride, 46.6 g potassium sulfate, 24.3 g magnesium oxide, 6.06 g ferric citrate, 1.65 g zinc carbonate, 0.63 g magnesium carbonate, 0.31 g cupric carbonate, 0.01 g potassium Iodate, 0.01025 sodium selenate, 0.00795 ammonium paramolybdate, 1.45 g sodium-metasilicate, 0.275 chromium potassium sulfate, 0.0174 lithium chloride, 0.0815 boric acid, 0.0635 sodium fluoride, 0.0318 nickel carbonate, hydroxide, tetrahydrate, 0.0066 ammonium vanadate, and 220.716 sucrose.

‡Supplied per kg of vitamin mix: 3 g nicotinic acid, 1.6 g calcium pentotenate, 0.7 g pyridoxine HCL, 0.6 g thiamin HCL, 0.6 g riboflavin, 0.2 g folic acid, 0.02 g D-biotin, 2.5 g vitamin B$_{12}$ (0.1% mannitol), 15 g DL-α tocopheryl acetate (500 IU/g), 0.8 g vitamin A palmitate (500,000 IU/g), 0.2 vitamin D$_3$ (cholecalciferol, 500,000 IU/g), 0.0075 vitamin K1 (phylloquinone), 974.705 g sucrose.

§The choline bitartrate concentrations have been increased from 2.5 g/kg in regular AIN-93G diets to 5 g/kg due to increased kcal density of high-fat diets.

¶Antioxidant (Sigma).

**Abscisic acid (ABA), or (2-*cis*,4-*trans*)-5-(1-hydroxy-2,6,6-trimethyl-4-oxo-2-cyclohexen-1-yl)-3-methyl-2,4-pentadienoic acid, was added as a 1:1 racemic mixture of the (S)-5 and (R)-5 isomers (Sigma).

collected and stored in RNA Later (Ambion) for RNA isolation and gene expression analyses, and in 10% buffered neutral formalin for histological evaluation. Weights were recorded for abdominal WAT and BAT.

Histopathology

Adipose tissue specimens were fixed in 10% phosphate buffered neutral formalin, embedded in paraffin, cut at thicknesses of 7 μm and later stained with hematoxylin and eosin (H&E) for histological examination of adipocyte hypertrophy and inflammatory lesions. The area of adipocytes from WAT was analyzed using Sigma Pro® 5.0 software at a magnification of 100 ×, and macrophage infiltration was determined by averaging the number of macrophages observed in five different fields at 400 ×. Analyses reflect data from experiments 1 and 2.

Quantitative real-time reverse transcriptase PCR

Total RNA was isolated from WAT using the RNA isolation Lipid Tissue Minikit (Qiagen) according to the manufacturer's instructions. Total RNA (1 μg) was used to generate complementary DNA (cDNA) template using the iScript cDNA Synthesis Kit (Bio-Rad, Hercules, CA). The total reaction volume was 20 μl with the reaction incubated as follows in the Tetrad Thermocycler: 5 min at 25 °C, 30 min at 52°, 5 min at 85 °C, hold at 4 °C. PCR was performed on the cDNA using Taq DNA polymerase obtained from Invitrogen and using previously described conditions.[14,15] Each gene amplicon was purified with the MiniElute PCR Purification Kit (Qiagen) and quantitated on an agarose gel by using a DNA mass ladder (Promega). These purified amplicons were used to optimize real-time PCR conditions and to generate standard

curves in the real-time PCR assay. Primer concentrations and annealing temperatures were optimized for the iCycler iQ system (Bio-Rad) for each set of primers using the system's gradient protocol. PCR efficiencies were maintained between 92% and 105% and correlation coefficients above 0.98 for each primer set (Table 2) during optimization and also during the real-time PCR of sample DNA.

cDNA concentrations for genes of interest were examined by real-time quantitative PCR using an iCycler IQ System and the iQ SYBR green supermix (Bio-Rad). A standard curve was generated for each gene using 10-fold dilutions of purified amplicons starting at 5 pg of cDNA and used later to calculate the starting amount of target cDNA in the unknowns. SYBR green I is a general double-stranded DNA intercalating dye and, therefore, may detect non-specific products and primer/dimers in addition to the amplicon of interest. In order to determine the number of products synthesized during the real-time PCR, a melting curve analysis was performed on each product. Real-time PCR was used to measure the starting amount of nucleic acid of each unknown sample of cDNA on the same 96-well plate. Results are presented as starting quantity of target cDNA (picograms) per microgram of total RNA from experiments 1 and 2.

Statistical analyses

Data were analyzed as a completely randomized design. To determine the statistical significance of the model, analysis of variance (ANOVA) was performed using the general linear model procedure of statistical analysis software (SAS) as previously described.[14] A $P < 0.05$ was considered to be significant. When the model was significant, ANOVA was followed by Sheffe's multiple comparison method. Non-

Table 2 Oligonucleotide sequences for quantitative real-time PCR.[*,†]

Primer	Sequence	Length	Accession No.
PPAR αF	5′-TGGGGATGAAGAGGGCTGAG-3′	143	NM_011144
PPAR αR	5′-GGGGACTGCCGTTGTCTGT-3′		
PPAR δF	5′-ACAGTGACCTGGCGCTCTTC-3′	96	U10375
PPAR δR	5′-TGGTGTCCTGGATGGCTTCT-3′		
PPAR γF	5′-CAGGCTTGCTGAACGTGAAG-3′	117	NM_011146
PPAR γR	5′-GGAGCACCTTGGCGAACA-3′		
CD36F	5′-CCGGGCCACGTAGAAAACA-3′	156	NM_007643
CD36R	5′-CCTCCAAACACAGCCAGGAC-3′		
β-actinF	5′-CCCAGGCATTGCTGACAGG-3′	141	X03672
β-actinR	5′-TGGAAGGTGGACAGTGAGGC-3′		
AdiponectinF	5′-ACAAGGCCGTTCTCTTCACC-3′	123	NM_009605
AdiponectinR	5′-CCCCATCCCCATACACCTG-3′		
aP2F	5′-TCTCTTATCAAAGGCTCTACTTCC-3′	78	BC054426
aP2R	5′-CAAAATTCCATCCAGGCCTCT-3′		
TNF-αF	5′-ACTGCCAGAAGAGGCACTCC-3′	137	NM_013693
TNF-αR	5′-CGATCACCCCGAAGTTCA-3′		

[*]F, forward; R, reverse. PCR primer pairs were designed for an optimal annealing temperature of 57 °C and product lengths between 78 and 157 base pairs.

[†]When plotting threshold cycle versus log starting quantity (pg), standard curves had slopes between −3.1 and −3.7; PCR efficiencies between 92 and 105 and R^2 above 0.98.

parametric data were analyzed by using the Mann–Whitney *U* test followed by a Dunn's multiple comparison's test.

Results

ABA activates PPARγ in 3T3-L1 pre-adipocytes in vitro

In order to establish whether ABA activated PPARγ in vitro, we cultured 3T3-L1 pre-adipocytes that were transfected with a PPARγ-luciferase plasmid in the presence of increasing concentrations (0, 3.125, 6.25, 12.5, 25, and 50 μM) of racemic ABA and rosiglitazone (1, 5, and 10 μM). We also cultured ABA (12.5 μM) or rosiglitazone (1 μM) in the presence of the PPARγ antagonist GW9662 (10 μM). ABA significantly increased the RLA of the transfected cells in a dose–response manner from 3.125 to 12.5 μM (Fig. 1). No additional increase in PPARγ activity was observed with the 25 and 50 μM ABA concentration. The PPARγ activation obtained from 12.5 μM ABA was similar to that observed with 1 μM rosiglitazone, indicating that either ABA has a weaker affinity for PPARγ than rosiglitazone or that that the uptake of ABA by cells is lower in comparison to the synthetic PPARγ ligand. Pretreatment of the pre-adipocytes with GW9662 for 1 h prior to administering ABA or rosiglitazone was equally effective in inhibiting PPARγ activation, suggesting that ABA, similar to rosiglitazone, increases PPARγ activity by binding the ligand-dependent transactivation domain (AF2).

Dietary ABA lowers fasting blood glucose and improves glucose tolerance

To test the efficacy of ABA to improve glucose homeostasis, we performed two separate experiments using prediabetic db/db mice to assess whether ABA exerted similar activities to TZDs in vivo. Experiment 1 was a dose-titration study where we fed 4–5-week-old db/db mice ($n = 25$) diabetogenic, high-fat diets containing 0, 100, 200, 400, or 800 mg racemic ABA mixture/kg diet. Experiment 2 was designed as a replicate of experiment 1 in which db/db mice ($n = 14$) were fed the lowest glucose-normalizing dose of ABA or a control diet. On day 36, mice fed the ABA-supplemented diets had significantly lower fasting blood glucose concentrations, regardless of the amount of dietary ABA (i.e., 100–800 mg/kg), than mice fed an isocaloric and isonitrogenous control diet without ABA (Table 1).

Based on readings showing no differences in fasting blood glucose concentrations among the ABA diets from 100 to 800 mg/kg, we chose the 100 mg/kg dose of ABA to continue on with further experiments. As demonstrated by the IPGTT, mice fed ABA had significantly improved their glucose-normalizing ability at every time point up to 100 min (Fig. 2).
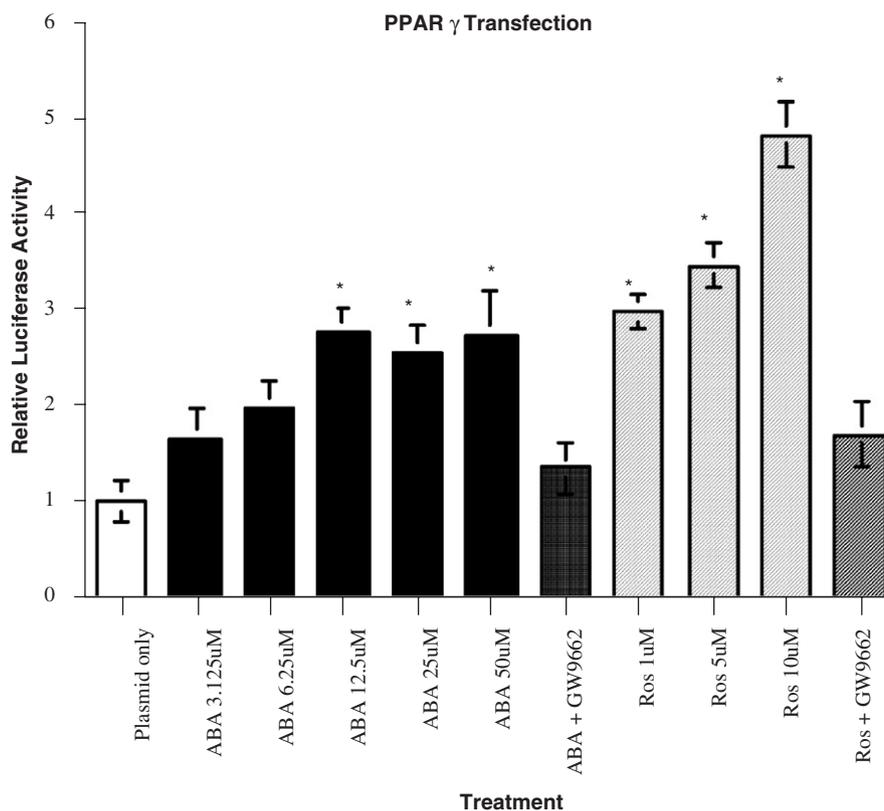
Figure 1 Transactivation of peroxisome proliferator-activated receptor γ (PPARγ) in 3T3-L1 pre-adipocytes cultured with abscisic acid (ABA) (0, 3.125, 6.25, 12.5, 25, 50 μM) or rosiglitazone (Ros) (1, 5, 10 μM). Cell were also pretreated with the PPARγ antagonist GW9662 1 h prior to treatment with ABA (12.5 μM) and Ros (1 μM). Relative luciferase activity (RLA) was calculated as the ratio of chemiluminescence 10 s before and after the reaction was stopped. Data are presented as average RLA ± standard error. Data points with an asterisk are significantly greater than control ($P < 0.05$).

Dietary ABA-supplementation increased WAT PPARγ and PPARγ-responsive gene expression and reduced WAT inflammation

To determine whether the glucose-normalizing effects of ABA were associated with activation of WAT PPARγ, we measured the expression of PPARγ and PPARγ-responsive

genes in WAT of ABA (100 mg/kg diet) and control-fed mice. We found that dietary ABA supplementation resulted in a significant increase in WAT expression of PPARγ ($P<0.01$) and the PPARγ responsive genes adiponectin ($P<0.05$), aP2 ($P<0.02$), and CD36 ($P<0.01$) (Fig. 3). There were no significant differences in mRNA expression of either PPARα or PPARδ (data not shown). No differences were found in the starting amount of cDNA for the housekeeping gene β-actin (data not shown).

Dietary ABA-supplementation ameliorates adipocyte hypertrophy and reduces macrophage infiltration and inflammation

PPARγ activation promotes adipogenesis, adipocyte differentiation, and inhibits the infiltration of bone-marrow-derived macrophages into WAT. In similar action, histological analysis of WAT confirmed that ABA-fed mice had significantly more small-size adipocytes and fewer hypertrophic adipocytes than WAT from control-fed mice (Fig. 4A–4C), which correlated with a significantly lower number of macrophages infiltrating WAT in ABA-fed mice in comparison to mice fed the control diet ($P<0.05$) (Fig. 5A). In line with the lower numbers of infiltrating macrophages, TNF-α mRNA expression was also down-regulated in WAT from ABA-fed mice ($P<0.05$) (Fig. 5B).

Dietary ABA-supplementation had no effect on body weight, feed intake or WAT weight

A common side effect of synthetic PPARγ agonists is increased body weight brought on by fluid retention and increased adipose tissue mass caused by enhanced adipocyte differentiation.[16] As expected, the db/db mice from both the control and ABA-fed groups gained a substantial amount of weight throughout the 36-day trial. However, as opposed to findings with TZDs,[17] there were no statistically significant differences in body weights between mice consuming ABA and control diet, including no differences in abdominal WAT weight. Interscapular BAT, however, was significantly increased in mice fed ABA (Table 3). The body weights of mice in the ABA-supplemented diet were

Figure 2 Effect of dietary abscisic acid (ABA) in response to an intraperitoneal glucose tolerance test (IPGTT). On day 36 of the experiment, after a 12-h fasting period, mice were given 2 mg/kg of glucose and the kinetics of blood glucose normalization was measured at different time points post-injection. Leptin receptor-deficient (db/db) mice were fed either 0 or 100 mg racemic ABA/kg diet. White circles = 0 mg; black circles = 100 mg. Data are presented as least square means±standard error. Data points with an asterisk are significantly different ($P<0.05$).

Figure 3 Effect of dietary abscisic acid (ABA)-supplementation at 100 mg/kg diet on mRNA expression of peroxisome proliferator-activated receptor γ (PPARγ) and PPARγ-responsive genes adiponectin, aP2, and CD36 in white adipose tissue. Expression of the house-keeping gene (β-actin) in both diets was approximately equal (not shown). Data are presented as least square means±standard error expressed as picograms (pg) of complementary DNA (cDNA) of each gene per microgram (ug) mRNA. An asterisk signifies that groups are significantly different ($P<0.05$).
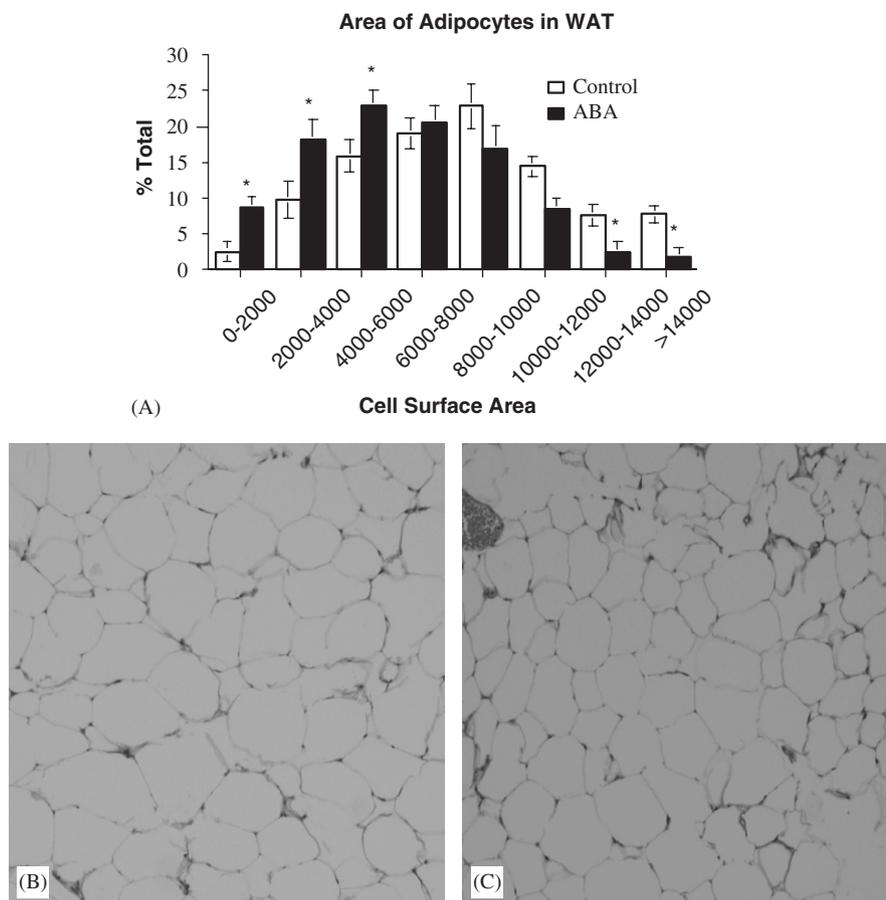
Figure 4 Effect of dietary abscisic acid (ABA)-supplementation on adipocyte hypertrophy and inflammation in white adipose tissue (WAT) (A) Area of adipocytes (micrograms^2) was assessed using SigmaPro$^{®}$ 5.0 software. Representative photomicrographs of WAT from mice fed diabetogenic, high-fat diets, supplemented with either 0 (B) or 100 mg ABA/kg diet (C) at 100 × magnification.
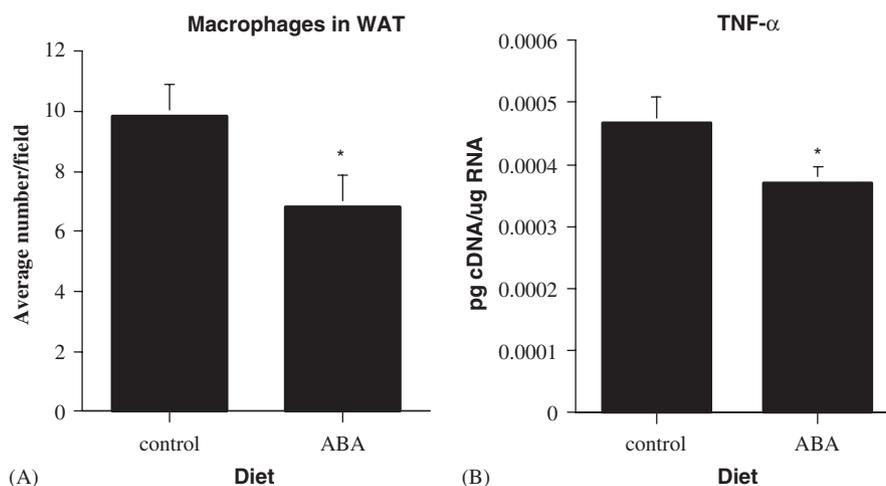
Figure 5 Effect of dietary abscisic acid (ABA)-supplementation on macrophage infiltration and tumor necrosis factor-α (TNF-α) expression in abdominal white adipose tissue (WAT) of db/db mice. Number of macrophages was obtained by averaging the results of 5 different fields at 400 × magnification. Data are presented as least square means ± standard error. TNF-α is expressed as picograms (pg) of complementary DNA (cDNA) per microgram (μg) mRNA. An asterisk signifies that values are significantly different ($P < 0.05$).

approximately 2.2 g lower than those of mice fed the control diet (41.34 g vs. 43.54 g), though none of the weigh data from any of the weekly time-points were statistically significant. Total feed intake also did not differ significantly between treatment groups (data not shown). Hence, the improved ability to regulate glucose homeostasis observed

Table 3 Effect of dietary abscisic acid (ABA)-supplementation on body and organ weights.[*,†,‡]

Diet	Initial body weight (g)	Final body weight (g)	WAT% body weight	Liver% body weight	BAT% body weight
Control	19.63	43.54	6.28	5.74	0.91
ABA	19.83	41.34	6.06	5.16#	1.37#
Pooled SEM	0.864	1.282	0.258	0.125	0.106
ANOVA P value	0.865	0.248	0.476	0.027	0.007

[*]Organs were excised and weighed on day 36 of experiment.
[†]Least squares means values in a column with a pound sign are significantly different ($P < 0.05$).
[‡]P-value of main effects of diet during the 36-day period. Data were analyzed as a completely randomized design.

in ABA-fed mice was not attributable to decreased energy intake.

Discussion

The objective of this study was to determine whether dietary ABA-supplementation could improve glucose homeostasis and obesity-related inflammation. The results from the transfection assay demonstrated for the first time that ABA-activated PPARγ in 3T3-L1 pre-adipocytes in vitro. Furthermore, we found that ABA was significantly less potent than the synthetic agonist rosiglitazone, although it remains unclear whether this decreased potency is caused by a weaker affinity of ABA for PPARγ or a more limited uptake by cells. Other natural and endogenous substances, including fatty acids and eicosanoids,[18] components of oxidized low-density lipoproteins,[19] and oxidized alkyl phospholipids,[20] have also been found to activate PPARγ in vitro· However, PPARγ activation in vitro does not always result in transcriptional regulation of PPAR-responsive genes or beneficial health effects in vivo.[18,21] Furthermore, molecular evidence in vivo is more definitive in assessing the potential PPARγ-activating abilities of natural agonistic ligands.[22]

In order to test the ability of ABA to activate PPARγ in vivo, we fed prediabetic db/db mice 0, 100, 200, 400, and 800 mg of a racemic ABA mixture/kg as part of a high-fat diet for 36 days. Though obesity in db/db mice is attributed to a monogenic mutation of the long leptin receptor, in similar action to patients with the metabolic syndrome, their development of insulin resistance is thought to stem from adipocyte hypertrophy and WAT macrophage infiltration and inflammation. Mice consuming the ABA-supplemented diets had significantly lower fasting blood glucose concentrations and responded better to an IPGTT than mice fed the isocaloric control diet. Moreover, all ABA-supplemented diets appeared to have a similar effect in improving glucose homeostasis, regardless of the amount of ABA from 100 to 800 mg/kg. This finding agrees with in vitro results indicating that concentrations above 12.5 μM ABA induced similar PPARγ transactivation, and this may yet indicate that doses lower than 100 mg/kg ABA may also be effective. Commensurate with the enhancement in glucose tolerance, we found that the expression of PPARγ and PPARγ-responsive genes adiponectin, CD36, and aP2 were significantly increased in WAT from db/db mice fed the ABA-supplemented diet. The increase in adiponectin production is

significant in itself as it has been shown to promote insulin-stimulated glucose disposal in muscle,[23] decrease hepatic glucose production,[24] and increase the oxidation of intramuscular fatty acids.[25] Consequently, it is possible that some of the improvements in glucose homeostasis brought on by dietary ABA supplementation are mediated by this important adipokine.

Another main effect of PPARγ activation in WAT is the reduction in hypertrophic adipocytes, which are less sensitive to insulin and secrete more pro-inflammatory adipokines than normal-sized adipocytes.[9,26,27] By promoting adipogenesis and adipocyte differentiation, TZDs create numerous smaller adipocytes which enhance the absorption of triglycerides, glucose, and free fatty acids from the bloodstream and prevent lipotoxicity in other organs.[27] These changes are also associated with a significant reduction in the expression of macrophage surface markers CD68, CD11b, and F4/80 in WAT,[8] suggesting decreased macrophage infiltration. The macrophages in the SVF, which also contains preadipocytes, T cells and endothelial cells, are the main producers of WAT-derived TNF-α (9), which impairs insulin signaling by increasing serine phosphorylation of IRS-1[28] and worsens obesity-related inflammation. Histological analysis of WAT revealed that mice receiving the ABA-supplemented diet had significantly more small adipocytes than control mice. This attenuation in adipocyte hypertrophy was associated with significant reductions in both macrophage infiltration and TNF-α expression.

While ABA and synthetic PPARγ agonists (i.e., rosiglitazone) elicit similar effects on adipose tissue morphology, treatment with ABA did not induce any weight gain, a major side effect associated with TZD treatment.[17] Initially thought to be solely related to the increase in adipogenesis, it is now believed that a main contributor to TZD-associated weight gain is increased fluid retention via the PPARγ-dependent induction of the Na+ transporter EnaC.[16] Conditional knockout of PPARγ in the renal collecting ducts prevents TZD-induced weight gain.[16] Approximately 10–15% of patients using TZDs are forced to discontinue treatment due to edema, and the increase in extracellular volume from excess fluid retention also poses a major problem for individuals with pre-existing congestive heart failure.[29,30] The lack of weight gain in our study suggests that fluid retention either does not occur or is very minimal in ABA-fed mice, and we suspect this may be due to the lower potency of ABA for PPARγ in comparison with TZDs. The significant increase in BAT may also have contributed to the slight, but insignificant, weight reduction of ABA-fed mice when

compared to controls due to the extra thermogenic capacity of this tissue. The finding that dietary ABA increases BAT is consistent with previous publications which found that PPARγ activation increases BAT differentiation.[31] While the effect of increased BAT in regard to glucose homeostasis is not fully understood, increased BAT in ABA-fed mice may also have contributed to their improved glucose tolerance, as the promotion of lipid accumulation and fatty acid oxidation in this tissue limit WAT adipocyte hypertrophy and lipid deposition into other peripheral tissues, such as liver and skeletal muscle. Accordingly, we observed a significant decrease in liver sizes, an observation that may be linked to reduced lipid accumulation as a result of increased WAT and BAT differentiation.

ABA is a widely studied naturally occurring phytohormone that plays a key role in many different processes in plants, including stress response, leaf abscission, growth and development, and germination.[32–35] Interestingly, ABA is also a key component of sugar sensitivity, as plants deficient of ABA are glucose insensitive.[35,36] While ABA is ubiquitously found in plants, and therefore consumed by humans as a part of the daily diets, its natural content ranges from 5–15 mg/kg in leaves.[37] Thus, the doses that can be attained by vegetable intake would be significantly lower than those required for efficacy against non-insulin dependent diabetic and pre-diabetic states. This is the first study to explore the effect of this bioactive molecule in the prevention of T2D. Our finding that ABA is a novel PPARγ ligand opens the possibility that this compound could be used as a safe and effective alternative to the synthetic agonists for the 20.8 million Americans with T2D and the millions more afflicted by prediabetes, though future studies will need to be conducted that confirm our preliminary findings that ABA appears both safe and non-toxic. The therapeutic potential of ABA against T2D is promising, and as more is learned about other uses of natural PPARγ agonists for treating chronic inflammatory diseases such as atherosclerosis, type 1 diabetes, multiple sclerosis and inflammatory bowel disease, this potential will only continue to grow.

Acknowledgements

References

1. Mokdad AH, Bowman BA, Ford ES, Vinicor F, Marks JS, Koplan JP. The continuing epidemics of obesity and diabetes in the United States. *JAMA* 2001;**286**:1195–200.
2. *CDC: national diabetes fact sheet: general information and national estimates on diabetes in the United States, 2005*. US Department of Health and Human Services, Center for Disease Control and Prevention, 2005 Atlanta, Georgia, 2005. p. 1–10
3. Narayan KM, Boyle JP, Thompson TJ, Sorensen SW, Williamson DF. Lifetime risk for diabetes mellitus in the United States. *JAMA* 2003;**290**:1884–90.
4. Wellen KE, Hotamisligil GS. Inflammation, stress, and diabetes. *J Clin Invest* 2005;**115**:1111–9.
5. Cinti S, Mitchell G, Barbatelli G, et al. Adipocyte death defines macrophage localization and function in adipose tissue of obese mice and humans. *J Lipid Res* 2005;**46**:2347–55.
6. Lehmann JM, Moore LB, Smith-Oliver TA, Wilkison WO, Willson TM, Kliewer SA. An antidiabetic thiazolidinedione is a high affinity ligand for peroxisome proliferator-activated receptor gamma (PPARgamma). *J Biol Chem* 1995;**270**: 12953–6.
7. Bassaganya-Riera J, Guri A, King J, Hontecillas R. Peroxisome proliferator-activated receptors: the nutritionally controlled molecular networks that integrate inflammation, immunity and metabolism. *Curr Nutr Food Sci* 2005;**1**:179–87.
8. Xu H, Barnes GT, Yang Q, et al. Chronic inflammation in fat plays a crucial role in the development of obesity-related insulin resistance. *J Clin Invest* 2003;**112**:1821–30.
9. Weisberg SP, McCann D, Desai M, Rosenbaum M, Leibel RL, Ferrante Jr. AW. Obesity is associated with macrophage accumulation in adipose tissue. *J Clin Invest* 2003;**112**: 1796–808.
10. Nesto RW, Bell D, Bonow RO. Thiazolidinedione use, fluid retention, and congestive heart failure: a consensus statement from the American Heart Association and American Diabetes Association. *Circulation* 2003; **108**: 2941–8.
11. Wysowski DK, Armstrong G, Governale L. Rapid increase in the use of oral antidiabetic drugs in the United States, 1990–2001. *Diabetes Care* 2003;**26**:1852–5.
12. Yu C, Chen L, Luo H, et al. Binding analyses between human PPARgamma-LBD and ligands. *Eur J Biochem* 2004;**271**: 386–97.
13. Lin BL, Wang HJ, Wang JS, Zaharia LI, Abrams SR. Abscisic acid regulation of heterophylly in *Marsilea quadrifolia* L.: effects of R-(−) and S-(+) isomers. *J Exp Bot* 2005;**56**:2935–48.
14. Hontecillas R, Wannemeulher MJ, Zimmerman DR, et al. Nutritional regulation of porcine bacterial-induced colitis by conjugated linoleic acid. *J Nutr* 2002;**132**:2019–27.
15. Bassaganya-Riera J, Pogranichniy RM, Jobgen SC, et al. Conjugated linoleic acid ameliorates viral infectivity in a pig model of virally induced immunosuppression. *J Nutr* 2003;**133**: 3204–14.
16. Guan Y, Hao C, Cha DR, et al. Thiazolidinediones expand body fluid volume through PPARgamma stimulation of ENaC-mediated renal salt absorption. *Nat Med* 2005;**11**:861–6.
17. Kawasaki F, Matsuda M, Kanda Y, Inoue H, Kaku K. Structural and functional analysis of pancreatic islets preserved by pioglitazone in db/db mice. *Am J Physiol Endocrinol Metab* 2005;**288**:E510–8.
18. Desvergne B, Wahli W. Peroxisome proliferator-activated receptors: nuclear control of metabolism. *Endocr Rev* 1999;**20**:649–88.
19. Nagy L, Tontonoz P, Alvarez JG, Chen H, Evans RM. Oxidized LDL regulates macrophage gene expression through ligand activation of PPARgamma. *Cell* 1998;**93**:229–40.
20. McIntyre TM, Pontsler AV, Silva AR, et al. Identification of an intracellular receptor for lysophosphatidic acid (LPA): LPA is a transcellular PPARgamma agonist. *Proc Natl Acad Sci USA* 2003;**100**:131–6.
21. Lehrke M, Lazar MA. The many faces of PPARgamma. *Cell* 2005;**123**:993–9.
22. Bassaganya-Riera J, Reynolds K, Martino-Catt S, et al. Activation of PPARgamma and delta by conjugated linoleic acid mediates protection from experimental inflammatory bowel disease. *Gastroenterology* 2004;**127**:777–91.
23. Ouchi N, Kihara S, Arita Y, et al. Adiponectin, an adipocyte-derived plasma protein, inhibits endothelial NF-kappaB signaling through a cAMP-dependent pathway. *Circulation* 2000;**102**:1296–301.

24. Berg AH, Combs TP, Du X, Brownlee M, Scherer PE. The adipocyte-secreted protein Acrp30 enhances hepatic insulin action. *Nat Med* 2001;**7**:947–53.

25. Fruebis J, Tsao TS, Javorschi S, et al. Proteolytic cleavage product of 30-kDa adipocyte complement-related protein increases fatty acid oxidation in muscle and causes weight loss in mice. *Proc Natl Acad Sci USA* 2001;**98**:2005–10.

26. Trayhurn P, Wood IS. Adipokines: inflammation and the pleiotropic role of white adipose tissue. *Br J Nutr* 2004;**92**: 347–55.

27. de Souza CJ, Eckhardt M, Gagen K, et al. Effects of pioglitazone on adipose tissue remodeling within the setting of obesity and insulin resistance. *Diabetes* 2001;**50**:1863–71.

28. Zick Y. Insulin resistance: a phosphorylation-based uncoupling of insulin signaling. *Trends Cell Biol* 2001;**11**:437–41.

29. Mudaliar S, Chang AR, Henry RR. Thiazolidinediones, peripheral edema, and type 2 diabetes: incidence, pathophysiology, and clinical implications. *Endocr Pract* 2003;**9**:406–16.

30. Page II RL, Gozansky WS, Ruscin JM. Possible heart failure exacerbation associated with rosiglitazone: case report and literature review. *Pharmacotherapy* 2003;**23**:945–54.

31. Tai TA, Jennermann C, Brown KK, et al. Activation of the nuclear receptor peroxisome proliferator-activated receptor gamma promotes brown adipocyte differentiation. *J Biol Chem* 1996;**271**:29909–14.

32. Gomez-Cadenas A, Tadeo FR, Talon M, Primo-Millo E. Leaf Abscission induced by ethylene in water-stressed intact seedlings of Cleopatra mandarin requires previous abscisic acid accumulation in roots. *Plant Physiol* 1996;**112**:401–8.

33. Gubler F, Millar AA, Jacobsen JV. Dormancy release, ABA and pre-harvest sprouting. *Curr Opin Plant Biol* 2005;**8**:183–7.

34. Goliber TE, Feldman LJ. Osmotic stress, endogenous abscisic acid and the control of leaf morphology in *Hippuris vulgaris* L. *Plant Cell Environ* 1989;**12**:163–71.

35. Finkelstein RR, Gibson SI. ABA and sugar interactions regulating development: cross-talk or voices in a crowd? *Curr Opin Plant Biol* 2002;**5**:26–32.

36. Arenas-Huertero F, Arroyo A, Zhou L, Sheen J, Leon P. Analysis of *Arabidopsis* glucose insensitive mutants, gin5 and gin6, reveals a central role of the plant hormone ABA in the regulation of plant vegetative development by sugar. *Genes Dev* 2000;**14**:2085–96.

37. Le Hir R, Leduc N, Jeannette E, Viemont JD, Pelleschi-Travier S. Variations in sucrose and ABA concentrations are concomitant with heteroblastic leaf shape changes in a rhythmically growing species (Quercus robur). *Tree Physiol* 2005;**26**:229–38.

45

CHAPTER 4: THE LOSS OF PPAR γ IN IMMUNE CELLS IMPAIRS THE ABILITY OF ABSCISIC ACID TO IMPROVE INSULIN SENSITIVITY BY SUPPRESSING MONOCYTE CHEMOATTRACTANT PROTEIN-1 EXPRESSION AND MACROPHAGE INFILTRATION INTO WHITE ADIPOSE TISSUE

The loss of PPAR γ in immune cells impairs the ability of abscisic acid to improve insulin sensitivity by suppressing monocyte chemoattractant protein-1 expression and macrophage infiltration into white adipose tissue

Amir J. Guri[1], Raquel Hontecillas[1], Gerardo Ferrer[1], Oriol Casagran[1], Umesh Wankhade[1], Alexis M. Noble[1], Decio L. Eizirik[2], Fernanda Ortis[2], Miriam Cnop[2], Dongmin Liu[1], Hongwei Si[1] and Josep Bassaganya-Riera[1]

[1]Laboratory of Nutritional Immunology and Molecular Nutrition; Virginia Polytechnic Institute and State University, Blacksburg, VA 24061 and [2]Laboratory of Experimental Medicine; Université Libre de Bruxelles, B-1070 Brussels, Belgium

Running head: Macrophage PPAR γ in obesity-related inflammation

CORRESPONDENCE: Dr. Josep Bassaganya-Riera: jbassaga@vt.edu

Abstract

Abcisic acid (ABA) is a natural phytohormone and PPARgamma agonist that significantly improves insulin sensitivity in db/db mice. Though it has become clear that obesity is associated with macrophage infiltration into white adipose tissue (WAT), the phenotype of adipose tissue macrophages (ATMs) and the mechanisms by which insulin-sensitizing compounds modulate their infiltration remains unknown. We used a loss-of-function approach to investigate whether ABA ameliorates insulin resistance through a mechanism dependent on immune cell PPARgamma. We characterized two phenotypically distinct ATM subsets in db/db mice based on their surface expression of F4/80. The F4/80^{hi} ATMs were more abundant and expressed greater concentrations of chemokine receptor 2 (CCR2) and CCR5 when compared to F4/80^{lo} ATMs. ABA significantly decreased CCR2^{+}F4/80^{hi} infiltration into WAT and suppressed monocyte chemoattractant protein-1 (MCP-1) expression in WAT and plasma. Furthermore, the deficiency of PPARgamma in immune cells, including macrophages, impaired the ability of ABA to suppress infiltration of F4/80^{hi} ATMs into WAT, repress WAT MCP-1 expression and improve glucose tolerance. We provide molecular evidence *in vivo* demonstrating that ABA improves insulin sensitivity and obesity-related inflammation by inhibiting MCP-1 expression and F4/80^{hi} ATM infiltration through a PPARgamma-dependent mechanism.

1. Introduction

Obesity is characterized by a low-grade chronic inflammation and insulin resistance. In parallel with the obesity epidemic, the prevalence of insulin resistance and type II diabetes (T2D) has also seen a precipitous growth [1]. Adipocyte hypertrophy is believed to be at the core of the pathogenesis of obesity-induced insulin resistance [2, 3]. Hypertrophic adipocytes are insulin resistant and secrete more free fatty acids (FFAs) and triglycerides (TGs) than they take up, leading to lipid deposition in peripheral tissues such as the liver and skeletal muscle; they also produce chemokines, such as monocyte chemoattractant protein 1 (MCP-1) and macrophage inflammatory protein 1α (MIP-1 α), which promote macrophage infiltration into white adipose tissue (WAT) [4-6]. Macrophages, and not adipocytes, are the main pro-inflammatory mediators in WAT and these cells play a prominent role in the induction and maintenance of obesity-induced inflammation and insulin resistance [2, 5].

Thiazolidinediones (TZDs) are drugs that improve systemic insulin sensitivity mostly by activating the nuclear receptor peroxisome proliferator-activated receptor γ (PPAR γ) [7]. This nuclear receptor is endogenously activated by some polyunsaturated fatty acids and products of lipid metabolism [8]. PPAR γ activation significantly attenuates adipocyte hypertrophy and inhibits WAT inflammation [5, 9]. The prevailing notion is that the beneficial actions of TZDs in uncoupling of obesity from insulin resistance are mediated by adipocyte PPAR γ, which induces the transcription of a number of adipogenic genes and is essential for the differentiation of pre-adipocytes into adipocytes [8, 10, 11]. The increased adipocyte differentiation induced by PPAR γ ligands significantly increases the number of small, insulin-sensitive adipocytes,

augmenting insulin-stimulated glucose, FFA, and TG uptake from circulation, and partitioning FFA away from skeletal muscle and liver; these effects will result in decreased extra-adipose fat deposition [12].

Immune cells, the key pro-inflammatory mediators in WAT of obese mice and humans, also express PPAR γ and are plausible therapeutic targets for PPAR γ agonists [13, 14]. Thus, it is possible that the clinically proven efficacy of PPAR γ agonists in type 2 diabetes prevention and treatment [15] is also mediated via the anti-inflammatory actions of PPAR γ activation in immune cells. At the molecular level, PPAR γ is a direct transcriptional repressor of chemokine receptor 2 (CCR2), the receptor for MCP-1 [16], which is prominently expressed in immune cells, including macrophages. Moreover, MCP-1 expression and secretion are significantly inhibited in WAT following treatment with synthetic PPAR γ ligands [4, 5]. Whole-body disruption of either the *Ccr2* or *Mcp-1* genes has recently been shown to ameliorate obesity-induced insulin resistance by dampening the recruitment of macrophages into WAT [17-19]. MCP-1 directly inhibits the insulin signaling pathway and may be involved in the progression of hepatic steatosis, which is a paradigm of insulin resistance states due to the preserved lipid storage capacity and enhanced gluconeogenesis in the insulin resistant liver [18, 19].

Despite the impressive and persistent benefits of synthetic PPAR γ ligands in improving systemic insulin sensitivity, their side-effects, including fluid retention, weight gain, and in some cases congestive heart failure [20], make them unlikely candidates for insulin resistance prevention. Against this background, our laboratory has recently begun examining the insulin-sensitizing effects of the phytochemical and novel PPAR γ agonist abscisic acid (ABA). Administration of ABA to db/db mice improves glucose tolerance

and upregulates PPAR γ and PPAR γ-responsive gene expression in WAT without affecting body weight [21]. We also observed a significant suppression in WAT TNF-α mRNA expression and macrophage infiltration in ABA-fed db/db mice [21].

To further characterize these promising findings, the present study aims to dissect the expression of PPAR γ-responsive and inflammatory genes by adipocytes versus stromal vascular cells (SVC)s in WAT. We also phenotypically characterized the subsets of adipose tissue macrophages (ATM) targeted by ABA and determine whether ABA ameliorates insulin resistance and obesity-related inflammation through a mechanism dependent upon immune cell PPAR γ. Our data demonstrate that SVCs, and not the adipocytes, are the main producers of PPAR γ-responsive genes and chemokines in WAT. In addition, we provide *in vivo* molecular evidence suggesting that ABA ameliorates glucose tolerance and obesity-related inflammation by suppressing MCP-1 expression and F4/80$^{\text{hi}}$ macrophage infiltration into WAT through a mechanism dependent on immune cell PPAR γ.

2. Materials and Methods

2.1. Mice and dietary treatments

BKS.Cg -+Lepr$^{\text{db}}$ /+Lepr$^{\text{db}}$ /OlaHsd (db/db), PPAR γ flfl; MMTV-Cre^{+} and PPAR γ flfl; MMTV-Cre^{-} mice in a C57BL/6J background were housed at the animal facilities at Virginia Polytechnic Institute and State University in a room maintained at 22° C, with a 12:12 h light-dark cycle starting from 6:00 AM. All experimental procedures were approved by the Institutional Animal Care and Use Committee of Virginia Polytechnic

Institute and State University and met or exceeded requirements of the Public Health Service/National Institutes of Health and the Animal Welfare Act.

Db/db mice (n=10) were fed high-fat diets with a previously described ingredient composition [21] containing 0 or 100 mg of racemic ABA (Sigma Aldrich, St. Louis, MS)/kg diet for 36 days. On day 36, fasted mice (12h) were sacrificed by CO_2 narcosis and blood was withdrawn directly from the heart for assessment of fasting glucose levels with an Accu-Chek® Glucometer (Roche, Indianapolis, IN). Plasma was also collected for analysis of MCP-1 protein levels and plasma triglycerides (TGs). Abdominal WAT was then excised to generate single cell suspensions for flow cytometry. Liver specimens were placed in 10% buffered neutral formalin for histological evaluation. Liver samples were also stored in RNA later (Ambion, Austin, TX), a commercial solution that inhibits RNases, for RNA isolation and quantitative gene expression analyses.

PPAR γ floxed mice expressing the Cre transgene (e.g., PPAR-γ fl/fl; MMTV-Cre) undergo premature termination of translation following the loss of the exon 2 of PPAR γ due to the enzymatic activity of the recombinase on genomic DNA [22, 23]. PPAR γ flfl; MMTV-Cre[+] and PPAR γ flfl; MMTV-Cre[-] littermate mice were fed high-fat diets with or without ABA (100 mg/kg). After 28 weeks, the mice were fasted for 6 hours and bled through the caudal vein for assessment of fasting blood glucose concentrations by using an Accu-Chek® Glucometer (Roche, Indianapolis, IN). The mice were then subjected to an intraperitoneal glucose tolerance test (2 g/kg body weight), with determination of glucose levels at 15, 30, and 90 minutes post-challenge. At the 90 minute timepoint, mice were sacrificed by CO_2 narcosis. Abdominal WAT was then excised to generate single-cell suspensions for flow cytometry or placed in 10% buffered

neutral formalin for histological evaluation and stored in RNA later (Ambion, Austin, TX) for RNA isolation and quantitative gene expression analyses.

2.2. WAT Digestion

Abdominal WAT was excised, weighed, minced into small <10 mg pieces and placed into digestion media consisting of DMEM (Mediatech, Herndon, VA) supplemented with 2.5% HEPES (Mediatech) and 10 mg/mL fatty-acid free bovine serum albumin (FAB-poor BSA, Sigma), Liberase Blendzyme 3 (0.03 mg/mL, Roche) and DNase I (50 U/mL, Qiagen, Valencia, CA). Samples were incubated in a rotating 37°C water bath for 90 minutes and then filtered through a 250 μm nylon mesh (Sefar America Inc., Depew, New York) to remove undigested particles and centrifuged at 4°C at 1,000 x g for 10 minutes. The pellet, consisting of stromal vascular cells (SVCs), containing endothelial cells, pre-adipocytes, macrophages and T cells, was washed with DMEM and centrifuged at 4°C at 1,000 x g for 10 minutes. The supernatant was discarded and erythrocytes were lysed by incubating the SVCs in 2 mL erythrocyte lysis buffer for 2 minutes before stopping the reaction with 9 mL 1X phosphate-buffered saline (PBS). Cells were then centrifuged again at 4°C at 1,000 x g for 10 minutes, suspended in 1 ml of 1X PBS, and enumerated with a Z1 Single Particle Counter (Beckman Coulter, Fullerton, CA). The SVCs were resuspended in FACS buffer (1X PBS, 1% normal goat serum, 0.2% sodium azide) at a concentration of 2×10^6 cells/mL. The SVCs not used in the resuspensions were centrifuged for 5 minutes at 10,000 x g, resuspended in RLT lysis buffer (Qiagen) containing 1% β-mercaptoethanol, and immediately frozen at -80°C for RNA isolation and gene expression analyses.

2.3. Flow Cytometry

SVCs (2 x 10^5 cells) were seeded into 96-well plates and centrifuged at 4°C at 1,800 x g

for 4 minutes. The cells were then incubated in the dark at 4°C for 20 minutes in

FcBlock (20 µg/ml; BD Pharmingen), and then for an additional 20 minutes with

fluorochrome-conjugated primary antibodies anti-F4/80-PE-Cy5 (5 µg/mL), anti-CD11b-

FITC (2 µg/mL) (eBioscience), anti-CCR5-PE or anti-CCR2-PE (R&D systems,

Minneapolis, MN). The specific antibody combinations used were F4/80, CD11b, CCR5

and F4/80, CD11b, CCR2. After incubation with primary antibodies, cells were

centrifuged at 4°C at 1,800 x g for 4 minutes and washed with 200 µL of FACS buffer.

After washing, cells were suspended in 200 µL PBS and 3-color data acquisition was

performed on a FACS Calibur flow cytometer. Data analyses were performed by using

the CellQuest software (BD).

2.4. Quantitative real-time reverse transcriptase PCR

Total RNA was isolated from SVCs and liver using the RNA isolation Minikit (Qiagen)

according to the manufacturer's instructions. RNA from the adipocyte fraction and WAT

was isolated using the Lipid Minikit (Qiagen). Total RNA (1 µg) was used to generate

complementary DNA (cDNA) template using the iScript cDNA Synthesis Kit (Bio-Rad,

Hercules, CA). The total reaction volume was 20 µL with the reaction incubated as

follows in an MJ MiniCycler: 5 minutes at 25°C, 30 minutes at 52°, 5 minutes at 85°C,

hold at 4°C. PCR was performed on the cDNA using Taq DNA polymerase obtained

from Invitrogen and using previously described conditions [23]. Each gene amplicon

was purified with the MiniElute PCR Purification Kit (Qiagen) and quantitated on an agarose gel by using a DNA mass ladder (Promega). These purified amplicons were used to optimize real-time PCR conditions and to generate standard curves in the real-time PCR assay. Primer concentrations and annealing temperatures were optimized for the iCycler iQ system (Bio-Rad) for each set of primers using the system's gradient protocol. PCR efficiencies were maintained between 92 and 105% and correlation coefficients above 0.98 for each primer set (Table 1) during optimization and also during the real-time PCR of sample DNA.

Complementary DNA (cDNA) concentrations for genes of interest were examined by real-time quantitative PCR using an iCycler IQ System and the iQ SYBR green supermix (Bio-Rad). A standard curve was generated for each gene using 10-fold dilutions of purified amplicons starting at 5 pg of cDNA and used later to calculate the starting amount of target cDNA in the unknown samples. SYBR green I is a general double-stranded DNA intercalating dye and may therefore detect nonspecific products and primer/dimers in addition to the amplicon of interest. In order to determine the number of products synthesized during the real-time PCR, a melting curve analysis was performed on each product. Real-time PCR was used to measure the starting amount of nucleic acid of each unknown sample of cDNA on the same 96-well plate. Results are presented as starting quantity of target cDNA (picograms) per microgram of total RNA.

2.5. Hepatic Steatosis, plasma MCP-1 and liver triglyceride content
Liver specimens were excised and immediately fixed in 10% phosphate buffered neutral formalin, embedded in paraffin, cut at thicknesses of 5 microns and stained with

hematoxylin and eosin (H&E) for histological examination. For hepatic triglyceride

assessment, livers fragments (50–100 mg) were extracted for 16 hours at 4°C with 4 ml

CHCl$_3$/methanol (2:1, vol/vol). Two milliliters of 0.6% NaCl were then added to the

extract, and the mixture was centrifuged at 2,000 g for 20 minutes. Lipids were isolated

by nitrogen evaporation, dissolved in 100 μL isopropanol, and quantified with a

triglyceride assay kit (Stanbio). The Triglyceride Assay Kit (Sigma) and Ready-set-go

MCP-1 ELISA (ebioscience) were used to quantify plasma TGs and MCP-1,

respectively, according to manufacturer's instructions.

2.6. Transfection of 3T3-L1 preadipocytes

A pCMX.PPAR γ expression plasmid (kindly provided by Dr. R.M. Evans, The Salk

Institute, San Diego, CA) and pMCP-1-514(enh) luc construct [24] were purified using

Qiagen's Maxi kit (Valencia, CA). 3T3-L1 cells (American Type Culture Collection,

Manassas, VA) were grown in 24-well plates in DMEM high glucose medium

(Invitrogen, Carlsbad, CA) containing 10% fetal bovine serum (FBS) until 60-70%

confluence. Before transfection, the medium was changed to 1% FBS. The cells cultured

in 24-well plates were co-transfected with 0.8 μg plasmid DNA and 1 ng of pRL reporter

control plasmid per well using F-1 transfection reagents (Targeting Systems, Santee, CA)

according to the manufacturer's protocol. Transfection efficiencies were determined by

cotransfecting the cells with a pcDNA™ 3.1/His/*lac*Z control vector at 24 h. The

transfected cells were then treated with either a racemic ABA mixture (12.5 μM; Sigma)

or rosiglitazone (1 μM; Cayman Chemicals, Ann Arbor, MI) for 24 hours. Designated

wells were also treated with the PPAR γ antagonist GW9662 (30 μM; Cayman

56

Chemicals). Transfected cells were harvested in reporter lysis reagent. Luciferase

activity, normalized to pRL activity in the cell extracts was determined by using the dual

luciferase reporter assay system (Promega, Madison, WI) in a TD-20/20 Single-Tube

Luminometer (Turner Biosystems, Sunnyvale, CA). Relative luciferase activity (RLA)

was calculated as a ratio of the chemiluminescence 10 seconds after the Luciferase Assay

Reagent II (Promega) was added over the chemiluminescence 10 seconds after the

Stop&Glo Reagent (Promega).

2.7. *Statistical Analyses*

For db/db experiment, data were analyzed as a completely randomized design. To

determine the statistical significance of the model, analysis of variance (ANOVA) was

performed using the general linear model procedure of Statistical Analysis Software

(SAS). In the experiment using PPAR γ flfl; MMTV-Cre$^+$ and PPAR γ flfl; MMTV-Cre$^-$

mice, data were analyzed as a 2×2 factorial arrangement within a completely

randomized design. The statistical model utilized was $Y_{ijk} = \mu +$ Genetic Background$_i +$

Diet$_j +$ (Genetic Background x Diet)$_{ij} +$ Error$_{ijk}$. To determine the statistical significance

of the model, analysis of variance (ANOVA) was performed using the general linear

model procedure of SAS, and probability value $(P) < 0.05$ was considered to be

significant. When the model was significant, ANOVA was followed by Fisher's

Protected Least Significant Difference multiple comparison method. Non-parametric data

were analyzed by using the Mann-Whitney *U* test followed by a Dunn's multiple

comparison's test.

3. Results

3.1. ABA improves fasting glucose and lowers plasma triglycerides in db/db mice without affecting body weight

ABA-supplementation to db/db mice for 36 days significantly lowers fasting glucose levels and improves their response to an intraperitoneal glucose tolerance test [21]. Similar to these previous findings, ABA did not alter food intake or body weights of the db/db mice throughout the course of the experiment (Figure 1A and B). In this study, the db/db mice fed the ABA-supplemented diet had significantly lower fasting blood glucose (FBG) and plasma TGs concentrations when compared to mice fed the control high-fat diet (Figure 1C and D).

3.2. The stromal-vascular fraction (SVF) contains two phenotypically distinct macrophage sub-populations

To characterize the phenotypical differences in ATM in the SVF we examined surface expression of F4/80 and CD11b and chemokine receptors (CCR2 and CCR5).   SVCs were isolated from adipocytes by gradient centrifugation and subsequently gated on the immune cell population based on forward versus side scatter (Figure 2A). We identified two phenotypically distinct sub-populations of $F4/80^+CD11b^+$ macrophages in the SVF of WAT which differed in their mean fluorescence intensity (MFI) for F4/80, yielding a macrophage subset expressing high surface concentrations of the F4/80 molecule ($F4/80^{hi}$) and a subset expressing low surface concentrations of the F4/80 molecule ($F4/80^{lo}$) (Figure 2B, 2C). The $F4/80^{hi}$ population was more abundant in WAT than the $F4/80^{lo}$ subset, encompassing approximately 75% of total macrophages versus 25% in

58

control-fed db/db mice, respectively (Figure 2B). The F4/80^{hi} macrophage subset also expressed higher surface concentrations of CCR2 and CCR5 when compared to the F4/80^{lo} subset (Figure 2G).

3.3. ABA inhibits F4/80^{hi} macrophage infiltration into WAT

After characterizing these two macrophage sub-populations, we next determined whether ABA targeted one of these populations or both. We found that ABA significantly suppressed F4/80^{hi} macrophage infiltration into WAT (*P*=0.05) but had no effect on the F4/80^{low} ATM (Figure 3). In addition, the amount of F4/80 expressed in the surface of F4/80^{hi} macrophages administered ABA, as measured by MFI, was significantly lower than that in mice fed the control diet (Figure 3L). The differences observed in the F4/80^{hi} population in mice fed ABA were due primarily to a reduction in a subset of F4/80^{hi}CD11b^{+}CCR2^{+}ATM (*P*=0.006).

3.4. ABA decreases MCP-1 mRNA expression in WAT, MCP-1 protein concentrations in plasma and attenuates liver triglyceride accumulation and hepatic steatosis

A significant reduction in the infiltration of the F4/80^{hi}CD11b^{+}CCR2^{+} macrophage subset into WAT could be due to attenuated CCR2 surface expression in monocytes, repression of CCR2 ligand expression in WAT, or both. CCR2 and its principal ligand, MCP-1, have been recently linked to the development of obesity-induced insulin resistance [17-19]. To determine whether ABA inhibited MCP-1 expression in WAT, we assessed levels of MCP-1 mRNA content in the stromal vascular fraction (i.e., macrophages, T cells, fibroblasts, preadipocytes and endothelial cells) and in the adipocyte fraction. Both

WAT fractions produce MCP-1 in obese mice and humans [2]. We found that ABA decreased the concentrations of MCP-1 mRNA by almost 15-fold in SVCs. There was also a significant reduction in MCP-1 mRNA in the adipocyte fraction following ABA-supplementation (P=0.05), though this reduction was not as drastic as the difference we observed in SVCs (Figure 4A). PPAR γ mRNA expression was higher in both SVCs and adipocytes (Figure 4B), but expression of the well-known PPAR γ-responsive gene and fatty acid transporter, CD36, was only significantly elevated in SVCs (Figure 4C). We did not see significant differences in the mRNA expression of MIP-1α or the innate immune receptor toll-like receptor 4 (TLR-4) in either SVCs or adipocytes (data not shown).

We next determined whether the suppressed MCP-1 expression observed in WAT of ABA-fed mice resulted in decreased plasma MCP-1 concentrations. MCP-1 protein concentrations were significantly decreased in plasma, but not in liver, from ABA-fed mice (Figures 4D and E), suggesting that WAT-derived MCP-1 may elicit systemic actions. In a recent study, MCP-1-overexpressing mice under control of the aP2-promoter (i.e., adipose tissue specific) had a significantly elevated risk of developing hepatic steatosis [18]. Upon histological examination of liver specimens, we found that the hepatic steatosis was less severe in ABA-fed mice (Figure 4 G). In line with this histological finding, the amount of liver triglycerides was significantly lower in mice fed the ABA-supplemented diet as compared to mice fed the control diet (Figure 4F).

3.5. Targeted deficiency of PPAR γ expression in immune cells impairs the ability of ABA to improve glucose tolerance

The greatest differences in MCP-1 and the PPAR γ-responsive gene CD36 induced by

ABA occurred in SVCs, suggesting that immune cell PPAR γ (and not adipocyte PPAR

γ) is the molecular target for ABA in WAT. To determine whether the ability of ABA to

normalize plasma glucose concentrations following a GTT was mediated through

immune cell PPAR γ, we next fed high-fat diets supplemented with or without ABA to

PPAR γ flfl; MMTV-Cre$^+$ mice, which do not express PPAR γ in hematopoetic cells, and

PPAR γ flfl; MMTV-Cre$^-$ littermates (wild-type phenotype). After 28 weeks of high-fat

feeding, the mice were overweight (Figure 5A). Similar to our findings with db/db mice,

ABA did not increase body weights in either MMTV-Cre$^+$ and MMTV-Cre$^-$ and did not

effect food intake (data not shown). The deficiency of PPAR γ in immune cells

abrogated ABA-induced normalization of fasting blood glucose concentrations 90

minutes following an intraperitoneal GTT (Figure 5B and C).

3.6. Deficient PPAR γ expression in immune cells impairs the ability of ABA to suppress

MCP-1 expression and infiltration of the F4/80^{hi} macrophage subset into WAT

To determine whether the observed differences in glucose tolerance corresponded to

phenotypic changes in SVF macrophage subsets, we investigated the effect of ABA on

both F4/80^{hi} and F4/80^{lo} ATM. Dietary ABA-supplementation significantly decreased

both total SVF macrophage infiltration and the amount of F4/80^{hi} macrophages in mice

expressing PPAR γ in immune cells (i.e., PPAR γ fl/fl; MMTV-Cre-). However, the

deficiency of PPAR γ in immune cells (i.e., PPAR γ fl/fl; MMTV-Cre+) abrogated the

ability of ABA to suppress infiltration of F4/80^{hi} into WAT. Of note, surface CCR2 was

expressed by a greater percentage of ATM from tissue-specific PPAR γ null mice (data not shown).

We next examined whether immune cell PPAR γ was required for the suppressive actions of ABA on WAT MCP-1 mRNA expression. ABA decreased both WAT and plasma MCP-1 levels in mice expressing PPAR γ in immune cells (Figure 6H). However, in line with our findings on F4/80[hi] macrophage infiltration into WAT, the ability of ABA to suppress the expression of MCP-1 in WAT was significantly impaired in tissue-specific PPAR γ null mice, suggesting that ABA acts through a mechanism requiring the expression of PPAR γ in immune cells. The SVF of WAT contains macrophages, T cells, endothelial cells, fibroblasts and pre-adipocytes, but the only cell subsets in this fraction lacking the PPAR γ gene in the tissue-specific PPAR γ null mouse would be the cells of hematopoietic origin i.e., bone marrow-derived macrophages and T cells. Thus, the differences in glucose tolerance observed might be attributed to one or both immune cell subsets.

3.7. ABA inhibits MCP-1 promoter activity through PPAR γ

To further examine the effect of ABA on MCP-1 transactivation 3T3-L1 pre-adipocytes were transfected with a MCP-1 promoter luciferase reporter construct and also co-transfected with a pCMX PPAR γ expression plasmid to increase endogenous PPAR γ activity. Cells were then treated with ABA (12.5 μM), rosiglitazone (1 μM), the PPAR γ antagonist GW9662 (30 μM), or a combination of agonist and inhibitor. We previously found that ABA (12.5 μM) and rosiglitazone (1 μM) were equally effective in inducing PPAR γ transactivation [21]. In this study, co-transfection with the PPAR γ expression

vector significantly enhanced the ability of both ABA and rosiglitazone to inhibit MCP-1 promoter activity (Figure 7). The effects on MCP-1 transactivation by both compounds were significantly inhibited by co-treatment with GW9662.

4. Discussion

The obesity and T2D epidemics follow a similar demographic pattern [1, 25], but little is known about the factors linking obesity to insulin resistance and T2D at the cellular and molecular level. The "FFA efflux theory" proposes that adipocyte dysfunction and extra-adipose fat storage are the central components in the pathogenesis of insulin resistance, highlighting the importance of adipocytes as cellular targets [26-28]. In contrast, the "endocrine theory" suggests that pro-inflammatory mediators play an essential immunopathogenic role, favoring immune cells as central cellular targets for therapies against T2D [29]. PPAR γ is expressed in both adipocytes and immune cells and has been identified as an important therapeutic target both in insulin resistance and T2D. In this report we show that PPAR γ and its responsive gene CD36 are expressed at higher concentrations in SVCs than in adipocytes and that treatment with a novel insulin-sensitizing PPAR γ agonist induces PPAR γ-responsive gene expression primarily in SVCs. These results are also suggestive that TZDs may elicit their insulin-sensitizing actions through PPAR γ expressed in immune cells infiltrating the WAT. Hence, PPAR γ activation in immune cells may be a central regulator of insulin resistance and obesity-related inflammation. In line with this hypothesis, obesity-induced insulin resistance is associated with the infiltration of bone-marrow-derived monocytes into WAT and differentiation into ATM [2, 5]. This study phenotypically characterized the subsets of

63

ATM targeted by ABA and investigated whether this compound ameliorates insulin resistance and obesity-related inflammation through a mechanism dependent upon immune cell PPAR γ.

We have previously found that ABA improves glucose tolerance and reduces total ATM infiltration and TNF-α expression in WAT of db/db mice [21]. To phenotypically characterize the actions of ABA on the ATM population, we presently isolated SVCs from WAT and assayed their expression of the glycoproteins F4/80 and CD11b and of the chemokine receptors CCR2 and CCR5. F4/80 contains extracellular epidermal growth factor (EGF)-like domains and a seven-span transmembrane (TM7) domain; it has been suggested to play a role in cell adhesion and cell signaling and it is widely used as a maturation marker for macrophages [30]. We report for the first time the presence of two phenotypically distinct subsets of macrophages in the SVF of WAT which differ in the amount of surface F4/80 (e.g., F4/80^{lo} and F4/80^{hi}). The newly identified F4/80^{hi} subset is more abundant (i.e., 75% of the macrophages in the SVF) and expresses higher surface concentrations of CCR2 and CCR5 in comparison to the F4/80^{lo} population.

The expression of F4/80 is tightly regulated according to the physiological status of cells. Because the precursor of tissue macrophages, the bone-marrow derived blood monocyte, expresses lower surface F4/80 than its mature counterparts [30], the F4/80^{hi} ATM subset is probably a mature cell type that contributes to obesity-related inflammation, whereas F4/80^{low} ATM may be monocytes, which have recently transmigrated into the WAT. Alternatively, a difference in the ontogeny of F4/80^{hi} and F4/80^{lo} macrophages could account for these two distinct ATM subsets. The SVF, in addition to containing bone marrow-derived cells of myeloid origin, includes pre-

adipocytes that can differentiate into adipocytes or F4/80-expressing macrophages of mesenchymal origin [31]. Resident macrophages from different organs differ considerably in the amount of F4/80 expressed on their surfaces [32]. Moreover, the limited expression of chemokine receptors on the majority of F4/80^{lo} ATMs may be indicative of a predominantly resident population [33].

After phenotypically characterizing these two ATM subsets, we next examined the ability of ABA to differentially modulate their numbers in WAT. We found that ABA decreased the amount of F4/80^{hi}CCR2^{+} ATM but had a negligible effect on the F4/80^{lo} population. Although the effect of synthetic PPAR γ ligands on the infiltration of F4/80^{hi}CCR2^{+} ATM has not been studied, the reduction of this subset of ATM by ABA is in line with the well-characterized ability of PPAR γ to suppress CCR2 expression. At the molecular level, the CCR2 gene contains two promoters which are both repressed by PPAR γ [16] and TZDs downregulate the MCP-1-induced chemotactic response in THP-1 monocytes [34]. Moreover, in obese mice matched for adiposity, *Ccr2* deficiency decreased macrophage content and WAT inflammation while ameliorating hepatic steatosis [17]. We propose that ABA activates PPAR γ in monocytes, which, in turn, suppresses surface CCR2 expression and infiltration of F4/80^{hi} ATM.

We next determined whether ABA downregulated the expression of MCP-1, the main ligand for CCR2, in WAT. Similar to CCR2, MCP-1 is inhibited following TZD treatment in both SVCs and adipocytes [35]. We found a 15-fold decrease in MCP-1 mRNA in the SVF of WAT and a 4-fold decrease in plasma MCP-1. The decrease observed in the SVCs was far greater than the approximately 2-fold decrease Xu et al. obtained following similar short-term intervention with rosiglitazone in ob/ob mice [5].

65

In addition to recruiting macrophages and directly impairing insulin signaling by blocking IRS-1 and Akt phosphorylation [19], MCP-1 was recently shown to increase the risk for hepatic steatosis by activating the gluconeogenic genes phophoenolpyruvate carboxykinase (PEPCK) and glucose-6-phosphatase (G6P) and preserving lipid storage capacity [18]. In line with the suppressed expression of MCP-1 mRNA in WAT and decreased concentrations of MCP-1 protein in plasma of ABA-fed mice, we observed a decreased severity in high-fat diet-induced hepatic steatosis which could not be attributed to differences in MCP-1 mRNA expression in the liver. In addition to the decreased systemic MCP-1 concentrations, the ABA-induced reduction in plasma TGs may contribute to the improvement of liver steatosis. To further characterize the role of PPAR γ in mediating ABA-induced repression of MCP-1, we co-transfected 3T3-L1 pre-adipocytes with a MCP-1 reporter construct and a PPAR γ expression vector. The presence of the expression vector significantly enhanced the ability of both ABA and rosiglitazone to inhibit MCP-1 promoter activity. The effects of both compounds were also inhibited by the selective PPAR γ antagonist GW9662. Because the MCP-1 promoter is not known to contain a PPRE, the inhibition of MCP-1 promoter activity may have occurred though PPAR γ-induced inhibition of NF-κB responsive genes. In 2005, Pascual et al. demonstrated that following ligand binding, the PPAR γ ligand-binding domain (LBD) becomes sumoylated, resulting in its migration to nuclear receptor corepressor (NCoR)-histone deacetylase-3 (HDAC3) complexes on inflammatory gene promoters [36].   The presence of PPAR γ at these sites inhibited the ubiquitination of NCoR that is required for NF-κB-induced transcription of pro-inflammatory genes [36].

Because macrophages are the main producers of MCP-1 in WAT, we next examined whether the deletion of PPAR γ in immune cells would impair the ability of ABA to ameliorate insulin resistance and obesity-related inflammation. For this purpose, we used a mouse model in which the PPAR γ gene has been disrupted in immune cells. While several studies have been performed on muscle specific [37] and adipose tissue-specific PPAR γ null mice [38], little is known about the importance of immune cell PPAR γ in the regulation of insulin resistance and T2D. The PPAR γ fl/fl; MMTV-Cre[+] mice lack PPAR γ in immune and epithelial cells but express it at normal concentrations in adipocytes. Thus, they represent an excellent model to dissect the immune cell-dependent mechanisms of PPAR γ action. We have previously used this loss-of-function approach to characterize *in vivo* the mechanism by which conjugated linoleic acid, another natural agonist of PPAR γ, prevents intestinal inflammation [23]. Our present findings indicate that the loss of PPAR γ in immune cells impairs the ability of ABA to improve glucose tolerance, suppress F4/80[hi] ATM infiltration and down-regulate MCP-1 expression in WAT, suggesting that the protective actions of ABA on insulin resistance are mediated, in part, through a mechanism dependent upon expression of PPAR γ in immune cells. These findings, however, do not preclude that possibility that ABA can also activate other extracellular or intracellular receptors to induce its insulin-sensitizing effects, and current work in our laboratory is being conducted to explore these options. Moreover, since we observed that fasting glucose levels were improved by ABA-supplementation in both the Cre[+] and Cre[-] mice, other cells and tissues including adipocytes, preadipocytes, skeletal muscle, liver, etc. may have played a role in the beneficial effects of ABA.

In summary, we have characterized for the first time two phenotypically distinct subsets of ATM (F4/80^{hi} and F4/80^{lo}) and demonstrated that a novel PPAR γ agonist decreases the infiltration of F4/80^{hi} ATM, MCP-1 expression in WAT, MCP-1 promoter activity and ameliorates insulin resistance through a mechanism requiring immune cell PPAR γ. These data further support the theory that immune cell-derived pro-inflammatory mediators are essential components in the pathogenesis of insulin resistance and T2D. While our data show that F4/80^{hi} ATM are important contributors to the immunopathogenesis of insulin resistance, additional work is needed to characterize the role of other immune cell subsets (i.e., natural killer cells, dendritic cells and regulatory T cells) in modulating this abnormal immune response. Of particular interest are infiltrating regulatory T cells given their higher concentrations of PPAR γ when compared to other T cell subsets and their ability to suppress established inflammation. Uncovering immunoregulatory mechanisms, such as PPAR γ action, by which insulin resistance can be prevented may take us one step closer to halting the epidemics of insulin resistance and T2D.

References

[1]   CDC. National Diabetes Fact Sheet: general information and national estimates on diabetes in the United States, 2005. In: U. S. Department of Health and Human Services, Center for Disease Control and Prevention, 2005. Atlanta, Georgia; 2005. p. 1-10.

[2]   Weisberg SP, McCann D, Desai M, Rosenbaum M, Leibel RL, Ferrante AW, Jr. Obesity is associated with macrophage accumulation in adipose tissue. J Clin Invest l2003;112: 1796-808.

[3]   Cinti S, Mitchell G, Barbatelli G, Murano I, Ceresi E, Faloia E, Wang S, Fortier M, Greenberg AS, Obin MS. Adipocyte death defines macrophage localization and function in adipose tissue of obese mice and humans. J Lipid Res l2005;46: 2347-55.

[4]   Bruun JM, Lihn AS, Pedersen SB, Richelsen B. Monocyte chemoattractant protein-1 release is higher in visceral than subcutaneous human adipose tissue (AT): implication of macrophages resident in the AT. J Clin Endocrinol Metab l2005;90: 2282-9.

[5]   Xu H, Barnes GT, Yang Q, Tan G, Yang D, Chou CJ, Sole J, Nichols A, Ross JS, Tartaglia LA, Chen H. Chronic inflammation in fat plays a crucial role in the development of obesity-related insulin resistance. J Clin Invest l2003;112: 1821-30.

[6]   Gerhardt CC, Romero IA, Cancello R, Camoin L, Strosberg AD. Chemokines control fat accumulation and leptin secretion by cultured human adipocytes. Mol Cell Endocrinol l2001;175: 81-92.

[7]   Lehmann JM, Moore LB, Smith-Oliver TA, Wilkison WO, Willson TM, Kliewer SA. An antidiabetic thiazolidinedione is a high affinity ligand for peroxisome proliferator-activated receptor gamma (PPAR gamma). J Biol Chem l1995;270: 12953-6.

[8]   Desvergne B, Wahli W. Peroxisome proliferator-activated receptors: nuclear control of metabolism. Endocr Rev l1999;20: 649-88.

[9]   Yamauchi T, Kamon J, Waki H, Murakami K, Motojima K, Komeda K, Ide T, Kubota N, Terauchi Y, Tobe K, Miki H, Tsuchida A, Akanuma Y, Nagai R, Kimura S, Kadowaki T. The mechanisms by which both heterozygous peroxisome proliferator-activated receptor gamma (PPARgamma) deficiency and PPARgamma agonist improve insulin resistance. J Biol Chem l2001;276: 41245-54.

[10]   Otto TC, Lane MD. Adipose development: from stem cell to adipocyte. Crit Rev Biochem Mol Biol l2005;40: 229-42.

[11]   Lehrke M, Lazar MA. The many faces of PPARgamma. Cell l2005;123: 993-9.

[12]   Guri AJ, Hontecillas R, Bassaganya-Riera J. Peroxisome proliferator-activated receptors: Bridging metabolic syndrome with molecular nutrition. Clin Nutr l2006;doi:10.1016/j.clnu.2006.08.006.

[13]   Braissant O, Foufelle F, Scotto C, Dauca M, Wahli W. Differential expression of peroxisome proliferator-activated receptors (PPARs): tissue distribution of PPAR-alpha, -beta, and -gamma in the adult rat. Endocrinology l1996;137: 354-66.

[14]   Welch JS, Ricote M, Akiyama TE, Gonzalez FJ, Glass CK. PPARgamma and PPARdelta negatively regulate specific subsets of lipopolysaccharide and IFN-gamma target genes in macrophages. Proc Natl Acad Sci U S A l2003;100: 6712-7.

[15]   Knowler WC, Hamman RF, Edelstein SL, Barrett-Connor E, Ehrmann DA, Walker EA, Fowler SE, Nathan DM, Kahn SE. Prevention of type 2 diabetes with troglitazone in the Diabetes Prevention Program. Diabetes l2005;54: 1150-6.

[16]   Chen Y, Green SR, Ho J, Li A, Almazan F, Quehenberger O. The mouse CCR2 gene is regulated by two promoters that are responsive to plasma cholesterol and peroxisome proliferator-activated receptor gamma ligands. Biochem Biophys Res Commun l2005;332: 188-93.

[17]   Weisberg SP, Hunter D, Huber R, Lemieux J, Slaymaker S, Vaddi K, Charo I, Leibel RL, Ferrante AW, Jr. CCR2 modulates inflammatory and metabolic effects of high-fat feeding. J Clin Invest l2006;116: 115-24.

[18]   Kanda H, Tateya S, Tamori Y, Kotani K, Hiasa K, Kitazawa R, Kitazawa S, Miyachi H, Maeda S, Egashira K, Kasuga M. MCP-1 contributes to macrophage infiltration into adipose tissue, insulin resistance, and hepatic steatosis in obesity. J Clin Invest l2006;116: 1494-505.

[19]   Kamei N, Tobe K, Suzuki R, Ohsugi M, Watanabe T, Kubota N, Ohtsuka-Kowatari N, Kumagai K, Sakamoto K, Kobayashi M, Yamauchi T, Ueki K, Oishi Y, Nishimura S, Manabe I, Hashimoto H, Ohnishi Y, Ogata H, Tokuyama K, Tsunoda M, Ide T, Murakami K, Nagai R, Kadowaki T. Overexpression of monocyte chemoattractant protein-1 in adipose tissues causes macrophage recruitment and insulin resistance. J Biol Chem l2006;281: 26602-14.

[20]   Nesto RW, Bell D, Bonow RO, Fonseca V, Grundy SM, Horton ES, Le Winter M, Porte D, Semenkovich CF, Smith S, Young LH, Kahn R. Thiazolidinedione use, fluid retention, and congestive heart failure: a consensus statement from the American Heart Association and American Diabetes Association. October 7, 2003. Circulation l2003;108: 2941-8.

[21]   Guri AJ, Hontecillas R, Si H, Liu D, Bassaganya-Riera J. Dietary abscisic acid ameliorates glucose tolerance and obesity-related inflammation in db/db mice fed high-fat diets. Clin Nutr l2006;doi:10.1016/j.clnu.2006.07.008.

[22]   Akiyama TE, Sakai S, Lambert G, Nicol CJ, Matsusue K, Pimprale S, Lee YH, Ricote M, Glass CK, Brewer HB, Jr., Gonzalez FJ. Conditional disruption of the peroxisome proliferator-activated receptor gamma gene in mice results in lowered expression of ABCA1, ABCG1, and apoE in macrophages and reduced cholesterol efflux. Mol Cell Biol l2002;22: 2607-19.

[23]   Bassaganya-Riera J, Reynolds K, Martino-Catt S, Cui Y, Hennighausen L, Gonzalez F, Rohrer J, Benninghoff AU, Hontecillas R. Activation of PPAR gamma and delta by conjugated linoleic acid mediates protection from experimental inflammatory bowel disease. Gastroenterology l2004;127: 777-91.

[24]   Kutlu B, Darville MI, Cardozo AK, Eizirik DL. Molecular regulation of monocyte chemoattractant protein-1 expression in pancreatic beta-cells. Diabetes l2003;52: 348-55.

[25]   Mokdad AH, Bowman BA, Ford ES, Vinicor F, Marks JS, Koplan JP. The continuing epidemics of obesity and diabetes in the United States. Jama l2001;286: 1195-200.

[26]   Arner P. Regional adipocity in man. J Endocrinol l1997;155: 191-2.

[27]   Holness MJ, Bulmer K, Smith ND, Sugden MC. Investigation of potential mechanisms regulating protein expression of hepatic pyruvate dehydrogenase kinase isoforms 2 and 4 by fatty acids and thyroid hormone. Biochem J l2003;369: 687-95.

[28]   Boden G. Fatty acid-induced inflammation and insulin resistance in skeletal muscle and liver. Curr Diab Rep l2006;6: 177-81.

[29]   Shoelson SE, Lee J, Goldfine AB. Inflammation and insulin resistance. J Clin Invest l2006;116: 1793-801.

[30]   Lin HH, Faunce DE, Stacey M, Terajewicz A, Nakamura T, Zhang-Hoover J, Kerley M, Mucenski ML, Gordon S, Stein-Streilein J. The macrophage F4/80 receptor is required for the induction of antigen-specific efferent regulatory T cells in peripheral tolerance. J Exp Med l2005;201: 1615-25.

[31]   Charriere G, Cousin B, Arnaud E, Andre M, Bacou F, Penicaud L, Casteilla L. Preadipocyte conversion to macrophage. Evidence of plasticity. J Biol Chem l2003;278: 9850-5.

[32]   Nibbering PH, Leijh PC, van Furth R. Quantitative immunocytochemical characterization of mononuclear phagocytes. I. Monoblasts, promonocytes, monocytes, and peritoneal and alveolar macrophages. Cell Immunol l1987;105: 374-85.

[33]   Phillips RJ, Lutz M, Premack B. Differential signaling mechanisms regulate expression of CC chemokine receptor-2 during monocyte maturation. J Inflamm (Lond) l2005;2: 14.

[34]   Tanaka T, Fukunaga Y, Itoh H, Doi K, Yamashita J, Chun TH, Inoue M, Masatsugu K, Saito T, Sawada N, Sakaguchi S, Arai H, Nakao K. Therapeutic potential of thiazolidinediones in activation of peroxisome proliferator-activated receptor gamma for monocyte recruitment and endothelial regeneration. Eur J Pharmacol l2005;508: 255-65.

[35]   Tsuchida A, Yamauchi T, Takekawa S, Hada Y, Ito Y, Maki T, Kadowaki T. Peroxisome proliferator-activated receptor (PPAR)alpha activation increases adiponectin receptors and reduces obesity-related inflammation in adipose tissue: comparison of activation of PPARalpha, PPARgamma, and their combination. Diabetes l2005;54: 3358-70.

[36]   Pascual G, Fong AL, Ogawa S, Gamliel A, Li AC, Perissi V, Rose DW, Willson TM, Rosenfeld MG, Glass CK. A SUMOylation-dependent pathway mediates transrepression of inflammatory response genes by PPAR-gamma. Nature l2005;437: 759-63.

[37]   Hevener AL, He W, Barak Y, Le J, Bandyopadhyay G, Olson P, Wilkes J, Evans RM, Olefsky J. Muscle-specific Pparg deletion causes insulin resistance. Nat Med l2003;9: 1491-7.

[38]   He W, Barak Y, Hevener A, Olson P, Liao D, Le J, Nelson M, Ong E, Olefsky JM, Evans RM. Adipose-specific peroxisome proliferator-activated receptor gamma knockout causes insulin resistance in fat and liver but not in muscle. Proc Natl Acad Sci U S A l2003;100: 15712-7.

FIGURE LEGENDS

Figure 1. Abscisic acid (ABA) ameliorates fasting glucose concentrations without inducing body weight gain. Effect of ABA on body weight, feed intake, fasting blood glucose and plasma lipids. Db/db mice were fed control or ABA-supplemented (100mg/kg diet) high-fat diets for 36 days. (A) Body weights and (B) food intake were assessed weekly. After dietary treatment, plasma was withdrawn from fasted mice (12h) to obtain (C) fasting blood glucose (FBG, milligrams/deciliter) and (D) plasma triglycerides (TGs, mg/mL). Data are presented as least square means ± standard error of 10 mice. The error bars at some time points (Figure 1A and B) are smaller than the symbols and cannot be seen in the figure. Data points with an asterisk are significantly different ($P<0.05$).

Figure 2. Phenotypic analysis of macrophage subsets within the stromal-vascular fraction (SVF) of white adipose tissue (WAT). (A) and (B) are representative dot plots from a control db/db mouse. The F4/80^{hi} and F4/80^{lo} subsets differed significantly in (C) total amount of macrophages and (D) mean fluorescence intensities (MFI). (E) and (F) are the MFI's of CCR2 and CCR5-expressing macrophages in each population, respectively. (G) represents the percentage of macrophages in each population expressing either CCR2 or CCR5. Data are presented as least square means ± standard error of 10 observations. Data points with an asterisk or number sign indicate a significant difference ($P<0.05$) between the separate macrophage populations.

Figure 3. Abscisic acid (ABA) decreases the numbers of F4/80^{hi} macrophages in white adipose tissue. (A), (B), and (C) are representative dot plots for total stromal-vascular fraction (SVF) macrophage infiltration and the percentages of CCR2+ macrophages in the F4/80^{hi} and F4/80^{lo} subsets, respectively, for control-fed db/db mice. (D), (E), and (F) are the respective dot plots for a representative ABA-fed db/db mouse. (G), (H), and (I) indicate the contribution of SVF macrophages, F4/80^{lo} macrophages, and F4/80^{hi} macrophages to the total amount of gated cells. The mean fluorescence intensities (MFIs) of each macrophage sub-population for (J) CCR2 and (K) CCR5. (L) is the difference in MFI of total SVF macrophages between control and ABA-fed mice. Data are presented as least square means ± standard error of 10 observations. Data points with different superscripts are significantly different ($P<0.05$).

Figure 4. Abscisic acid (ABA) induces PPAR γ and suppresses the expression of MCP-1 in white adipose tissue. Effect of dietary abscisic acid (ABA) supplementation on white adipose tissue and liver gene expression, MCP-1 protein levels, liver triglyceride concentrations and hepatic steatosis scores. Db/db mice were fed high-fat diets with (black bars) or without (empty bars) ABA (100 mg/kg) for 36 days. Gene expression in RNA isolated from stromal-vascular cells (SVCs) and adipocytes was analyzed by real-time qRT-PCR for (A) monocyte chemoattractant protein 1 (MCP-1), (B) peroxisome proliferator-activated receptor γ (PPAR γ), and (C) CD36. (D) Liver MCP-1 expression, (E) plasma MCP-1 (picograms/milliliter), and (F) liver triglycerides (TG, mg/gram tissue) were also assessed. Gene expression values are expressed as a relative ratio to the housekeeping gene β-actin. Data are presented as least square means

± standard error of 10 observations. Data points with an asterisk are significantly different (*P*<0.05). (G) Liver histology scores. (H) and (I) are representative photomicrographs of liver histology specimens stained with hemotoxylin and eosin (H&E).

Figure 5. The beneficial effects of abscisic acid (ABA) on insulin resistance are abrogated in immune cell-specific PPAR γ null mice. PPAR γ flfl; MMTV-Cre[+] and PPAR γ flfl; MMTV-Cre[-] littermates (wild-type phenotype) were fed high-fat diets with or without ABA (100 mg/kg). (A) Final body weights and (B) response to an intraperitoneal glucose challenge (2 g glucose/kg body weight) in fasted mice (6h) were assessed after 28 weeks of dietary supplementation. Data are presented as least square means ± standard error of 8 mice. The error bars at some time points (Figure 5B and C) are smaller than the symbols and cannot be seen in the figure. Data points with different superscripts are significantly different (*P*<0.05).

Figure 6. The beneficial effects of abscisic acid (ABA) on the infiltration of monocytes and chemokine production in white adipose tissue are abrogated in immune cell-specific PPAR γ null mice. Effect of dietary abscisic acid (ABA)-supplementation and tissue-specific deletion of peroxisome proliferator-activated receptor γ (PPAR γ) in immune cells on adipose tissue macrophage (ATM) phenotype. (A), (B), and (C) represent the effects of ABA on total macrophage infiltration and the percentage of F4/80[lo] and F4/80[hi] ATM in PPAR γ flfl; MMTV-Cre[+] and PPAR γ flfl; MMTV-Cre[-] mice. (D) and (E) are representative dot plots for stromal-vascular fraction

(SVF) infiltration of ATMs in PPAR γ flfl; MMTV-Cre[+] and PPAR γ flfl; MMTV-Cre[-]

mice fed the control high-fat diet. (F) and (G) are the respective dot plots for ABA-fed

mice. Real-time qRT-PCR was used to assess the expression of monocyte

chemoattractant protein 1 (MCP-1) (H). Data are presented as least square means ±

standard error of 8 mice. The error bars at some time points (Figure 6B) are smaller than

the symbols and cannot be seen in the figure. Data points with different superscripts are

significantly different ($P<0.05$).

Figure 7. Abscisic acid (ABA) inhibits MCP-1 promoter activity by acting through

PPAR γ. 3T3-L1 pre-adipocytes were transfected with a MCP-1 promoter luciferase

reporter construct with (black bars) or without (empty bars) co-transfection with a

pCMX.PPAR γ expression plasmid. After 20 hours, cells were treated with the PPAR γ

antagonist GW9662 (GW, 30 μM), ABA (12.5 μM), rosiglitazone (Ros, 1 μM), ABA and

GW, or Ros and GW. The results were normalized for *Renilla* activity. Data are

presented as least square means ± standard error of 4 observations. Data points with an

asterisk are significantly different ($P<0.05$).

Figure 1
Click here to download high resolution image
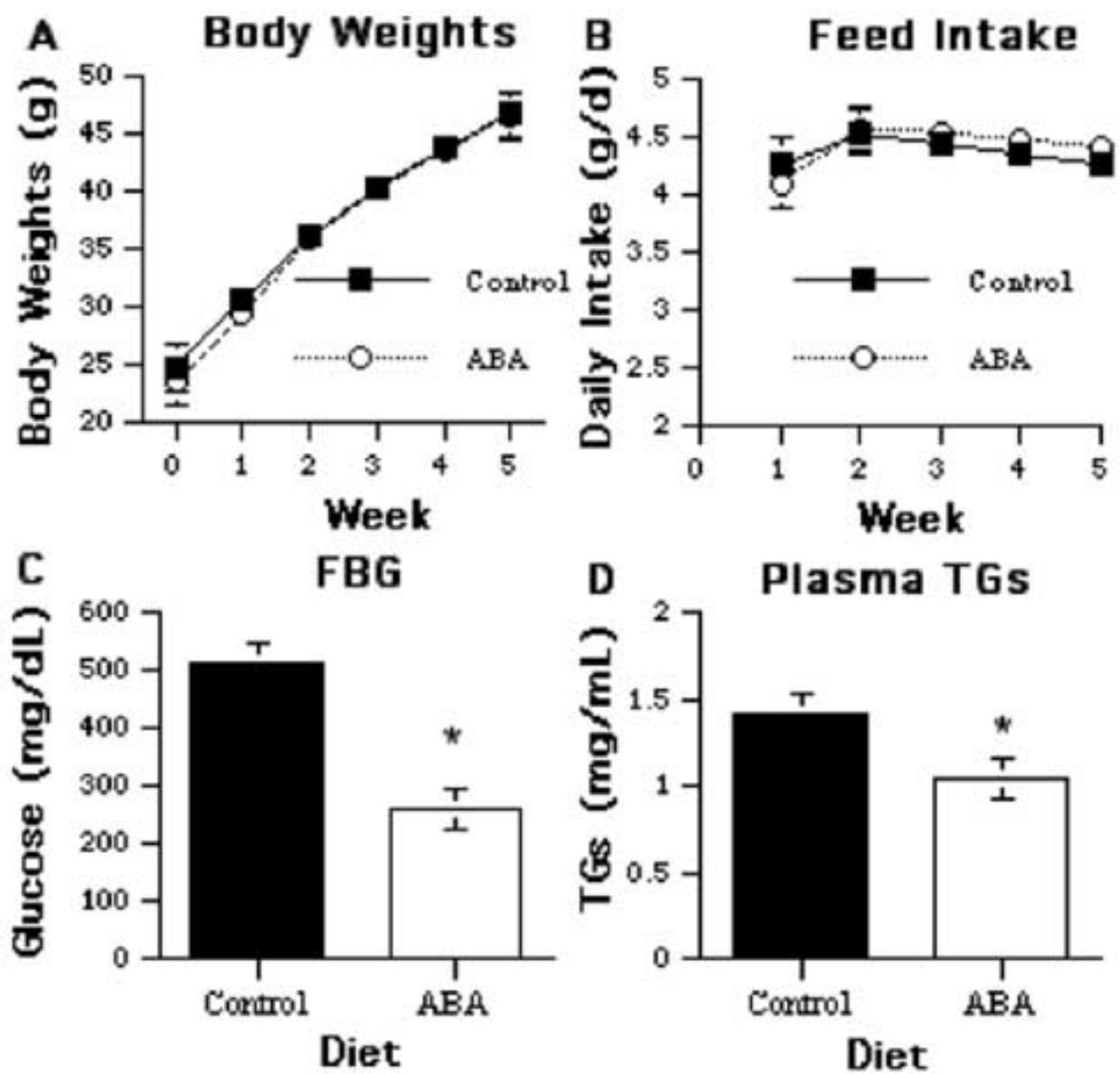
Figure 1

Figure 2
Click here to download high resolution image

78
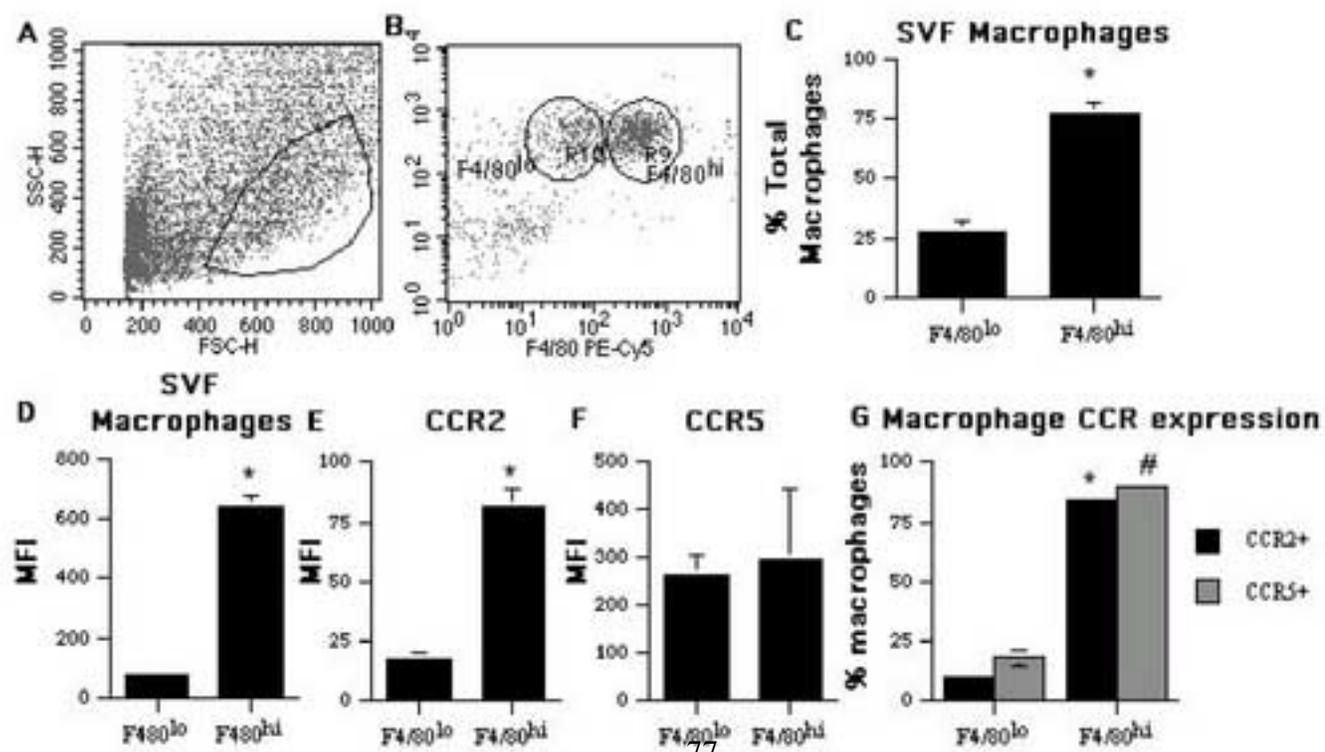
Figure 4
Click here to download high resolution image
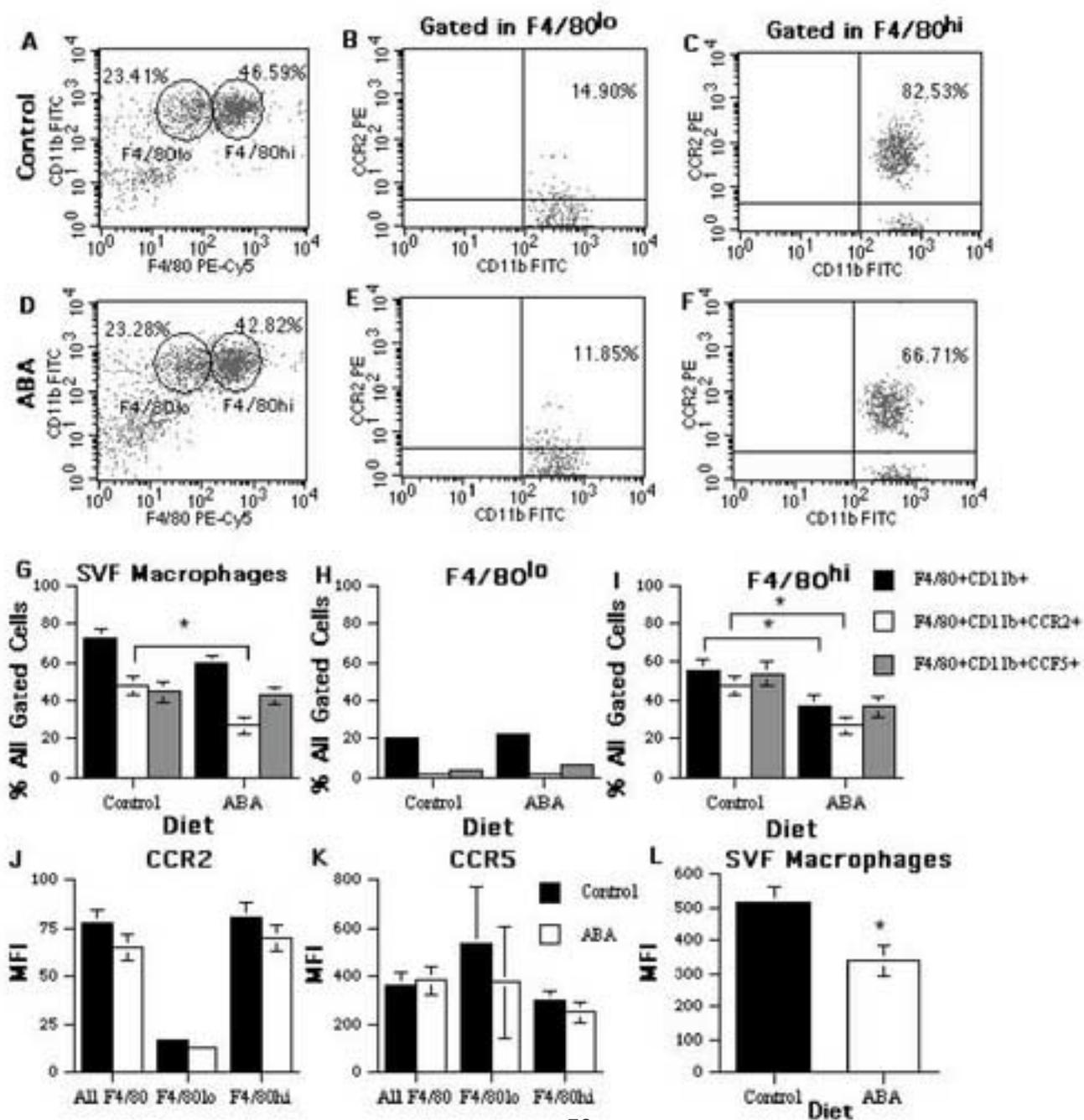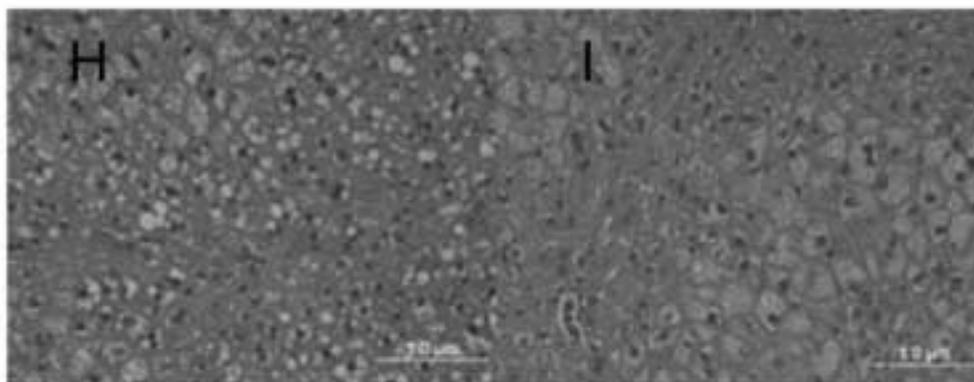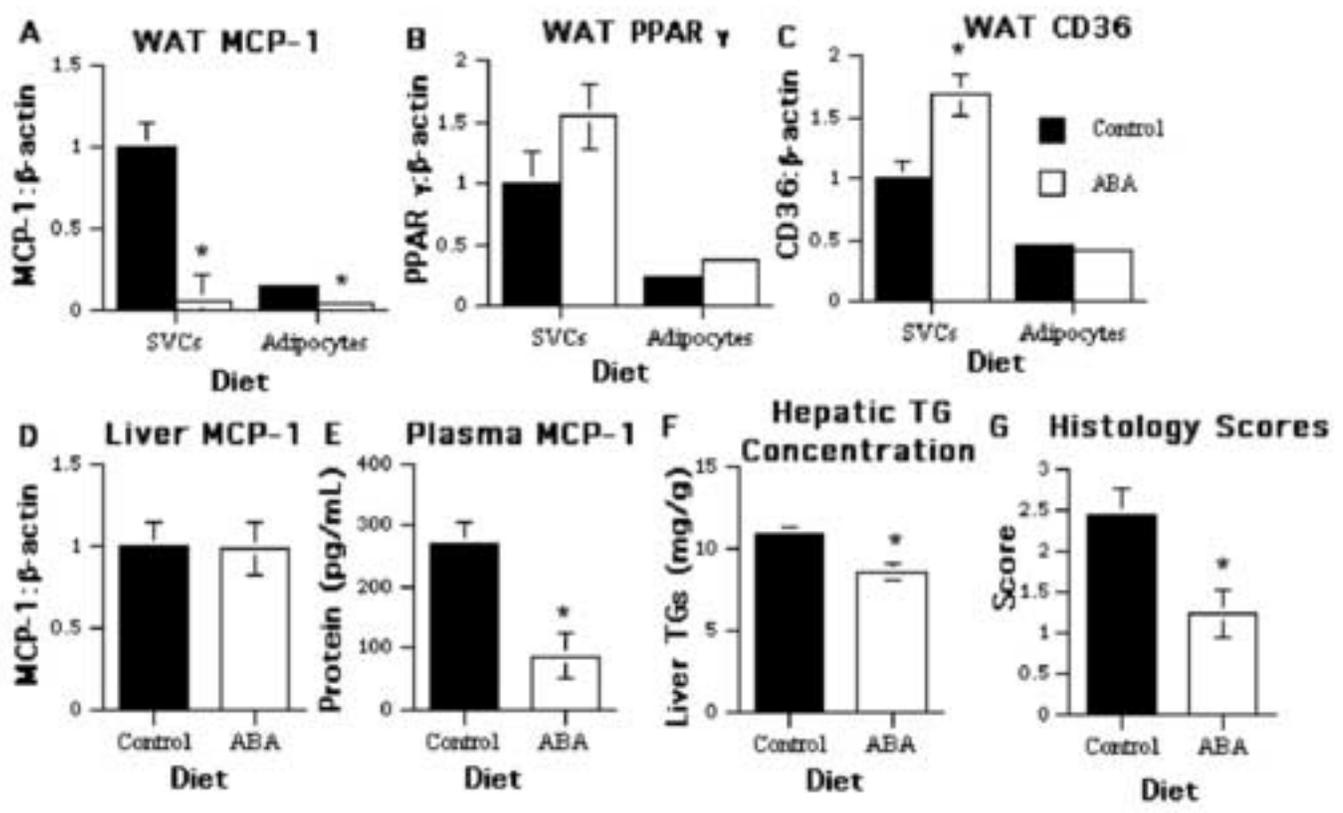
Figure 5
Click here to download high resolution image

A Body Weights

B Glucose Tolerance Test

C Glucose Tolerance Test

80
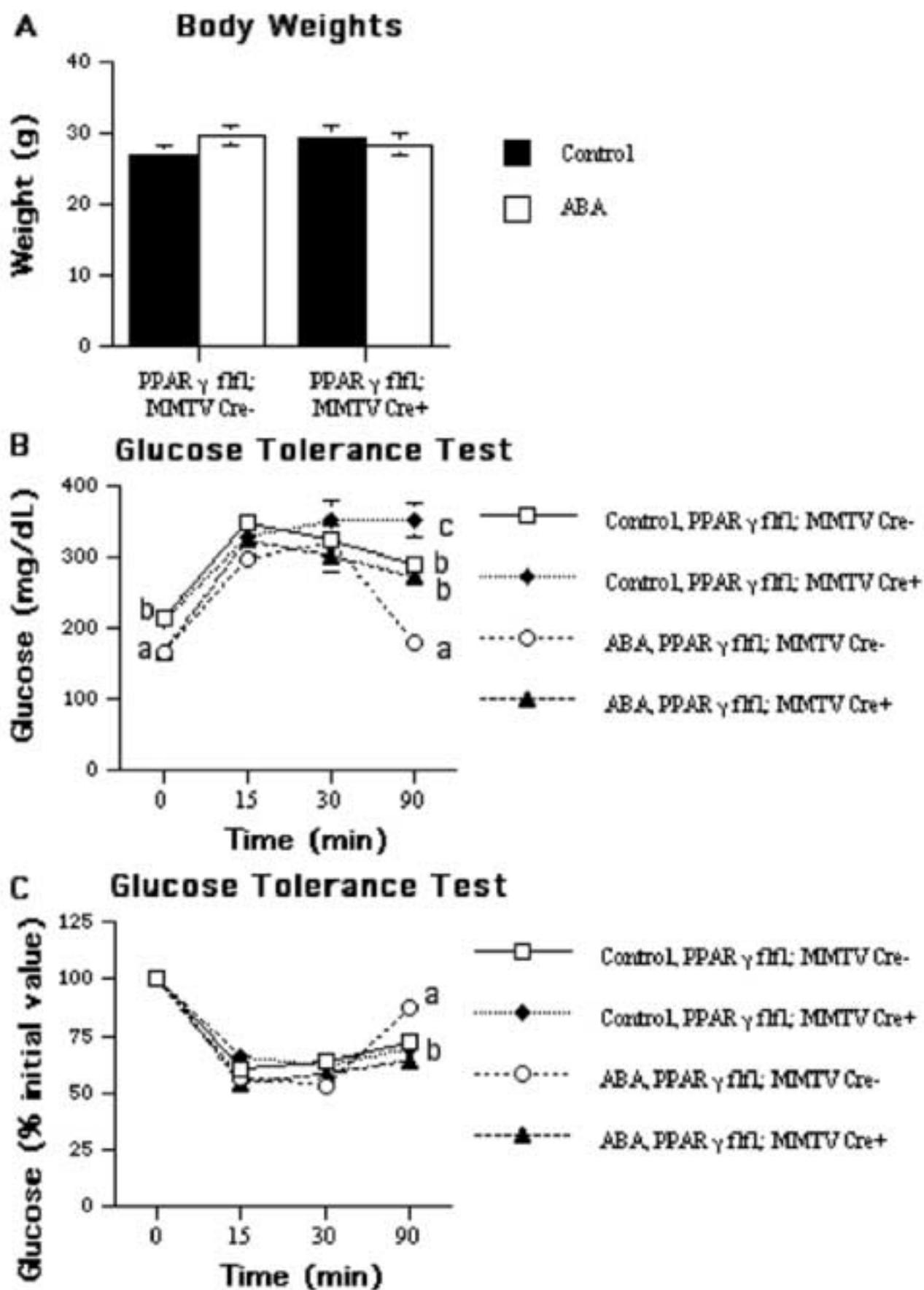
Figure 6
Click here to download high resolution image

Figure 6

81
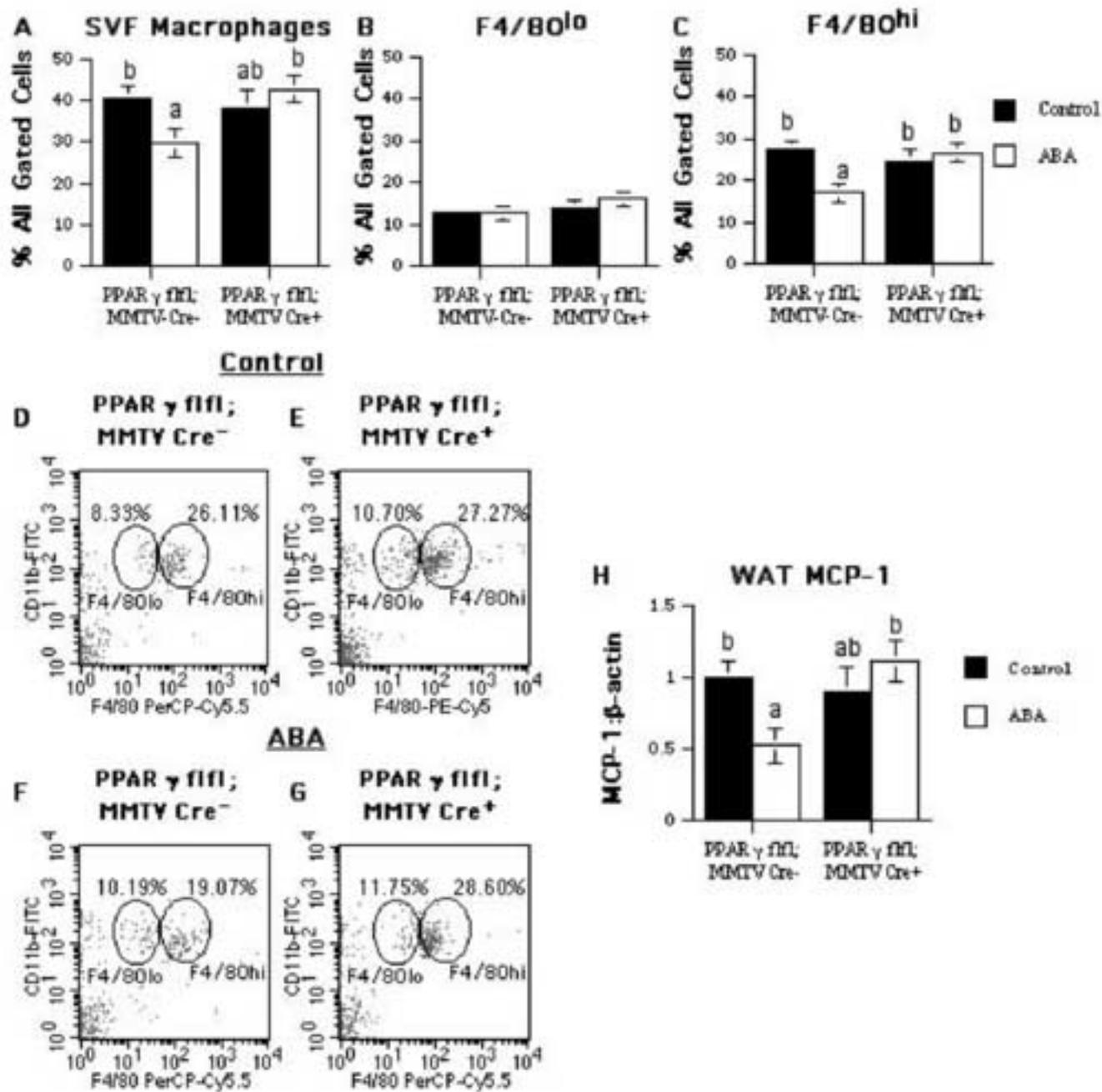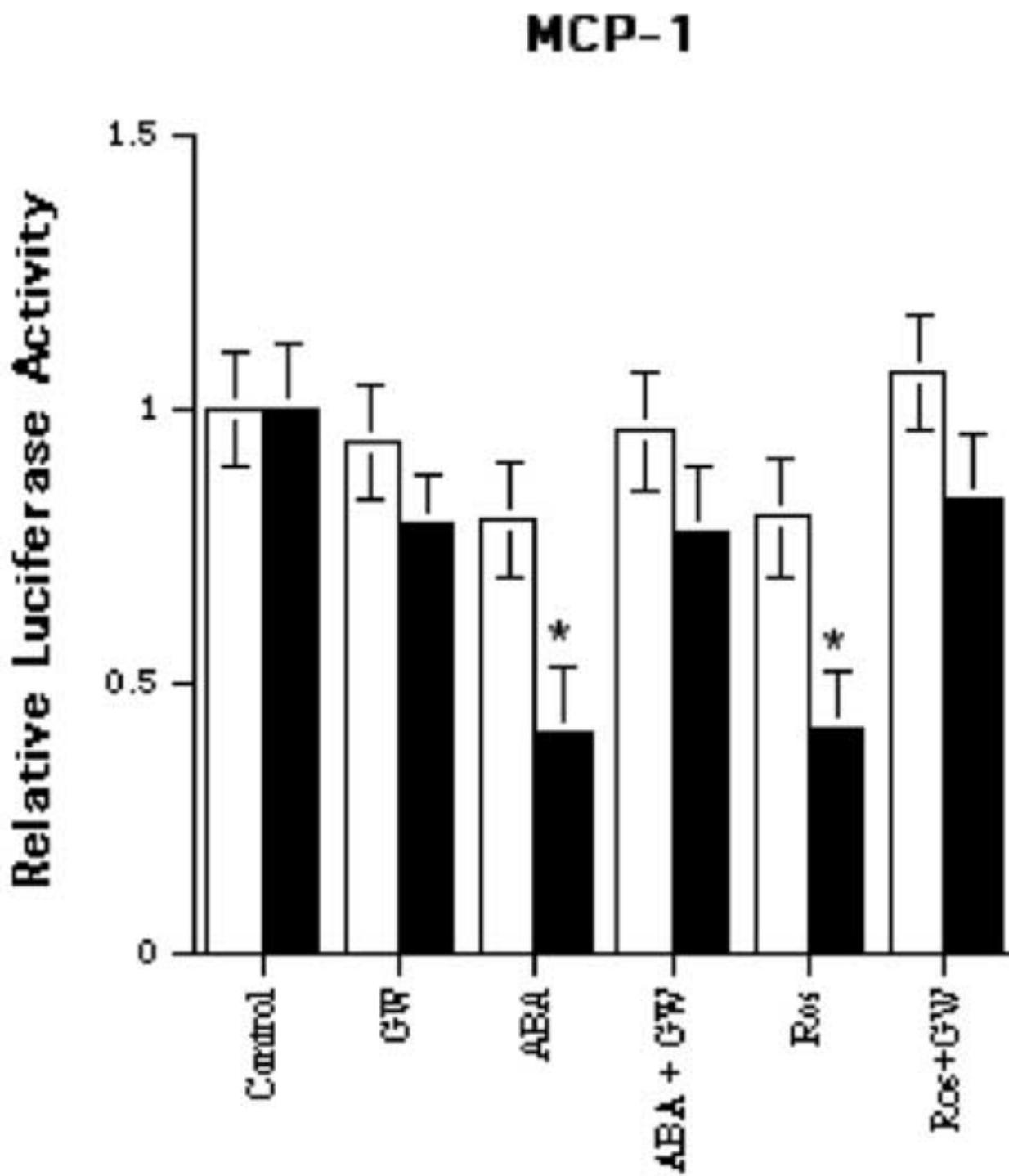
MCP-1

Table 1

Table 1. Oligonucleotide sequences for quantitative real-time PCR. [a, b]

Primer	Sequence	Length	Accession Number
β-actinF	5'CCCAGGCATTGCTGACAGG3'	141	X03672
β-actinR	5'TGGAAGGTGGACAGTGAGGC3'		
MCP-1F	5'CTTGCCTAATCCACAGACTG'3	146	AJ238892
MCP-1R	5'GCCTGAACAGCACCACTA'3		
PPAR γF	5'CAGGCTTGCTGAACGTGAAG3'	117	NM_011146
PPAR γR	5'GGAGCACCTTGGCGAACA3'		
CD36F	5'CCGGGCCACGTAGAAAACA3'	156	NM_007643
CD36R	5'CCTCCAAACACAGCCAGGAC3'		
TLR-4	5'GGCGCTCCGAGTTGTGA'3	73	NM_009841
TLR-4	5'GTACCTGCTTCAGCCCAGTG'3		

1 [a] F, forward; R, reverse. PCR primer pairs were designed for 73 and 157 base pairs.

2 Annealing temperatures are 57ºC for β-actin, TNF-α, PPAR γ, and CD36, and 54ºC for

3 MCP-1 and TLR-4.

4 [b] When plotting threshold cycle versus log starting quantity (pg), standard curves had

5 slopes between -3.1 and -3.7; PCR efficiencies between 92 and 105 and R^2 above 0.98.

6

CHAPTER 5: OBESITY PROMOTES MACROPAHGE INFILTRATION INTO BOTH ADIPOSE TISSUE AND SKELETAL MUSCLE AND IMPAIRS THE REGULATORY CD4+ T CELL COMPARTMENT

Obesity promotes macrophage infiltration into both adipose tissue and skeletal muscle and impairs the regulatory CD4+ T cell compartment

Amir J. Guri, Raquel Hontecillas and Josep Bassaganya-Riera

Laboratory of Nutritional Immunology and Molecular Nutrition; Virginia Polytechnic Institute and State University, Blacksburg, VA 24061

Running head: Immunomodulation in Obesity and Insulin Resistance

Correspondence: Dr. Josep Bassaganya-Riera, Laboratory of Nutritional Immunology & Molecular Nutrition, 319 Wallace Hall, Virginia Tech, Blacksburg, VA 24061

E-mail: jbassaga@vt.edu

Abstract

Background: Macrophage infiltration into white adipose tissue (WAT) is an emerging hallmark of obesity-induced insulin resistance. We have previously shown that adipose tissue macrophages (ATMs) consist of two phenotypically distinct CD11b$^+$ subsets which differ in surface expression of the glycoprotein F4/80 and chemokine receptor 2 (CCR2). **Objective:** To characterize the effect of diet-induced obesity (DIO) on the kinetics of macrophage and T-cell infiltration into WAT, skeletal muscle (SM) and liver. **Methods and results:** Mice fed high-fat diets had more abdominal WAT and were glucose intolerant at days 70 and 140 of high-fat feeding in comparison to control mice fed low-fat diets. Diet-induced obesity (DIO) significantly increased the percent of F4/80^{hi} ATMs, which were also CCR2^{hi}, and, over time, CD11c protein levels were significantly elevated in both F4/80^{hi} and F4/80^{lo} ATMs. In SM, an organ responsible for 80% of insulin-stimulated glucose disposal, DIO induced the infiltration of F4/80^{lo} skeletal muscle macrophages (SMPs), and the infiltration of this subset was associated with a significant increase in MCP-1 mRNA in the stromal fraction of SM. We also found that the percent of CD4$^+$FOXP3$^+$ regulatory T-cells (Treg) in both WAT and liver was significantly reduced in HFD-fed mice. **Conclusion:** DIO is associated with infiltration of CCR2^{hi}F4/80^{hi} ATMs and the eventual conversion of both infiltrating and resident ATMs subsets into a CD11c$^+$ pro-inflammatory phenotype. This inflammatory process may be accentuated if the Treg compartment is impaired by high fat feeding.

Keywords: Adipose tissue, macrophage**,** inflammation, CD11c, skeletal muscle, high saturated fat feeding, Treg.

Introduction

The recent worldwide obesity epidemic has resulted in a significant increase in the number of individuals diagnosed with diseases associated with insulin resistance, including type 2 diabetes (T2D), cardiovascular disease, atherosclerosis, stroke, and hypertension (1). While it is implicit that insulin resistance stems from metabolic dysfunctions in one or more of the three main tissues responsible for maintaining glucose homeostasis, including the liver, skeletal muscle (SM), and white adipose tissue (WAT), the etiology of the disease and mechanisms responsible for its pathogenesis, including immunoinflammatory mechanisms, are not entirely understood.

One theory which has gained much ground over recent years delves into the interplay between insulin resistance and the low-grade chronic inflammation associated with obesity. While it was discovered back in 1876 that anti-inflammatory agents such as salicylates can alleviate glycosuria and impaired glucose tolerance (2, 3), the ability to generate targeted knockout mice or neutralize key inflammatory pathways and mediators, including jun-c activated kinase (JNK) (4), inhibitor of nuclear factor κB (NF-κB) kinase (IKK) (5), toll-like receptor 4 (TLR-4) (6, 7), and tumor necrosis factor α (TNF-α) (8, 9) has portrayed a necessary role for inflammation in the pathogenesis of insulin resistance. More specifically, Arkan et al showed that disrupting IKK-β in myeloid cells protects both liver and SM from the development of insulin resistance (10).

In 2003, studies by Weisberg et al (11) and Xu et al (12) demonstrated that macrophages infiltrate WAT of obese mice and humans and produce significant amounts of pro-inflammatory cytokines and chemokines. The vast majority of adipose tissue macrophages (ATMs) surround dead adipocytes in the stromal-vascular fraction (SVF)

and form characteristic crown-like structures and multinucleated giant cells (13). The reasons why ATMs infiltrate and function in a reportedly deleterious manner are debatable. However, by altering the ability of macrophages to migrate through overexpressing monocyte chemoattractant protein 1 (MCP-1) (14) in adipocytes or disrupting its main receptor chemokine receptor 2 (CCR2) (15), the tight link between ATM infiltration and the progression of systemic insulin resistance has been visualized. Interestingly, deletion of the *Ccr2* or *Mcp-1* genes does not completely abrogate macrophage infiltration into WAT, suggesting the existence of mechanisms dependent and independent of the MCP-1/CCR2 axis (15-17) as well as a possible role of additional immune cell subsets found in the SVF. Among the immune cell subsets are the anti-inflammatory and immunoregulatory $CD4^+FOXP3^+$ regulatory T-cells (Treg), whose presence in the SVF may correlate with the decreased severity of obesity-induced inflammation. On the other hand, interventions resulting in functional or numerical impairments in the Treg compartment could result in enhanced severity of inflammation. Thus, the limited knowledge on the phenotypic and functional heterogeneity of immune cell subsets infiltrating WAT weakens our understanding of the mechanisms of immunopathogenesis of insulin resistance during obesity.

On this pretense, our laboratory sought to characterize the phenotype of ATMs in obese mice to gain a better understanding of the mechanisms involved in infiltration and persistence of ATM subsets in WAT. In doing so, we reported for the first time the existence of two distinct ATM populations which all expressed the integrin CD11b but differed in the amount of the glycoprotein F4/80, a maturation marker expressed on the surface of monocytes/macrophages ($F4/80^{hi}$ vs $F4/80^{lo}$) (18). Phenotypically, in db/db

mice fed high-fat diets (HFDs), a greater percentage of F4/80^{hi} ATMs also expressed the chemokine receptors CCR2 and CCR5 than F4/80^{lo} ATMs and had a significantly higher concentration of CCR2 on their surface, suggesting a heightened responsiveness to MCP-1-mediated recruitment (18). In response to the insulin-sensitizing agent abscisic acid (ABA), we observed a significant reduction in F4/80^{hi} ATMs that necessitated expression of peroxisome proliferator-activated receptor γ (PPAR γ) in hematopoietic cells (18). The present study further characterizes the effect of obesity on immune cell infiltration into liver, WAT and SM by utilizing the diet-induced obesity (DIO) model in C57BL6J mice. Our findings reveal that 140 days of feeding HFD induces a significant increase in large, F4/80^{hi} ATMs, which similar to our previous findings were CCR2^{hi} when compared to the F4/80^{lo} and also consisted of more larger, mature ATMs. In both ATM populations, we observed a progressive rise over time in the surface integrin CD11c. These changes in WAT coincided with a significant decrease in the percent of CD4^{+}FOXP3^{+} Treg cells in the DIO mice. In SM, we also observed increased infiltration of skeletal muscle macrophages (SMPs), though in this tissue it was the F4/80^{lo} which was affected in the DIO mice. With the increase in SMP infiltration, there was a concomitant upregulation in MCP-1 mRNA from the SVF of SM. Overall, our findings suggest that F4/80^{hi} ATMs may represent the infiltrating, M1 polarized phenotype described previously by Lumeng et al (19) whereas the F4/80^{lo} ATMs could be a resident ATM population. Over time, both these subsets evolve into a pro-inflammatory phenotype characterized by enhanced surface expression of the CD11c integrin.

Materials and Methods

Mice and dietary treatments

Six week-old, male C57BL6/J mice were housed at the animal facilities at Virginia Polytechnic Institute and State University in a room maintained at 75° F, with a 12:12 h light-dark cycle starting from 6:00 AM. All experimental procedures were approved by the Institutional Animal Care and Use Committee of Virginia Polytechnic Institute and State University and met or exceeded requirements of the Public Health Service/National Institutes of Health and the Animal Welfare Act.

Mice (n=48) were fed either: 1) a low-fat AIN-93G diet containing 7% fat and 0.02 total cholesterol and obtaining 14.5% of kilocalories (Kcal) from fat (20) or 2) a high saturated fat (AIN-93G-based) diet containing 19.6% fat and 0.2% total cholesterol and obtaining 40.1% of Kcal from fat (4.4 Kcal/g) (21). The experimental diets were fed for 0, 70 or 140 days. The energy density of the high saturated fat diet is approximately 16% higher than the control low-fat diet. The mice were weighed and their food intake was recorded weekly. At the conclusion of each dietary period, fasted mice underwent intraperitoneal glucose tolerance test (IPGTT) as previously described (21). Briefly, mice were bled at 0, 15, 45, and 90 minutes following the administration of glucose (2 g/kg body weight) for measurement of plasma glucose concentrations with an AccuChek® Glucometer (Roche, Indianapolis, IN). Two days after the IPGTT, fasted mice (12h) were euthanized by CO_2 narcosis. WAT was excised and weighed, and, along with both SM and liver samples, was stored in RNA later (Ambion) for gene expression analyses.

WAT Fractionation

Abdominal WAT was excised, weighed, minced into small <10 mg pieces and placed into digestion media. WAT digestion media consisted of DMEM (Mediatech, Herndon, VA) supplemented with 2.5% HEPES (Mediatech) and 10 mg/mL fatty-acid free bovine serum albumin (FAB-poor BSA, Sigma), Liberase Blendzyme 3 (0.03 mg/mL, Roche) and DNase I (50 U/mL, Sigma). Samples were incubated in a rotating 37°C water bath for 90 minutes, filtered through a 250 μm nylon mesh (Sefar America Inc., Depew, New York) to remove undigested particles and centrifuged at 4°C at 2250 rpm for 10 minutes. The pellet, consisting of stromal vascular cells (SVCs), containing endothelial cells, pre-adipocytes, macrophages and T cells was washed with DMEM and then centrifuged at 4°C at 2250 rpm for 10 minutes. After discarding supernatant, erythrocytes were lysed by incubating cells with 2 mL of erythrocyte lysis buffer for 2 minutes before stopping the reaction with 9 mL of ice cold phosphate-buffered saline (PBS). SVCs were centrifuged again at 4°C at 2250 rpm for 10 minutes, suspended in 1 ml of 1X PBS, enumerated with a Z1 Single Particle Counter (Beckman Coulter, Fullerton, CA), and then resuspended in FACS buffer (1X PBS, 1% normal goat serum, 0.2% sodium azide) at a concentration of 2×10^6 cells/mL. SVCs not used for immunophenotyping were stored in RLT/βME and immediately frozen at -80°C for RNA isolation and gene expression analyses.

SM Fractionation

Utilizing a modified protocol from the laboratory of Goodall et al., SM from mouse hindlimbs were excised, placed into a petri dish containing approximately 10 mL

of Hanks Balanced Sodium Salt Solution (HBSS), and minced into a fine slurry of 1 mm^2 or smaller pieces. Minced muscle was then centrifuged at 1200 rpm for 10 minutes at 4°C. After discarding supernatant, containing subcutaneous adipose tissue, samples were digested in 0.2% type II collagenase (Worthington Biochemicals) for 90 minutes. To stop the reaction, 35 mL HBSS were added to each sample. Digested samples were then centrifuged at 1200 rpm for 10 minutes at 4°C. After, supernatant was discarded and samples were resuspended in DMEM containing 10% horse serum. Samples were then triturated, passed through a 100 μM filter (BD), and centrifuged at 3000 rpm for 6 minutes at 4°C. To separate immune fraction from SM-derived fraction, the supernatant was discarded and samples were resuspended in 5 mL 40% Percoll (Sigma). They were then overlaid over 5 mL of 70% percoll and centrifuged at 1800 rpm for 20 minutes at room temperature. Cells from the interface were collected, washed twice with PBS, and enumerated with a Z1 Single Particle Counter (Beckman Coulter). Cells not utilized for immunophenotyping were stored in RLT/β-ME.

Liver Fractionation

Livers from mice were perfused with 1XPBS through the hepatic portal vein, minced into small pieces and digested in HBSS containing 0.3% Liberase (Roche) and DNase I (50U/mL, Sigma) for 1 hour in a rotating 37°C water bath. After incubation, samples were filtered through a 250 μm nylon mesh (Sefar), washed with HBSS, and centrifuged at 3000 rpm for 6 minutes. Separation of immune layer was accomplished by spinning samples in 20/50% Percoll (Sigma) at 1500 rpm for 20 minutes. After immune

cell isolation, samples were washed twice with PBS, resuspended in FACS buffer, and enumerated with a Z1 Single Particle Counter (Beckman Coulter).

Flow Cytometry

SVCs, SM stromal cells, and liver immune cells (2×10^5 cells) were seeded into 96-well plates and centrifuged at 4°C at 3000 rpm for 4 minutes. To assess differential monocyte/macrophage infiltration across, the cells were then incubated in the dark at 4°C for 20 minutes in FcBlock (20 µg/ml; BD Pharmingen) for macrophage assessment, and then for an additional 20 minutes with fluorochrome-conjugated primary antibodies anti-F4/80-PE-Cy5 (5 µg/mL), anti-CD11b-FITC (2 µg/mL, eBioscience), anti-CD11c-APC (2 µg/mL), or anti-CCR2-PE (R&D systems, Minneapolis, MN). For lymphocyte assessment, cells were incubated with CD4-FITC (FITC (2 µg/mL; BD Pharmingen) and FOXP3-PE (2 µg/mL; eBioscience). After incubation with primary antibodies, cells were centrifuged at 4°C at 3000 rpm for 4 minutes and washed with 200 µL of FACS buffer. After washing, cells were suspended in 200 µL PBS and 3-color data acquisition was performed on a FACS Calibur flow cytometer. Data analyses were performed by using the CellQuest software (BD).

Real-Time Quantitative PCR

Total RNA was isolated using the RNA isolation Minikit (Qiagen) according to the manufacturer's instructions. Total RNA (0.5 µg) was used to generate complementary DNA (cDNA) template using the iScript cDNA Synthesis Kit (Bio-Rad, Hercules, CA). The total reaction volume was 20 µL with the reaction incubated as

follows in an MJ MiniCycler: 5 minutes at 25°C, 30 minutes at 52°, 5 minutes at 85°C, hold at 4°C. PCR was performed on the cDNA using Taq DNA polymerase obtained from Invitrogen and using previously described conditions (20). Each gene amplicon was purified with the MiniElute PCR Purification Kit (Qiagen) and quantified on an agarose gel by using a DNA mass ladder (Promega). These purified amplicons were used to optimize real-time PCR conditions and to generate standard curves in the real-time PCR assay. Primer concentrations and annealing temperatures were optimized for the iCycler iQ system (Bio-Rad) for each set of primers using the system's gradient protocol. PCR efficiencies were maintained between 92 and 105% and correlation coefficients above 0.98 for each primer set during optimization and also during the real-time PCR of sample DNA. Sequences, annealing temperatures, and base pair lengths for each primer set were previously described (18).

Complementary DNA (cDNA) concentrations for genes of interest were examined by real-time quantitative PCR using an iCycler iQ System and the iQ SYBR green supermix (Bio-Rad). A standard curve was generated for each gene using 10-fold dilutions of purified amplicons starting at 5 pg of cDNA and used later to calculate the starting amount of target cDNA in the unknown samples. SYBR green I is a general double-stranded DNA intercalating dye and may therefore detect nonspecific products and primer/dimers in addition to the amplicon of interest. In order to determine the number of products synthesized during the real-time PCR, a melting curve analysis was performed on each product. Real-time PCR was used to measure the starting amount of nucleic acid of each unknown sample of cDNA on the same 96-well plate. Results are presented as starting quantity of target cDNA (picograms) per microgram of total RNA.

In vitro glucose uptake in macrophage co-culture studies

C2C12 myoblasts (American Type Culture Collection, Manassas, VA) and RAW 264.7 macrophages (ATCC) were both grown in high glucose DMEM containing 10% fetal bovine serum (FBS, Mediatech) and 1% penicillin/streptomycin solution. When 50-60% confluent, C2C12 myoblasts were seeded into 12-well plates at 1.5 x 10^5 cells/well and cultured in differentiation media (DMEM, 10% horse serum). Media was changed every other day until differentiated myotubes were formed. Five days after differentiation, RAW 264.7 were added onto myotubes or empty wells at 1.5 x 10^5 or 3.0 x 10^5 cells/well and cells incubated overnight in serum free αMEM. To assess glucose uptake, cells were treated with or without 100nM insulin for 15 minutes. Afterwards, αMEM containing 2-deoxy-D-[^{3}H] glucose (0.5 μCi/mL, 10 μmol/L cold 2-DG) was added to cells for 20 minutes. The reaction was stopped by washing cells three times with cold 1XPBS and cells were lysed with 30 mM NaOH. An aliquot was removed for protein analysis (Bio-rad) and incorporation of 2-deoxy-D-[^{3}H] glucose in cells was assessed by with liquid scintillation and is presented as relative counts per million (CPM). Protein values did not differ significantly among C2C12-seeded wells (*P*=0.89).

Statistical Analyses

Kinetic data were analyzed as a repeated measures completely randomized design. The statistical model utilized was $Y_{ijk} = \mu + Time_i + Diet_j + (Time \times Diet)_{ij} + Error_{ijk}$. To determine the statistical significance of the model, analysis of variance (ANOVA) was performed using the general linear model procedure of Statistical

95

Analysis Software (SAS), and probability value $(P) < 0.05$ was considered to be

significant. When the model was significant, ANOVA was followed by Fisher's

Protected Least Significant Difference multiple comparison method. Non-parametric data

were analyzed by using the Mann-Whitney U test followed by a Dunn's multiple

comparison's test.

Results

Body weights and glucose tolerance

To examine the effect of DIO on macrophage infiltration into WAT and SM, we fed high

saturated fat (HFD) and control diets (i.e., 16% lower energy value) to C57BL6/J mice

for 0, 70, and 140 days. Mice from both dietary treatments gained weight throughout the

treatment period, and day 140 mice fed the HFD had gained significantly more weight

than mice fed the control diets (Figure 1a). Mice fed the HFD also had accumulated

significantly more abdominal WAT on days 70 and 140 (Figure 1b) and had significantly

impaired glucose tolerance when compared to mice fed the control diets (Figure 1c-e).

Phenotypic characterization of ATM infiltration

We previously characterized two phenotypically distinct ATM populations in db/db mice

which differed in the amount of surface expression of the F4/80 glycoprotein (18) (i.e.,

F4/80^{hi} and F4/80^{lo} subsets) – a well-characterized monocyte/macrophage maturation

marker. F4/80 surface concentrations increase as monocytes mature and differentiate into

macrophages, a process that involves a significant increase in size and phagocytic ability

(22). The F4/80^{hi} population was more abundant and expressed significantly more of the chemokine receptors CCR2 and CCR5 than the F4/80l^{lo} subset. Here, we found that C57BL6/J mice on both control and HFDs also contained these differing ATM populations (Figure 2A). Similar to our past findings using the db/db model, we observed a significant increase in both total and F4/80^{hi} ATM infiltration with no significant difference in the F4/80^{lo} subset (Figures 2B-2D). The F4/80^{hi} population had a higher CCR2 expression (i.e., more F4/80^{hi} cells expressed CCR2) than the F4/80^{lo} along with a significantly higher ($P<0.0001$) mean fluorescence intensity (MFI), and therefore a higher surface CCR2 concentration, in F4/80^{hi} cells (Figures 2E-2G). These phenotypic differences were consistent throughout days 0 to 140 and were present in both dietary treatments.

It has been previously shown that macrophages expressing the surface integrin CD11c significantly increase in adipose tissue in response to obesity (17, 23). To assess the kinetics of this distinct population of macrophages during DOI we examined both CCR2^{+}F4/80^{lo} and CCR2^{+}F4/80^{hi} ATMs for the presence and surface concentrations of CD11c. We observed that the majority of CCR2^{+}F4/80^{lo} and CCR2^{+}F4/80^{hi} ATMs expressed CD11c. After 140 days, the percent of CCR2^{+}F4/80^{hi} ATMs which were also CD11c^{+} was significantly greater in the DIO mice (87.7 vs 81.7%, P=0.04), and there were no significant differences in the F4/80^{lo} subset (Figure 2H). The CD11c surface expression for CCR2^{+}F4/80^{hi} ATMs was also significantly upregulated by DIO after 70 and 140 days of dietary treatment. In CCR2^{+}F4/80^{lo} ATMs, the CD11c surface concentration was significantly greater in mice fed HFD on day 140 (Figures 2I, 2J).

To further characterize the effect of high saturated fat feeding on ATM phenotype, we examined both the F4/80^{hi} and F4/80^{lo} ATM populations based on their forward scatter (FSC) in order to differentiate the number of mature and immature ATMs. FSC is proportional to cell size, whereby larger cells scatter more light and therefore have a higher detected signal. For our analysis, we subdivided the cells into small, medium, and large ATMs based on the distribution of the macrophage gate throughout FSC (Figure 3A). The average sizes, as measured by FSC, were <914 (small); 915-1019 (medium); and >1019 (large) microns. Of note, the MFI, and thus the surface concentration, of the F4/80 glycoprotein (a maturation marker for monocytes/macrophages) were proportional to macrophage size in both the F4/80^{lo} and F4/80^{hi} populations (Figures 3B). At day 140, we observed that a significantly greater percentage of F4/80^{hi} ATMs were large in the DIO mice when compared to control mice, who had significantly more small ATMs. High-fat feeding had no apparent effect on ATM size in the F4/80^{lo} subset (Figures 3C and 3D). In both F4/80^{lo} and F4/80^{hi} ATMs, the CCR2 surface expression increased proportionately with cell size (Figures 3E and 3F). Interestingly, the CCR2 MFI of F4/80^{hi} ATMs was consistently higher in macrophages of all sizes in the control, LFD-fed mice.

Thus far, we have found that DIO results in a significant increase in CCR2^{+}F4/80^{hi} ATMs, which have a greater CCR2 MFI than the CCR2^{+}F4/80^{lo} ATMs. Also, the amount of CD11c protein expressed on these ATMs increased progressively throughout the dietary intervention period in both populations and it increased at a higher rate in adipose tissue from mice fed high saturated fat diets. We next asked whether the level of CD11c integrin expressed on the surface of ATMs was associated with size and

maturation stage, thereby helping us to determine whether WAT is specifically attracting

ATMs with high CD11c protein or whether CD11c is upregulated in response to

inflammatory mediators in WAT. Our findings show that in the F4/80^{lo} population, the

MFI of CD11c significantly increases with time in ATMs of all sizes (Figures 3H-3J). In

the F4/80^{hi} subset, however, the population which increases in response to DIO, only

large, mature ATMs have increased CD11c MFI (Figures 3K-3M).

Skeletal Muscle Macrophage (SMP) Phenotype

While it is known that SM accounts for 80% of insulin-mediated glucose disposal,

little is known about the role of SM infiltrating macrophages on insulin resistance,

muscle function and obesity-related inflammation. Herein we examine for the first time

the effect of DIO on macrophage infiltration into SM. Specifically, we extracted hindlimb

SM and separated the stromal vascular fraction, containing macrophages, from the

myocyte fraction using a tissue digestion protocol followed by a 40/70% Percoll-based

gradient separation. Similar to our findings in WAT, we observed a significant increase

in skeletal muscle macrophages (SMPs) and identified two distinct SMP populations

which differed in F4/80 intensity (Figure 4A). The majority of these macrophages were

large and mature and we did not find any differences in SMP size among the different

dietary treatments in obese versus control mice. There were also no differences in

CD11c MFI between the DIO and control mice (data not shown), though the CD11c MFI

of the F4/80^{hi} subset was significantly higher than the F4/80^{lo}, whose CD11c surface

concentration more closely resembled that of the ATM populations (Figures 4C). As

opposed to our observations in WAT where the F4/80^{hi} subset predominated, the

increased macrophage infiltration in SM was directly associated with an increase in the

F4/80^{lo} population. To determine a potential cause of SMP infiltration, we measured

MCP-1 expression – the ligand for CCR2 -- in the stromal vascular fraction (SVF) of SM

and found increases on days 70 and 140, with the increase at day 140 being statistically

significant (P=0.02).

Macrophage/myotube Co-culture studies

To gain a better understanding of the effect of macrophages on skeletal muscle

insulin sensitivity, we cocultured differentiated C2C12 myotubes with and without RAW

264.7 macrophages at 1:1 and 1:2 ratios and performed a glucose uptake assay (Figure 5).

When cultured alone, the C2C12 myotubes showed a significant insulin response. The

macrophages also incorporated a significant amount of glucose but did not respond to

insulin. When cocultured together at a 1:1 ratio, the uptake of radiolabeled 2-

deoxyglucose was additive. At the 1:2 ratio of myotubes to macrophages, however, the

total insulin response was diminished, suggesting that macrophages alter the function of

muscle fibers by impairing their ability to take up glucose.

WAT and Liver infiltration of CD4^{+}FOXP3^{+} Regulatory Cells

While a number of studies have chronicled the infiltration of macrophages within

various metabolic tissues, very few have looked at lymphocytes. While the best

characterized lymphocyte functions are the effector function (i.e., induction of immune

responses to foreign antigens), which may contribute to obesity-related inflammation,

recent discoveries in lymphocyte biology illustrate other important roles for T cells as

down-regulators of inflammation. This study focused on the CD4^{+}Foxp3^{+} regulatory T cell (Treg) population and found in both WAT and liver, the percent of these cells significantly decreases in response to DIO (Figure 6). Because these cells are primary down-regulators of autoimmune and inflammatory responses, the Treg-mediated immunoregulatory activity at these important metabolic sites is likely to be impaired following high saturated fat feeding.

Discussion

Obesity is a debilitating and widespread illness characterized by systemic low-grade chronic inflammation, of which the principal mediators are believed to be macrophages infiltrating WAT (11). However, it is possible that macrophages and other immune cells also contribute to the immunopathogenesis and/or prevention of insulin resistance by infiltrating other important metabolic organs (i.e., SM and liver). In this study, we sought to further characterize the phenotype and kinetics of macrophage infiltration into WAT. Furthermore, we investigated whether macrophages and T cells infiltrated the SM and liver of mice fed HFD.

In support of our previous findings, we found that WAT tissue consists of two phenotypically distinct populations of CD11b^{+} ATMs which differ in F4/80 surface expression (18). In db/db mice, which have impaired leptin receptor signaling and rapidly become obese and diabetic, we had shown that F4/80[hi] ATMs were more numerous and had higher CCR2 and CCR5 expression than F4/80[lo] ATMs (18). In the DIO model, the total percentage of F4/80[hi] and F4/80[lo] ATMs were similar to each other, and a greater percentage of the F4/80[hi] ATMs expressed CCR2 and had a significantly

higher CCR2 MFI when compared to F4/80^{lo} ATMs. The differences in total percentage of F4/80^{hi} macrophages between the db/db and DIO mice may be due to the more rapid onset of obesity, impaired leptin signaling, and higher body weights (equivalent to morbidly obese individuals) of the db/db mice in comparison to wild-type mice. In agreement with our previous findings, we observed a significant increase in F4/80^{hi} ATMs with no significant differences in the F4/80^{lo} population. In this study, we also observed a gradual increase over time in surface CD11c expression, a common integrin expressed by macrophages and dendritic cells that functions in phagocytosis and immune surveillance. Overall, the F4/80^{lo} and F4/80^{hi} ATMs respectively resemble the resident and infiltrating macrophages recently described by Lumeng *et al*., who found that the infiltrating ATMs overexpress CCR2 and whose arrival is associated with the development of obesity-induced inflammation (19), characteristics very much in line with the F4/80^{hi} subset identified by our group.

To further expand on the observed phenotypic differences between F4/80^{lo} and F4/80^{hi} ATMs, we classified both populations on the basis of size to distinguish immature versus mature macrophages. Larger ATMs had greater levels of the maturation marker F4/80 than small or medium ATMs, and in the F4/80^{hi} subset, we saw a shift towards the larger phenotype in DIO mice. One possible reason for this finding may involve increased lifespan as anti-apoptotic factors such as macrophage-colony stimulating factor (M-CSF) and macrophage migratory inhibitory factor (MIF) have both been shown to be upregulated in WAT of obese mice (24-26). Interestingly, we also found that levels of CCR2 protein were enhanced in ATMs of all three sizes in the control mice, which may

correspond with the control mice secreting less MCP-1 than mice fed HFD and therefore needing a higher CCR2 threshold to attract ATMs.

Recent studies have reported an increase in $CD11b^+CD11c^+F4/80^+$ macrophages in obese mice (17, 23). These ATMs were associated with a pro-inflammatory M1 or classically activated phenotype in WAT, and lean and CCR2 KO mice had negligible accumulation of pro-inflammatory, $CD11c^+$ ATMs. To better describe the manner in which ATM infiltration leads to inflammation, Lumeng et al. proposed a mechanism by which the M1 polarized $CCR2^+$ monocytes infiltrate WAT of obese mice, differentiate into $CD11c^+$ ATMs and eventually drown out the M2, alternatively activated resident ATMs (17, 19). Our findings point to a similar but subtlety different mechanism. The combined results from this and our previous study strongly suggest that the $F4/80^{lo}$ ATMs represent the described resident ATM population, while the $F4/80^{hi}CCR2^{hi}$ ATMs represent the bone marrow-derived, M1 polarized, pro-inflammatory ATMs.

We show that after 70 and 140 days of high saturated fat feeding the $F4/80^{hi}$ ATMs differentiate into macrophages expressing high levels of CD11c, a pro-inflammatory marker in ATMs (17, 23). By separating ATMs by size and maturation state, we have shown that immature $F4/80^{hi}$ ATMs do not highly express CD11c, showing it to be a marker that develops after infiltration into WAT. What our data also demonstrates is that by day 140, $F4/80^{lo}$ ATMs also begin to express high levels of CD11c, and because they are a resident population, these levels are significantly increased in macrophages of all maturation states. Thus, it appears that during the period of high saturated fat feeding, both populations may be undergoing a shift towards the pro-inflammatory, M1 phenotype.

While we cannot be sure which specific factors induce the pro-inflammatory phenotype of ATMs, the finding that CCR2 KO mice fail to develop CD11c^{hi} ATMs may indicate that the shift involves adipocyte-derived factors in combination with cytokines secreted by other infiltrating cells that express CCR2, such as macrophages and/or effector lymphocyte subsets, and earlier studies have shown that interferon-γ (IFN-γ) in conjunction M-CSF induces both monocyte differentiation and an upregulation in CD11c (27). In this regard, we also assessed whether the Treg compartment, which inhibits the secretion of IFN-γ, suppresses inflammation and autoimmunity was modified in the DIO model. In DIO mice, we observed a significant reduction in Treg cells in both WAT and liver. While our current data only allows us to speculate as to the role of these immune cells in adipose tissue, it would be worthwhile to pursue whether the reduction in this Treg population plays a role in preventing the shift of ATMs into an M1 phenotype.

Our next objective in this study was to assess the role of DIO on the infiltration of SMPs. Recently, Hevener *et al* demonstrated that in myeloid cell-specific PPAR γ knockouts, the PPAR γ-deficient mice have significantly increased F4/80 staining in SM (28). There was also an upward trend in MCP-1 expression in those mice with increased macrophage infiltration in SM (28). Here, our approach was to analyze SMP content within the SVF of SM by flow cytometry and then to assess subset-specific infiltration as we did in WAT. In doing so, we found a significant increase in the infiltration of CD11b^{+}F4/80^{+} SMPs on day 140 resulting from a significant increase in the F4/80^{lo} subset of SM. Similar to WAT, SMPs of larger size from both subsets had elevated protein levels of both F4/80 and CCR2, and we found a significant increase in MCP-1 mRNA arising from the stromal fraction of SM. As opposed to the ATM populations,

DIO had no effect on SMP size or CD11c expression. Interestingly, however, the CD11c levels were much higher in the F4/80^{hi} ATM population.

To gain a better insight on role of macrophages in mediating insulin sensitivity in SM, we cocultured C2C12 myotubes with RAW 264.7 macrophages and performed a glucose uptake assay. When cultured in a 1:1 ratio, there was no adverse effect on insulin sensitivity. At the 1:2 myotube to macrophage ratio, however, the insulin response was significantly diminished, indicating that an increase in muscle macrophage content may exert a negative impact on skeletal muscle insulin sensitivity.

In conclusion, our results point to macrophage infiltration into both WAT and SM as being associated with obesity-induced insulin resistance and describe a novel mechanism by which CCR2^{hi} F4/80^{hi} ATM infiltration may also be involved in the pro-inflammatory shift of the CCR2^{lo} F4/80^{lo} subset. This is also the first study to show that the adipose and hepatic Treg compartments are numerically impaired by high saturated fat feeding. We previously demonstrated that the immunoregulatory activity of Treg is tightly controlled by endogenously activated PPAR γ (29). Thus, our finding that the Treg compartment is affected by DIO may be of importance for the development of Treg-based therapies against obesity-related inflammation and insulin resistance.

ACKNOWLEDGEMENTS

REFERENCES

1.   CDC. National Diabetes Fact Sheet: general information and national estimates on diabetes in the United States, 2005. U S Department of Health and Human Services, Center for Disease Control and Prevention, 2005: Atlanta, Georgia, 2005, pp 1-10.
2.   Shoelson SE, Lee J, Goldfine AB. Inflammation and insulin resistance. The Journal of clinical investigation 2006; 116: 1793-1801.
3.   Reid J, Macdougall AI, Andrews MM. Aspirin and diabetes mellitus. British medical journal 1957; 2: 1071-1074.
4.   Hirosumi J, Tuncman G, Chang L, Gorgun CZ, Uysal KT, Maeda K, et al. A central role for JNK in obesity and insulin resistance. Nature 2002; 420: 333-336.
5.   Shoelson SE, Lee J, Yuan M. Inflammation and the IKK beta/I kappa B/NF-kappa B axis in obesity- and diet-induced insulin resistance. Int J Obes Relat Metab Disord 2003; 27 Suppl 3: S49-52.
6.   Tsukumo DM, Carvalho-Filho MA, Carvalheira JB, Prada PO, Hirabara SM, Schenka AA, et al. Loss-of-function mutation in TLR4 prevents diet-induced obesity and insulin resistance. Diabetes 2007.
7.   Kim F, Pham M, Luttrell I, Bannerman DD, Tupper J, Thaler J, et al. Toll-like receptor-4 mediates vascular inflammation and insulin resistance in diet-induced obesity. Circulation research 2007; 100: 1589-1596.
8.   Hotamisligil GS, Shargill NS, Spiegelman BM. Adipose expression of tumor necrosis factor-alpha: direct role in obesity-linked insulin resistance. Science (New York, NY 1993; 259: 87-91.
9.   Feinstein R, Kanety H, Papa MZ, Lunenfeld B, Karasik A. Tumor necrosis factor-alpha suppresses insulin-induced tyrosine phosphorylation of insulin receptor and its substrates. The Journal of biological chemistry 1993; 268: 26055-26058.
10.   Arkan MC, Hevener AL, Greten FR, Maeda S, Li ZW, Long JM, et al. IKK-beta links inflammation to obesity-induced insulin resistance. Nature medicine 2005; 11: 191-198.
11.   Weisberg SP, McCann D, Desai M, Rosenbaum M, Leibel RL, Ferrante AW, Jr. Obesity is associated with macrophage accumulation in adipose tissue. The Journal of clinical investigation 2003; 112: 1796-1808.
12.   Xu H, Barnes GT, Yang Q, Tan G, Yang D, Chou CJ, et al. Chronic inflammation in fat plays a crucial role in the development of obesity-related insulin resistance. The Journal of clinical investigation 2003; 112: 1821-1830.
13.   Cinti S, Mitchell G, Barbatelli G, Murano I, Ceresi E, Faloia E, et al. Adipocyte death defines macrophage localization and function in adipose tissue of obese mice and humans. J Lipid Res 2005; 46: 2347-2355.
14.   Kamei N, Tobe K, Suzuki R, Ohsugi M, Watanabe T, Kubota N, et al. Overexpression of monocyte chemoattractant protein-1 in adipose tissues causes

macrophage recruitment and insulin resistance. The Journal of biological chemistry 2006; 281: 26602-26614.

15. Weisberg SP, Hunter D, Huber R, Lemieux J, Slaymaker S, Vaddi K, et al. CCR2 modulates inflammatory and metabolic effects of high-fat feeding. The Journal of clinical investigation 2006; 116: 115-124.

16. Kanda H, Tateya S, Tamori Y, Kotani K, Hiasa K, Kitazawa R, et al. MCP-1 contributes to macrophage infiltration into adipose tissue, insulin resistance, and hepatic steatosis in obesity. The Journal of clinical investigation 2006; 116: 1494-1505.

17. Lumeng CN, Bodzin JL, Saltiel AR. Obesity induces a phenotypic switch in adipose tissue macrophage polarization. The Journal of clinical investigation 2007; 117: 175-184.

18. Guri AJ, Hontecillas R, Ferrer G, Casagran O, Wankhade U, Noble AM, et al. Loss of PPARgamma in immune cells impairs the ability of abscisic acid to improve insulin sensitivity by suppressing monocyte chemoattractant protein-1 expression and macrophage infiltration into white adipose tissue. J Nutr Biochem 2007.

19. Lumeng CN, Deyoung SM, Bodzin JL, Saltiel AR. Increased inflammatory properties of adipose tissue macrophages recruited during diet-induced obesity. Diabetes 2007; 56: 16-23.

20. Bassaganya-Riera J, Reynolds K, Martino-Catt S, Cui Y, Hennighausen L, Gonzalez F, et al. Activation of PPAR gamma and delta by conjugated linoleic acid mediates protection from experimental inflammatory bowel disease. Gastroenterology 2004; 127: 777-791.

21. Guri AJ, Hontecillas R, Si H, Liu D, Bassaganya-Riera J. Dietary abscisic acid ameliorates glucose tolerance and obesity-related inflammation in db/db mice fed high-fat diets. Clin Nutr 2006; doi:10.1016/j.clnu.2006.07.008.

22. Austyn JM, Gordon S. F4/80, a monoclonal antibody directed specifically against the mouse macrophage. European journal of immunology 1981; 11: 805-815.

23. Brake DK, Smith EO, Mersmann H, Smith CW, Robker RL. ICAM-1 expression in adipose tissue: effects of diet-induced obesity in mice. Am J Physiol Cell Physiol 2006; 291: C1232-1239.

24. Skurk T, Herder C, Kraft I, Muller-Scholze S, Hauner H, Kolb H. Production and release of macrophage migration inhibitory factor from human adipocytes. Endocrinology 2005; 146: 1006-1011.

25. Hirokawa J, Sakaue S, Tagami S, Kawakami Y, Sakai M, Nishi S, et al. Identification of macrophage migration inhibitory factor in adipose tissue and its induction by tumor necrosis factor-alpha. Biochemical and biophysical research communications 1997; 235: 94-98.

26. Levine JA, Jensen MD, Eberhardt NL, O'Brien T. Adipocyte macrophage colony-stimulating factor is a mediator of adipose tissue growth. The Journal of clinical investigation 1998; 101: 1557-1564.

27. Maciejewski J, Wachter M, Elstner E, Weber H, Diezel W, Seiler FR, et al. Cytofluorometric and cytomorphologic analysis of human bone marrow cells derived from stromal cultures stimulated by granulocyte-macrophage colony-

stimulating factor, interferon-gamma and splenopentin pentapeptide. European journal of immunology 1990; 20: 1209-1213.

28. Hevener AL, Olefsky JM, Reichart D, Nguyen MT, Bandyopadyhay G, Leung HY, et al. Macrophage PPARgamma is required for normal skeletal muscle and hepatic insulin sensitivity and full antidiabetic effects of thiazolidinediones. The Journal of clinical investigation 2007; 117: 1658-1669.

29. Hontecillas R, Bassaganya-Riera J. Peroxisome proliferator-activated receptor gamma is required for regulatory CD4+ T cell-mediated protection against colitis. J Immunol 2007; 178: 2940-2949.

FIGURE CAPTIONS

Figure 1. The effect of diet-induced obesity on (A) body weights, (B) abdominal white adipose tissue (WAT) weights, and (C-E) glucose tolerance. Mice were fed either a high saturated fat diet (HFD) or control diet for 0, 70, or 140 days. At each timepoint mice underwent an intraperitoneal glucose tolerance test (IPGTT). Data are presented as least square means ± standard error. Data points with an asterisk are significantly different ($P<0.05$).

Figure 2. The effect of diet-induced obesity on the subset-specific infiltration adipose tissue macrophages (ATMs). Mice were fed either a high-fat diet (HFD) or control diet for 0, 70, or 140 days. (A) Phenotypical analysis yielded two distinct ATM populations, F4/80lo and F4/80hi. The total percentage of total F4/80$^+$ ATMs (B), F4/80^{lo} ATMs, and F4/80^{hi} ATMs (D) was then calculated throughout the 140-day treatment period. Gating each population individually illustrated that the F4/80^{lo} subset (E) contained significantly fewer CCR2$^+$ cells than the F4/80hi (E). The F4/80^{hi} subset was also CCR2^{hi} when compared to the F4/80^{lo} ATMs (F). On day 140, DIO increased the percent of F4/80^{hi} ATMs that were CD11c$^+$ (G) and increased CD11c protein expression, as indicated by mean fluorescence intensity (MFI), in both the F4/80^{lo} (H) and F4/80^{hi} ATMs. Data are

presented as least square means ± standard error. Data points with an asterisk are significantly different ($P<0.05$).

Figure 3. Effect of diet-induced obesity on the size of adipose tissue macrophages (ATMs). (A) F4/80^{lo} and F4/80^{hi} ATMs were analyzed by forward scatter (FSC) mean fluorescence intensity (MFI), which is indicative of overall cell size. F4/80 mean fluorescence intensity (MFI) was associated with cell size in both the F4/80^{lo} (B) and F4/80^{hi} (C) subsets, and the percent of small, medium, and large ATMs for both the F4/80^{lo} (D) and F4/80^{hi} (E) subsets were assessed along with the MFI of CCR2 (F-G) for day 140. The change in CD11c MFI over time for macrophages in all three maturation states was also determined for both the F4/80^{lo} (H-J) and F4/80^{hi} (K-M) ATMs. Data are presented as least square means ± standard error. Data points with an asterisk or with different subscripts are significantly different ($P<0.05$).

Figure 4. Effect of diet-induced obesity (DIO) on skeletal muscle macrophage (SMP) infiltration. (A) SMPs were divided into two distinct populations on basis of F4/80 mean fluorescence intensity (MFI). (B) Forward scatter (FSC) was utilized to assess the percent of small, medium, and large SMPs in both populations, and the mean fluorescence intensity (MFI) of CD11c was calculated for SMPs of all sizes (C). The total percentage of total F4/80^{+} SMPs (D), F4/80^{lo} SMPs (E), and F4/80^{hi} SMPs (F) was then calculated throughout the 140-day treatment period, and monocyte chemoattractant protein 1 (MCP-1) mRNA expression in the stromal fraction of skeletal muscle (SM) was calculated by real time quantitative RT-PCR (G). In both the F4/80^{lo} (H, I) and F4/80hi

(J, K) SMP subsets, the MFI of F4/80 and CCR2 was associated with size. Data are presented as least square means ± standard error. Data points with an asterisk are significantly different ($P<0.05$).

Figure 5. Glucose uptake in C2C12 myotubes cocultured with RAW 264.7 macrophages. Differentiated myotubes alone, myotubes and macrophages seeded at 1:1 or 1:2 ratios, or macrophages alone were seeded onto 12-well plates and cultured overnight. Cells were treated with or without 100nM insulin for 15 min. and the incorporation of H^3-2-deoxyglucose after 20 minute incubation was assessed. Afterwards, protein levels were assessed with Bio-rad protein assay and did not differ significantly among C2C12-treated wells ($P=0.89$). Data are presented as least square means of relative counts per million (CPM) ± standard error. Data points with an asterisk are significantly different ($P<0.05$).

Figure 6. Regulatory T cell (Treg) infiltration into white adipose tissue (WAT) and liver. Mice were fed either a high-fat diet (HFD) or control diet for 0, 70, or 140 days and the infiltration of CD4+FOXP3+ Treg into WAT (A) and liver (B) was assessed by flow cytometry. Data are presented as least square means ± standard error. Data points with an asterisk are significantly different ($P<0.05$).
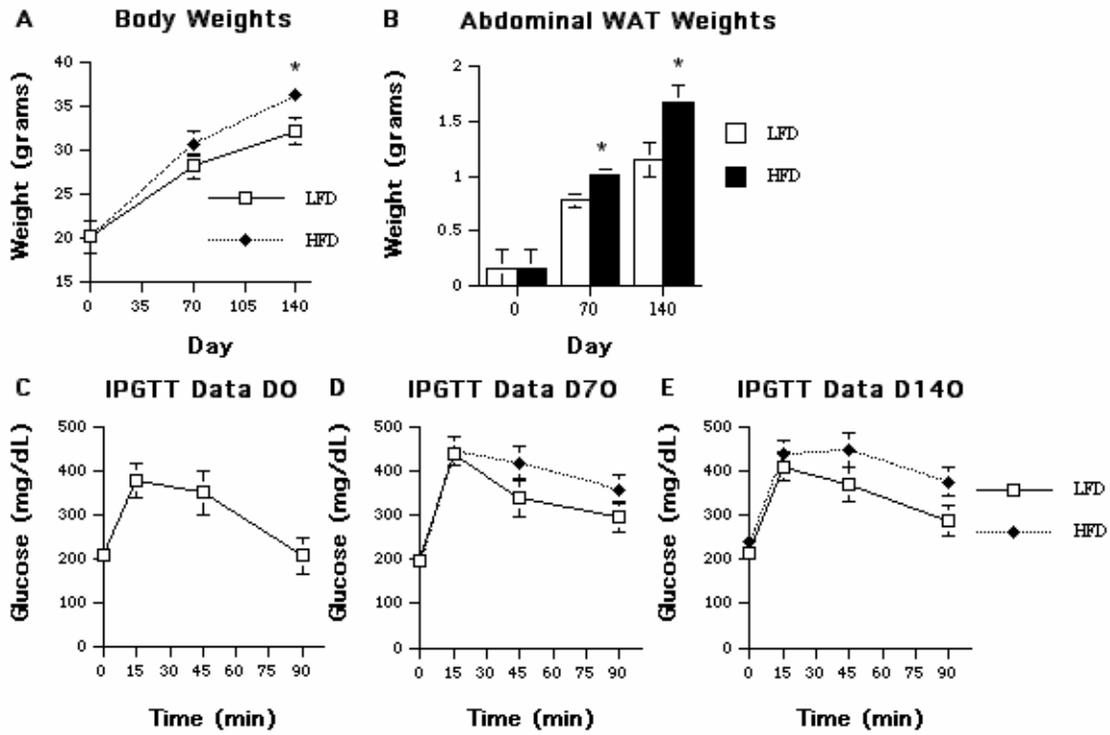
**FIGURE 1**

FIGURE 2
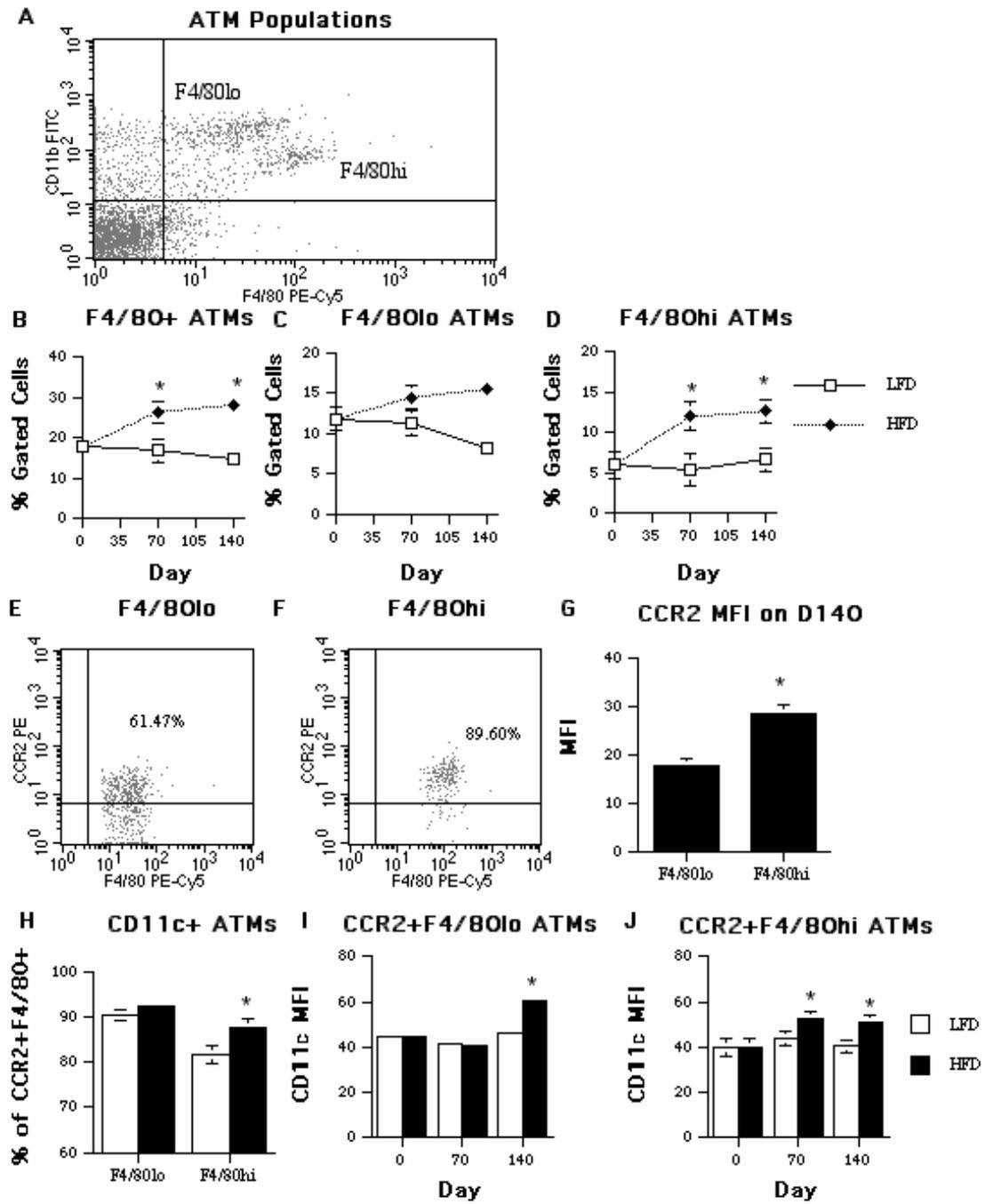
**FIGURE 3**

FIGURE 4

FIGURE 5


Glucose Uptake
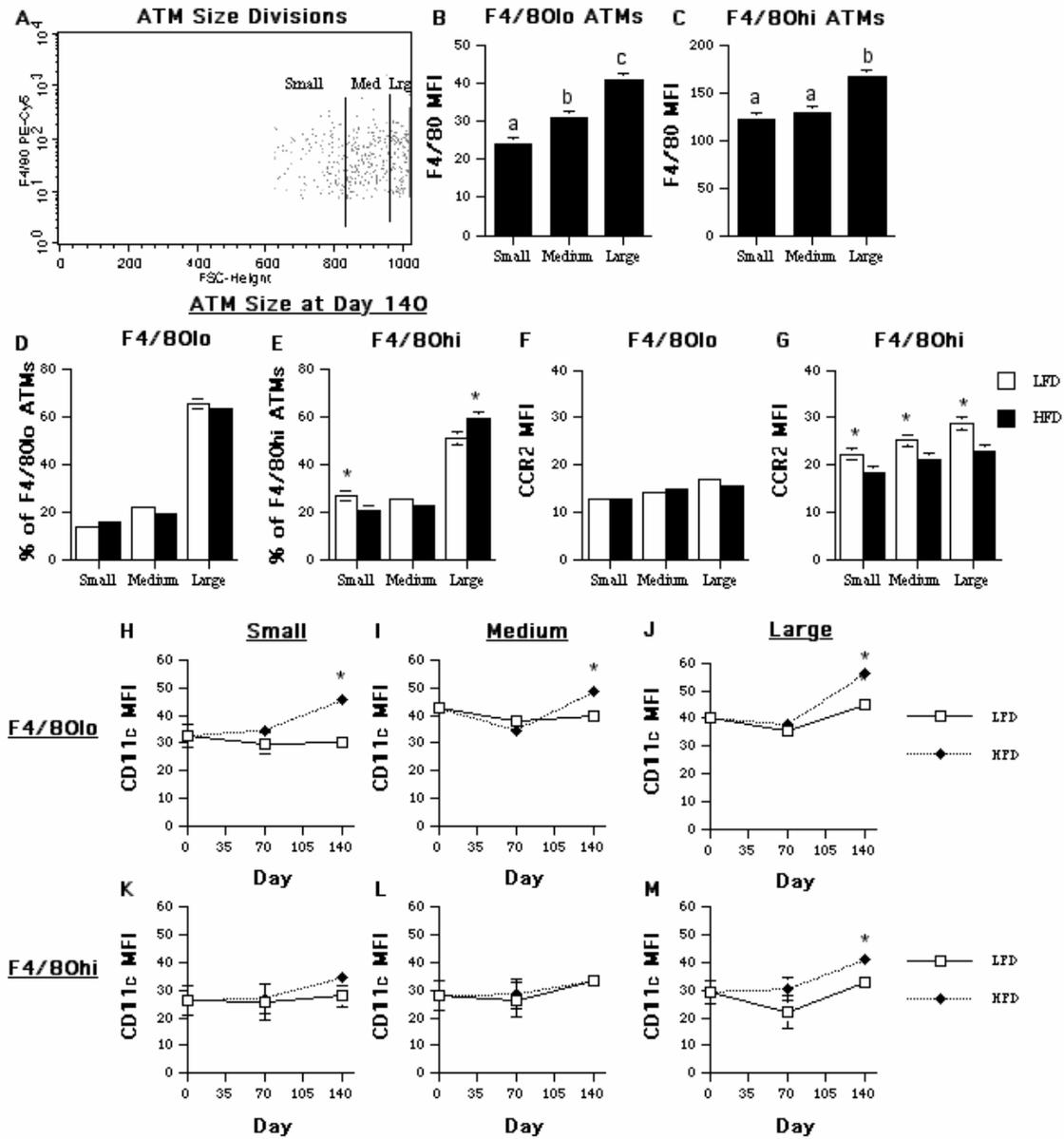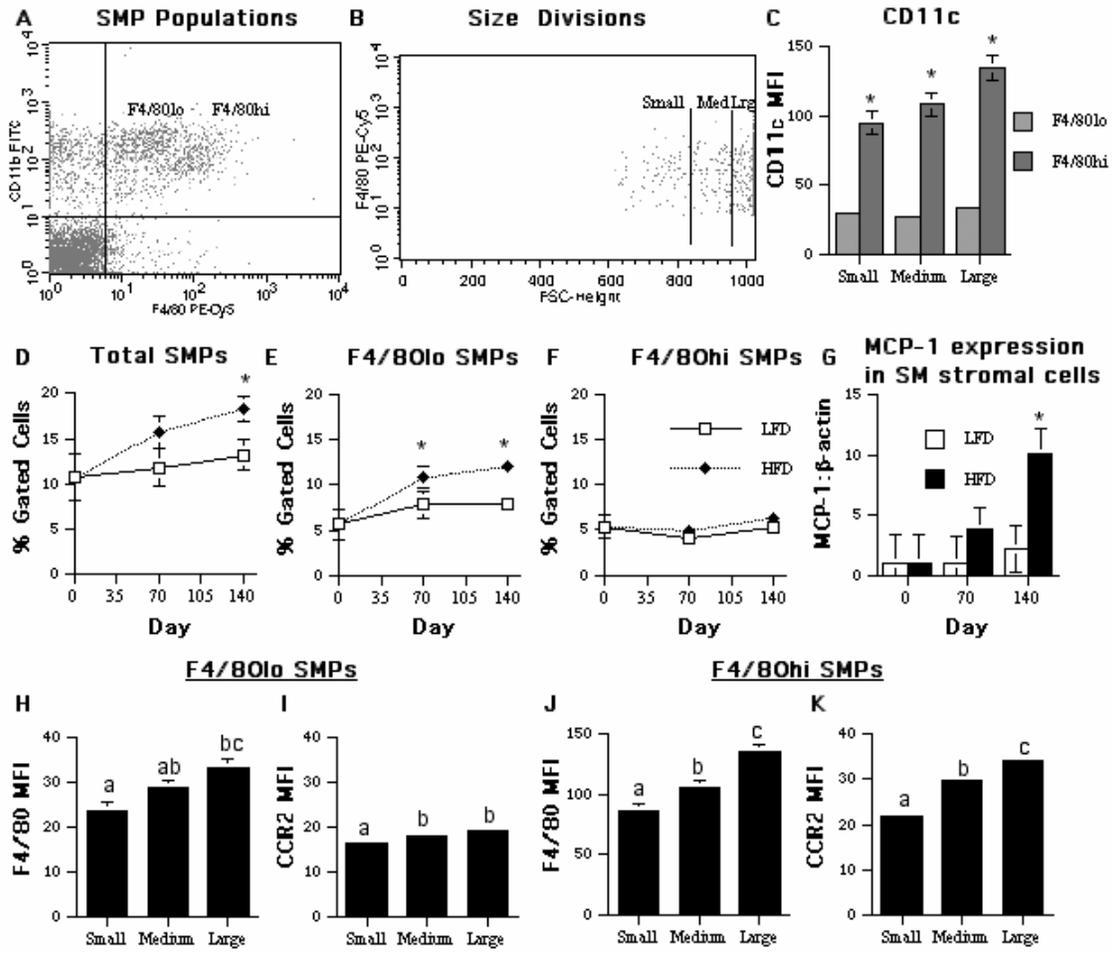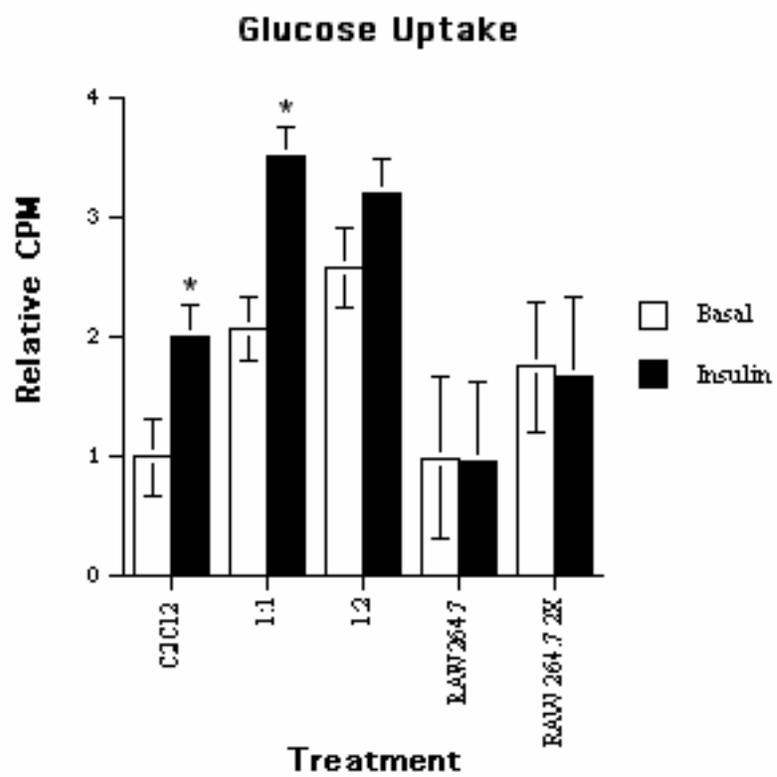
FIGURE 6
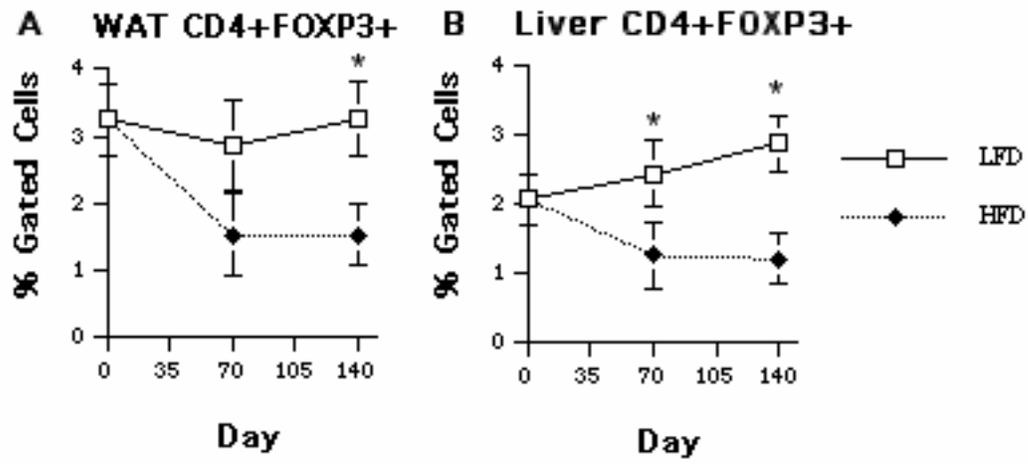
CHAPTER 6: CONCLUSIONS AND FUTURE DIRECTIONS

Obesity is a state characterized by insulin resistance and lipid infiltration into peripheral tissues, leading to the onset of chronic diseases (1). Among the reasons why PPAR agonists have been so effective is their ability to keep lipids in adipose tissue. In our first study, we demonstrated that ABA activates PPAR γ *in vitro* in 3T3-L1 pre-adipocytes and that dietary supplementation of ABA improves glucose homeostasis in obese db/db mice without inducing the side-effects associated with TZDs. These effects were associated with the induction of PPAR-responsive genes in WAT, an increase in the number of small adipocytes, and the inhibition of macrophage infiltration and inflammation, all of which correspond with an increase in PPAR γ activity (2).

In our next study, our goal was to differentiate the effect of ABA on the two cell populations in WAT, adipocytes and stromal vascular cells (SVCs), and to closely examine the role of ABA in influencing the phenotype of adipose tissue macrophages (ATMs) with flow cytometry. With regard to the latter, we unexpectedly discovered two phenotypically distinct CD11b$^+$ ATM populations which differed in their intensity of the surface glycoprotein F4/80 (F4/80^{hi} vs F4/80^{lo}) in db/db mice. Among the key differences we observed between these two populations was that the F4/80^{hi} population appeared to have a much greater migratory capability, whereby a significantly greater percentage of F4/80^{hi} ATMs expressed chemokine receptors CCR2 and CCR5 and the amount of CCR2 protein, as determined by CCR2 mean fluorescence intensity (MFI), was also significantly elevated.

When examining the effect of ABA on these individual populations, we found that mice fed the ABA-supplemented diets had significantly decreased F4/80^{hi} ATMs.

117

The diet had no effect on the percent of F4/80^{lo} ATMs. Moreover, these differences were associated with an approximately 15-fold decrease in MCP-1 expression in the SVF of ABA-fed mice and a significant reduction in plasma MCP-1 levels.

To assess whether PPAR γ in immune cells was necessary for the full antidiabetic effects of ABA, we fed high-fat diets with or without ABA to PPAR γ flfl; MMTV Cre$^+$, who lack PPAR γ specifically in hematopoietic cells, or PPAR γ expressing littermates for 27 weeks. In mice lacking PPAR γ in immune cells, ABA-supplementation was unable to reduce F4/80^{hi} ATM infiltration. The beneficial effects of ABA on glucose homeostasis were also significantly reduced. By transfecting 3T3-L1 pre-adipocytes with and without a PPAR γ expression vector, we determined that the inhibition of MCP-1 promoter activity by ABA also occurred through a PPAR γ-dependent mechanism.

In our final study, our objective was to more closely examine how ABA ameliorates WAT inflammation, and to better understand the pathogenesis of obesity-induced inflammation in WAT, by examining in closer detail the ATM population specifically inhibited by ABA-supplementation. At the time our second study was *in press*, a series of articles by Lumeng et al. (3, 4) and Brake et al. (5) also discovered two separate ATM populations. While they did not examine differing levels of F4/80 in their populations, they were able to differentiate the ATMs based on CD11c, which was later proposed to be a pro-inflammatory marker in ATMs (5). Lumeng et al. also hypothesized a model by which M1-polarized monocytes from the bone marrow infiltrate WAT and eventually overwhelm the M2-polarized resident ATM population (3). Thus, with this new information at hand, our goal was to determine how the populations described in these studies related to the populations discovered in our laboratory. Additionally, we

assessed the effect of diet-induced obesity (DIO) on the phenotype of immune cells in the other two important metabolic organs, liver and skeletal muscle (SM).

In our final study, C57BL6/J mice were fed high-fat or low-fat diets for 0, 70, or 140 days. Similar to our findings with db/db mice, we found two distinct ATM populations in WAT of the DIO mice. The F4/80^{hi} ATMs were CCR2^{hi} and significantly increased in WAT of HFD-fed mice. The amount of CD11c protein on CCR2^{+}F4/80^{hi} ATMs was significantly increased from day 0 on days 70 and 140 in DIO mice. We also observed a significant increase in CD11c MFI on the F4/80^{lo} ATMs on day 140.

To further assess the effect of DIO on ATM phenotype, we divided cells from each population based on size/maturation state using forward scatter (FSC) MFI. Our most significant finding concerned how CD11c protein levels changed through the different maturation states over time in HFD-fed mice. Based on these findings, combined with previous data from the cited literature, we proposed that F4/80^{hi} ATMs represent the infiltrating M1-polarized population. Once in WAT, they mature into a pro-inflammatory, CD11c^{+} phenotype, as exhibited by the increase in CD11c throughout maturation. These ATMs may then play a role in triggering the resident F4/80^{lo} population to become pro-inflammatory as well. Because they are a resident population and exposed to the environment throughout their entire maturation process, CD11c is elevated in F4/80^{lo} ATMs of all sizes. Thus, the role of ABA in preventing obesity-induced inflammation may result from inhibiting the ability of these M1-polarzied ATMs from migrating to WAT and thereby inhibiting this cascade from initiating. In this study, we also found an obesity-induced decrease in skeletal muscle macrophages (SMPs) and regulatory T-cells (T-regs) in liver and WAT. Because T-regs in particular express high

levels of PPAR γ and are important mediators of inflammation, the regulation of this population may also prove to be involved in the insulin-sensitizing effects of ABA.

In looking towards the future, there are still a number of avenues available to explore concerning both ABA and the mechanisms of insulin resistance. We have shown that ABA acts through a PPAR γ-dependent mechanism and inhibits the infiltration of a specific ATM population. There is still the question of whether ABA activates PPAR γ directly or perhaps through indirect mechanisms. In plants, where the actions of ABA have been more extensively examined, researchers recently discovered two ABA-binding proteins, one in the plasma membrane and the other in the nucleus (6, 7). There is also evidence in human cells that ABA can act through a G protein coupled receptor (GPCR), and this mechanism of action may prove to be an interesting one to explore (8).

Because ABA has been shown to be effective in ameliorating insulin resistance, it would be worth while to determine whether supplementation of ABA could be useful in preventing other obesity-related chronic diseases, including CVD and atherosclerosis. While ABA is a compound found ubiquitously in nature, the potential for toxicity at high doses will also have to be fully excluded. Nonetheless, our findings have not shown there to be toxic side effects associated with long-term exposure to an ABA-supplemented diet, and based on our initial findings we believe that ABA holds a considerable amount of potential as an alternative option to TZDs and other insulin-sensitizing drugs and glucostatic agents.

References

1.   Guri A, Hontecillas R, Bassaganya-Riera J. Peroxisome Proliferator-Activated Receptors: Bridging Metabolic Syndrome with Molecular Nutrition. Clinical Nutrition 2006.

2. Guri AJ, Hontecillas R, Si H, Liu D, Bassaganya-Riera J. Dietary abscisic acid ameliorates glucose tolerance and obesity-related inflammation in db/db mice fed high-fat diets. Clin Nutr 2006.
3. Lumeng CN, Bodzin JL, Saltiel AR. Obesity induces a phenotypic switch in adipose tissue macrophage polarization. The Journal of clinical investigation 2007; 117: 175-184.
4. Lumeng CN, Deyoung SM, Bodzin JL, Saltiel AR. Increased inflammatory properties of adipose tissue macrophages recruited during diet-induced obesity. Diabetes 2007; 56: 16-23.
5. Brake DK, Smith EO, Mersmann H, Smith CW, Robker RL. ICAM-1 expression in adipose tissue: effects of diet-induced obesity in mice. Am J Physiol Cell Physiol 2006; 291: C1232-1239.
6. Razem FA, Luo M, Liu JH, Abrams SR, Hill RD. Purification and characterization of a barley aleurone abscisic acid-binding protein. The Journal of biological chemistry 2004; 279: 9922-9929.
7. Razem FA, El-Kereamy A, Abrams SR, Hill RD. The RNA-binding protein FCA is an abscisic acid receptor. Nature 2006; 439: 290-294.
8. Bruzzone S, Moreschi I, Usai C, Guida L, Damonte G, Salis A, et al. Abscisic acid is an endogenous cytokine in human granulocytes with cyclic ADP-ribose as second messenger. Proceedings of the National Academy of Sciences of the United States of America 2007; 104: 5759-5764.

Curriculum Vita

Amir Joseph Guri

Nutritional Immunology and Molecular Nutrition Laboratory
336A Wallace Hall
Virginia Polytechnic Institute and State University
Blacksburg, VA 24061
(540)231-1759
guri@vt.edu

Education:

2004-2007   Ph.D., Nutritional Biochemistry, Virginia Polytechnic Institute and State University, Blacksburg, VA.

1999-2003   B.S., Nutrition major. Rutgers University, New Brunswick, NJ

Professional Memberships:

2005-2007   American Society for Nutrition (ASN)
2006   Montgomery County Coalition for Health Students

Honors and Awards:

2007   One of 12 abstracts chosen for the ASN/Procter and Gamble Graduate Student Research Awards Competition in subject of "Nutrition and Mebabolism."

2006   Became two-time recipient of Margaret Ellen Carter Hepler Memorial Research Scholarship

2005   Recipient Margaret Ellen Carter Hepler Memorial Research Scholarship

2004   Awarded John Lee Pratt Fellowship

2003   Graduated with Highest Honors from Rutgers University

2003   Named Most Outstanding Undergraduate Student in Nutrition Department

2003   Graduated as George H. Cook Honors Program Scholar

2002   Willard Chandler Thompson Scholarship

1999   Edward Bloustein Scholarship

1999   Outstanding Scholars Award

Publications:

1. Guri AJ, Hontecillas R, Ferrer G, Casagran O, Wankhade U, Noble AM, et al. (2007) Loss of PPARgamma in immune cells impairs the ability of abscisic acid to improve

insulin sensitivity by suppressing monocyte chemoattractant protein-1 expression and macrophage infiltration into white adipose tissue. J Nutr Biochem.

2. Bassaganya-Riera, J., A.J. Guri, A.M. Noble, K.A. Reynolds, J. King, C. Wood, M. Ashby, D. Rai, and R. Hontecillas (2007) Docosahexaenoic and arachidonic acid-enriched infant formulas modulate antigen-specific T cell responses to influenza virus in neonatal piglets. Am. J. Clin. Nutr.

3. Guri AJ, Hontecillas R, Bassaganya-Riera J. Dietary Modulators of Peroxisome Proliferator-Activated Receptors: Implications for the Prevention and Treatment of Metabolic Syndrome (2007). Journal of Nutrigenetics and Nutrigenomics. *In press*

4. Guri AJ, Hontecillas R, Si H, Liu D, Bassaganya-Riera J. Dietary abscisic acid ameliorates glucose tolerance and obesity-related inflammation in db/db mice fed high-fat diets (2007). *Clinical Nutrition*; 26: 107-116.

5. Guri A, Hontecillas R, Bassaganya-Riera J (2006) Peroxisome Proliferator-Activated Receptors: Bridging Metabolic Syndrome with Molecular Nutrition. *Clinical Nutrition*, 25 (6): 871-885.

6. Bassaganya-Riera J, A. Guri, J. King, and R. Hontecillas (2005) Peroxisome Proliferator-Activated Receptors: the Nutritionally Controlled Molecular Networks that Integrate Inflammation, Immunity and Metabolism. *Current Nutrition & Food Science.* 1:179-187

7. Guri AJ, Hontecillas R, Reynolds KA, Bassaganya-Riera J. Obesity promotes macrophage infiltration into both adipose tissue and skeletal muscle and impairs the regulatory CD4+ T cell compartment. Submitted 2007.

Abstracts
Guri, A.J., R. Hontecillas, G. Ferrer, O. Casagran, U. Wankhade, A.M. Noble and J. Bassaganya-Riera (2007) The loss of PPAR γ in immune cells abrogates the ability of abscisic acid to improve insulin sensitivity through a mechanism involving suppression of MCP-1 expression and macrophage infiltration into white adipose tissue. FASEB Meetings, Washington, D.C.; (Abstract #934).

Bassaganya-Riera, J., A.J. Guri, A.M. Noble, K.A. Reynolds, J. King, C. Wood, M. Ashby, D. Rai, and R. Hontecillas (2007) Docosahexaenoic and arachidonic acid-enriched infant formulas modulate antigen-specific T cell responses in the neonatal piglet. FASEB Meetings, Washington, D.C.; (Abstract #2530).

Hontecillas, R., A.J. Guri, U. Wankhade, G. Lopez-Velasco, J. Bassaganya-Riera (2007) Dietary abscisic acid modulates T cell proliferation and cytokine production. FASEB Meetings, Washington, D.C.; (Abstract #4269).

Patents
Bassaganya-Riera, J., A.J. Guri, and R. Hontecillas
Method of Using Abscisic Acid to Treat and Prevent Diabetes and Inflammation.
U.S. Patent Application No: 60/771,033.

(1)

1.   Guri AJ, Hontecillas R, Si H, Liu D, Bassaganya-Riera J. Dietary abscisic
        acid ameliorates glucose tolerance and obesity-related inflammation in
        db/db mice fed high-fat diets. Clinical nutrition (Edinburgh, Scotland)
        2007; 26: 107-116.